Identification of signaling peptides involved in immune responses in *Zea mays*

Inaugural-Dissertation

zur Erlangung des Doktorgrades der Naturwissenschaften
Dr. rer. nat.

der Mathematisch-Naturwissenschaftlichen Fakultät
der Universität zu Köln

angenommen im Jahr 2025

vorgelegt von

M. Sc. Philipp Michael Katzy

Summary

The phytohormone salicylic acid (SA) plays a crucial role in regulating plant immunity, particularly against biotrophic pathogens. SA modulates a variety of molecular processes including the transcriptional regulation of *pathogenesis-related* (*PR*) genes and the activation of apoplastic proteases. So far, neither early responses within the first 24 hours are described in maize nor have serine hydrolases, an important class of apoplastic proteases, been implicated in SA-induced responses. Thus, the first part of this study focused on profiling and identifying active SHs after SA treatments. A significant increase in the activity of SHs was observed 3 hours upon SA treatment and three activated subtilases: ZmSBT7, ZmSBT1.9 and ZmSBT4, were identified. So far, their role in maize immunity has not been elucidated. However, orthologs of these subtilases were shown to be involved in resistance against biotrophic pathogens.

As the activation of certain proteases was demonstrated to result in the release of signaling peptides (phytocytokines), the second aim of this study was to identify novel SA-related phytocytokines and elucidate their role in immunity. Numerous peptides were identified being uniquely present at 3 hours upon SA treatment. 14 peptides were selected as phytocytokine candidates (PC1 to PC14) of which six were found to induce *PR*-gene expression, indicating a role in SA signaling. Notably, the presence of two PCs modulated the virulence of *Ustilago maydis*, a biotrophic maize pathogen. PC13 was found to significantly reduce the virulence of *U. maydis*, while SIGGI (PC14) was observed to increase *U. maydis* virulence. Transcriptome analysis in response to SIGGI revealed its ability to induce genes involved in ubiquitination, proteolysis and SA-biosynthesis pointing to a potential role in modulating protein homeostasis and SA signaling. In contrast, PC13 triggered the upregulation of genes associated with programmed cell death (PCD), hypersensitive response (HR) and negative regulation of the jasmonic acid (JA) signaling pathway. This suggests that PC13 may influence the balance between defense mechanisms potentially by modulating the SA-JA crosstalk.

In conclusion, this study shows an early increase in serine hydrolase activity, specifically subtilases, upon SA treatments. These subtilases could likely release potential phytocytokines to modulate immune related hormonal pathways. These results deepen our knowledge about proteases and substrates involved in the plant immune system.

List of Abbreviations

ABA	Abscisic acid
ABPP	Activity Based Protein Profiling
AF	Apoplastic fluid
Ala	alanine
APF	Apoplastic peptide fraction
Asn	asparagine
Asp	aspartic acid
Avr	avirulence
BAK1	BRI1-ASSOCIATED RECEPTOR KINASE 1
Bax	BCL2-associated X
BIK1	*BOTRYTIS*-INDUCED KINASE 1
BR1	BRASSINOSTEROID INSENSITIVE 1
CatB	Cathepsin B
CC	coiled-coil
CERK1	CHITIN ELICITOR RECEPTOR KINASE 1
Cmu1	chorismate mutase 1
CNL	coiled-coil-type NLRs
CPK	Calcium-dependent protein kinases
CRP1	CONSTITUTIVE EXPRESSOR OF PR GENES 1
CSP	cold-shock protein
Cys	cysteine
CYS6	Cytokinase 6
DAMP	Damage-associated molecular pattern
DCI	3,4-Dichloroisocoumarin (SH inhibitor)
DEG	Differentially expressed gene
DMSO	dimethyl sulfoxide
DNA	Deoxyribonucleic acid
DORN1	DOES NOT RESPOND TO NUCLEOTIDES 1
dpi	Days post infection
E64	PLCP inhibitor
eATP	extracellular ATP
EDS1	ENHANCED DISEASE SUSCEPTIBILITY 1
EDTA	Ethylenediaminetetraacetic acid
ER	endoplasmic reticulum
ERF	Ethylene-Responsive Factor
ET	Ethylene
ETI	Effector-triggered immunity
ETS	Effector-triggered susceptibility

FC	Fold change
FER	FERONIA
FLS2	FLAGELLIN SENSING 2
Fn3	fibronectin type III
GB	Golden Bantam
GC	glucocorticoids
GLV	GOLVEN
GO	Gene Ontology
HECT	Homologous to E6-associated protein C-Terminus
His	histidine
hpi	hours post infiltration
HR	Hypersensitive response
HypSys	hydroxyproline-rich systemins
ICS	isochorismate synthase
IL	interleukin
IRP	immune-related peptide
JA	Jasmonic acid
JAZ	JASMONATE ZIM-DOMAIN
LAZ1	LAZARUS 1
LPS	lipopolysaccharide
MAMP	Microbe-associated molecular pattern
MAP1	Maize apoplastic peptide 1
MC	METACASPASE
MDL	MIF/D-DT-like
MeJA	Methyl jasmonate
MIF	Macrophage Migration Inhibitory Factor
MIK2	MALE DISCOVERER 1-INTERACTING RECEPTOR-LIKE KINASE 2
MS	Mass-spectrometry
NB-LRR	Nucleotide binding-leucine rich repeat
NF-κB	Nuclear factor kappa B
NHP	N-hydroxypipecolic acid
NLR	nucleotide-binding leucine-rich repeat receptors
NPC	No-probe control
NPR1	non-expressor of PR1 protein
OBD	On-bead digest
PA	Protease Associated
PAD4	PHYTOALEXIN DEFICIENT 4

padj	adjusted p-value
PAMP	Pathogen-associated molecular pattern
PC	Phytocytokine candidate
PCA	Principal component analysis
PCD	programmed cell death
PD	Pull-down
PDF1.2	PLANT DEFENSIN 1.2
PEP	plant elicitor peptide
PICS	protease cleavage sites
PIP1/2	PAMP-induced secreted peptide 1/2
PLCP	Papain-like cysteine protease
PMSF	Phenylmethylsulfonyl fluoride (SH inhibitor)
PR	Pathogenesis-related protein
PRR	Pattern recognition receptors
PSK	phytosulfokines
PSY1	peptide containing sulfated tyrosine 1
PTI	Pattern-triggered immunity
PUB	plant U-box
qRT-PCR	quantitative real-time PCR
RALF	rapid alkalization factor
RBOHD	RESPIRATORY BURST OXIDASE HOMOLOG D
RD21	Responsive to Dehydration 21
RGI	RGF1 INSENSITIVE
RIN4	RPM1-interacting protein 4
RING	Really Interesting New Gene
RLCK	receptor-like cytoplasmic kinases
RLK	Receptor-like kinases
RNA	Ribonucleic acid
RNAseq	RNA sequencing
RPM1	Resistance to *Pseudomonas syringae pv*. *maculicola* 1
S1P	SITE-1 PROTEASE
SA	Salicylic acid
SAG12	Senescence-associated reference gene
SAP	stress associated protein
SAP1/2	secreted aspartic protease 1/2
SAR	Systemic acquired resistance
SARD1	SAR DEFICIENT 1
SBT	Subtilisin-like protease
SCOOP	serine-rich endogenous peptide
SCP	carboxypeptidase
Ser	serine
SH	Serine Hydrolases
SINA	Seven in absentia

SNC1	SUPPRESSOR OF npr1-1 CONSTITUTIVE 1
SP	serine proteases
TAK1	Transforming growth factor-β activated kinase-1
TF	Transcription factor
TIR	Toll/interleukin-1 receptor/Resistance protein
TLR4-MD2	Toll-like receptor 4/myeloid differentiation factor 2
TNF	tumor necrosis factor
TNLs	TIR-type NLRs
TRAF6	tumor necrosis factor-6
Tukey HSD	Tukey Honestly Significant Difference
XCP1	Xylem Cysteine Protease 1
XCP1/2	Xylem cysteine protease
ZIM	Zinc finger protein expressed in Inflorescence Meristem
Zip1	*Zea mays* immune peptide 1

Table of Contents

1. Introduction

1.1. The plant immune system

Plants evolved a highly complex immune system including different immune responses and powerful defense mechanisms. This is required to successfully defend against diverse pathogens, including viruses, bacteria, fungi, oomycetes, herbivores, and parasitic plants (Ngou et al., 2022). As a first physical barrier the pathogen faces the cell wall, which they can overcome through open stomata, prior wounding or with the help of enzymes. After the pathogen has overcome the plant cell wall, it faces the plasma membrane. Pattern recognition receptors (PRR) are located at the plasma membrane that can recognize conserved molecular patterns which are called pathogen- or microbe-associated molecular patterns (PAMPs/MAMPs) (Fig. 1.1). These molecular structures are present in the pathogen/microbe but not in the plant itself (Yuan et al., 2021a). The probably best studied example of a MAMP and its respective PRR is the recognition of the bacterial protein flagellin. The active MAMP epitope of flagellin is recognized in *Arabidopsis thaliana* (hereafter: Arabidopsis) by the ubiquitously expressed PRR FLAGELLIN SENSING 2 (FLS2) (Bittel & Robatzek, 2007; Gómez-Gómez & Boller, 2000). To sense fungal infections, the cell surface is equipped with the PRR CHITIN ELICITOR RECEPTOR KINASE 1 (CERK1), which recognizes chitin. As chitin is an essential component of every fungal cell wall, the recognition of oligosaccharides is very conserved in plants. Orthologues of CERK1 can be found in monocotyledons as well as in dicotyledons. The probably best studied chitin receptors are Arabidopsis CERK1 (AtCERK1) and *Oryza sativa* CERK1 (rice, OsCERK1), but the receptor is also found in maize (ZmCERK1) and *Nicotiana benthamiana* (NbCERK1) (Li et al., 2024; Miya et al., 2007; Sánchez-Vallet et al., 2015; Shimizu et al., 2010; Yang et al., 2022). In addition to MAMPs, damage-associated molecular patterns (DAMPs) which are released by the plant after damage caused by e.g. a feeding insect can be sensed by PRRs (Ngou et al., 2022). Damage or rupture of cells leads for example to an increase of extracellular ATP (eATP), which is sensed by the PRR DOES NOT RESPOND TO NUCLEOTIDES 1 (DORN1) (Choi et al., 2014; Tanaka et al., 2014). After ligand binding by PRRs, co-receptors are recruited to form receptor complexes, which in turn activate receptor-like cytoplasmic kinases (RLCKs) (Fig. 1.1). Subsequently, these RLCKs phosphorylate other

components of the plant immune system resulting in further immune responses, including RESPIRATORY BURST OXIDASE HOMOLOG D (RBOHD), which induces the generation of reactive oxygen species (ROS), cyclic nucleotide-gated ion channel for calcium (Ca^{2+}) influx, MAPKKKs to induce MAPK signaling cascade and WRKYs transcription factors, which induce the expression of defense genes like *pathogenesis-related (PR*)-genes and phytohormone production of e.g. salicylic acid (SA) and jasmonic acid (JA) (Lee et al., 2020; Thulasi Devendrakumar et al., 2018; Wang et al., 2023; Yu et al., 2024; Yuan et al., 2021b). The recognition of MAMPs/DAMPs by PRRs and the resulting responses are referred to as PAMP triggered immunity (PTI) (Yuan et al., 2021b).

Some pathogens have evolved the capacity to suppress PTI through the secretion of effectors. Effector are proteins which have the capacity to mitigate plant defense responses and alter plant physiology so that it enabled the pathogen to establish infection (Selin et al., 2016). Thus, effectors are able to suppress PTI by interrupting the signaling cascade which results in effector-triggered susceptibility (ETS). Effectors can have different modes of action, e.g. shield the pathogen cell wall and thereby preventing MAMP recognition. The tomato pathogen *Cladosporium fulvum* secretes the effector protein avirulence4 (Avr4) to protect chitin within the fungal cell wall from secreted tomato chitinases (Wang et al., 2022). Other effectors were reported to directly target plant proteins. For example, the bacterial effector AvrRpt2 targets the Arabidopsis Resistance to *Pseudomonas syringae pv*. *maculicola* 1 (RPM1)-interacting protein 4 (RIN4) for degradation which is important for the regulation of stomatal apertures (Rose et al., 2012; Tsuda & Katagiri, 2010a). To counteract the action of effectors, plants have evolved intracellular nucleotide-binding leucine-rich repeat receptors (NLRs) to detect effectors, which are often encoded by Resistance (R) genes (Ngou et al., 2022). Upon effector perception, NLRs form resistosomes, which are distinguished based on their N-terminal domain, for instance coiled-coil (CC)-type NLRs (CNLs) or Toll/interleukin-1 receptor/Resistance protein (TIR)-type NLRs (TNLs) (Fig. 1.1). Upon resistosome formation, different immune responses are induced, which are summarized as effector triggered immunity (ETI). The CNL resistosome induces calcium-dependent protein kinases (CPKs), which subsequently boosts RBOHD activity and the generation of ROS.

Also, they enhance the phosphorylation of MAPKKK indirectly which starts the MAPK cascade. Both immune responses, the generation of ROS and the MAPK cascade, are also part of PTI and are enhanced upon recognition of effectors. Besides, the CNL as well as the TNL resistosome can induce the expression of defense genes through CPKs and other yet unknown factors resulting in the augmentation of RLCK phosphorylation. In case of AvrRpt2, the NLR protein RPS2 recognizes the degradation of RIN4 in Arabidopsis (Tsuda & Katagiri, 2010b). *P. syringae* suppresses tomato immunity by secretion of the effector AvrPto, which inhibits host kinase activity and thus, immune responses. The tomato plant counteracts this effector activity with guarding the decoy kinase Pto with CNL Prf, which detecting the influences of AvrPto activities and induce ETI (Ngou et al., 2022).

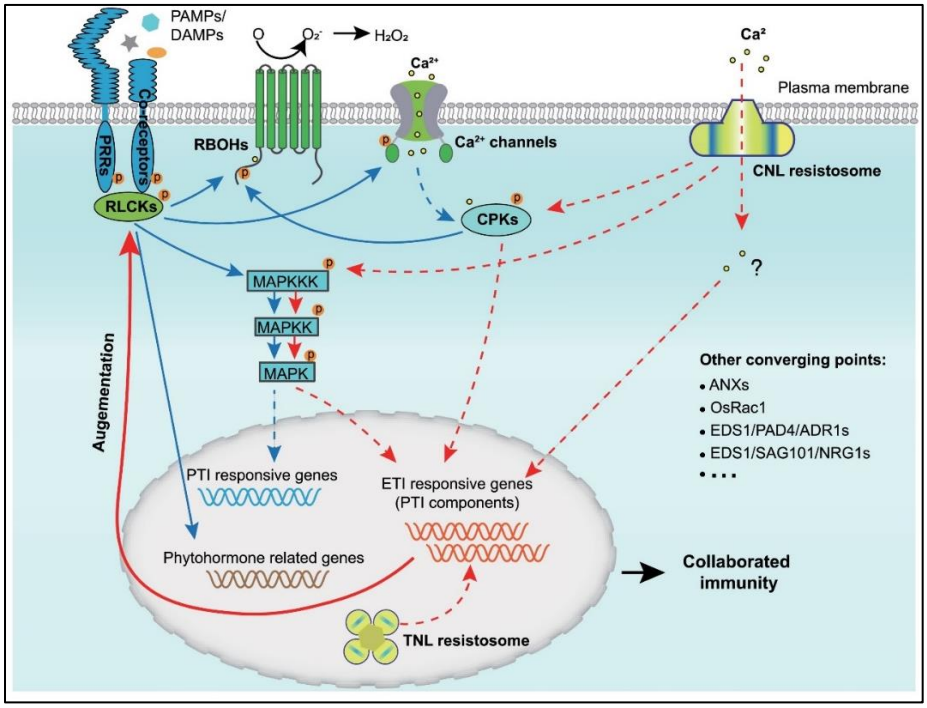

Figure 1.1: PRR and NLR pathways regulate immune responses in overlapping ways. Upon recognition of PAMPs and DAMPs by PRRs, co-receptors are recruited to form receptor complexes, which activate RLCKs. Subsequently, these RLCKs phosphorylate components, including RBOHD, CNGCs and MAPKKKs, thereby triggering a ROS burst, Ca^{2+} influx, MAPK activation, phytohormone production and transcriptional reprogramming. Activation of NLRs (CNLs and TNLs) forms resistosomes, resulting in overlapping immune responses but differing in dynamics. Studies show that several components, including RBOHD, RLCKs, CPKs and MAPK cascades, play a role in both PTI and ETI and are regulated by these processes. Furthermore, the development of ETI resistance and elicitation of responses depends on PTI pathway components. The potentiation of PTI by ETI represents a crucial aspect of the immune response, and the two signaling cascades work together to ensure effective immunity. Solid arrows indicate direct, and dashed arrows indirect effects, while question marks indicate mechanisms yet to be fully understood. Figure adapted from Yuan et al., 2021b.

1.2 Phytohormones – key players in plant immunity

Phytohormones, like salicylic acid (SA), jasmonic acid (JA), ethylene (ET), auxin, abscisic acid (ABA) and gibberellin, are essential in the regulation of developmental processes, interactions between plants or responses to biotic and abiotic environmental stresses. Every hormone initiates a specific pathway and is crucial for certain responses. The various hormone pathways are integrated into a complex network of interactions, including synergistic, antagonistic, and additive relationships. This inter-pathway communication is referred to as hormone crosstalk (Aerts et al., 2021).

The most extensively studied defense pathways are those involving the phytohormones SA and JA. These two phytohormones form the backbone of the hormone-regulated part of the immune system and act as antagonistic regulators (Wasternack & Song, 2017; Y. Zhang & Li, 2019). SA influences developmental processes, regulation of photosynthesis, but is considered to be mostly directed in plant defense against pathogens (Arif et al., 2020; Goodluck et al., 2022). All studied TNL receptors activated by pathogen effectors in ETI signal via the non-NLR protein ENHANCED DISEASE SUSCEPTIBILITY 1 (EDS1) and its interacting partner, PHYTOALEXIN DEFICIENT 4 (PAD4), which are required for SA accumulation (Fig. 1.2) (Lapin et al., 2019; Wiermer et al., 2005). The accumulation of SA occurs generally upon infection with biotrophic pathogens and is linked to many key compounds in plant defense (Goodluck et al., 2022). SA binds directly to the constitutively expressed non-expressor of PR1 protein (NPR1) in its oligomeric form and causes conformational changes, which results in biologically active monomers (Wu et al., 2012). The monomers serve as a transcriptional co-activator and influence the activity of transcription factors (TFs), which regulate the transcription of SA responsive genes (Fan & Dong, 2002). One example is the increased expression of SA-dependent *PR*-genes, which are frequently used as a robust marker to determine and characterize the SA-response (Goodluck et al., 2022; Withers & Dong, 2016). Interestingly, also protease activity is affected by SA. Upon exogenous application of SA, the activity of papain like cysteine proteases (PLCPs) increases at 24 hpi (Ziemann et al., 2018). Furthermore, SA induces the release of phytocytokines. For example, the maize phytocytokine *Zea mays* immune signaling peptide 1 (Zip1) was found in the apoplast upon SA treatments, which is specific for *Z. mays* and its wild ancestor teosinte and is able to induces *PR*-gene

expression upon detection (Depotter et al., 2022b; Ziemann et al., 2018). Phytocytokines are small plant endogenous signaling peptides and can be recognized as MAMPs and DAMPs by cell surface localized PRRs. These peptides transfer the immune signal to the neighboring cell and can induce an amplification loop and their release in the apoplast after proteolytic cleavage is strictly regulated (Hou, Liu, & He, 2021; Koenig et al., 2023; Ziemann et al., 2018). SA induced molecules are also transported from the infected site to distal tissues, thereby facilitating the establishment of systemic acquired resistance (SAR). This process confers long-lasting and broad-spectrum protection for the whole plant and enables a more robust defense against subsequent infections by related and unrelated pathogens (Kamle et al., 2020). Exogenously applied SA can mimic infections with biotrophic pathogens resulting in the induction of *PR*-gene expression and establishment of SAR (Cao et al., 1994). The SA signaling has a negative effect on the signaling of the phytohormone auxin, which acts as internal regulator of growth and root development in soil (Jan et al., 2024; Pieterse et al., 2009). In turn, auxin as well as ABA, which is crucial in abiotic stress responses, have a negative effect on the SA established defense against biotrophic pathogens, (Checker et al., 2018; Pieterse et al., 2009; A. Singh & Roychoudhury, 2023)

Over the past decades, the roles of phytohormone JA and their derivatives have been identified as crucial signaling compounds involved in stress, defense and plant development. The JA pathway is generally inhibited by JASMONATE ZIM-DOMAIN (JAZ), as these proteins inhibit crucial TFs of the JA pathway (Fig 1.2). Upon ubiquitination and degradation of JAZ, the TFs MYC and Ethylene-Responsive Factor (ERF) become active. MYC regulates the JA responses in plant defenses against attacks of insects (Ghorbel et al., 2021a). This TF activates JA responsive genes, like *WRKY*-genes, regulates JA biosynthesis, by targeting the JA biosynthesis genes LOX2, LOX3, LOX4, LOX6 and AOS, but also affects negatively the expression of JAZ (Ghorbel et al., 2021b; Zander et al., 2020). Further, MYC negatively regulates SA responsive TFs, which in turn also negatively regulate MYC expressions. Additionally, MYC negatively influences the expression of ERF1, which targets the promoter of *PLANT DEFENSIN 1.2* (*PDF1.2*). PDF1.2 is important in resisting the infection of necrotrophic and hemibiotrophic pathogens (Ghorbel et al., 2021b). ERF1 is in parallel also an important TF in the ET

pathway, which is therefore directly influenced by JAZ and MYC activity. ET plays an important role in the defense against necrotrophic and hemibiotrophic pathogens, but also has a positive effect on SA accumulation and thus, indirectly a negative to MYC expression (Checker et al., 2018; Pieterse et al., 2009). The ubiquitination of JAZ is indirectly inhibited by gibberellin signaling, which is a main plant growth regulator (Castro-Camba et al., 2022; Pieterse et al., 2009)

This complex antagonistic interaction of SA and JA is also employed by pathogens such as the biotroph *P. syringae.* The secretion of the JA-mimicking toxin coronatine has the effect of repressing salicylic acid-mediated immune responses, which consequently enhances virulence (Spoel & Dong, 2024b).

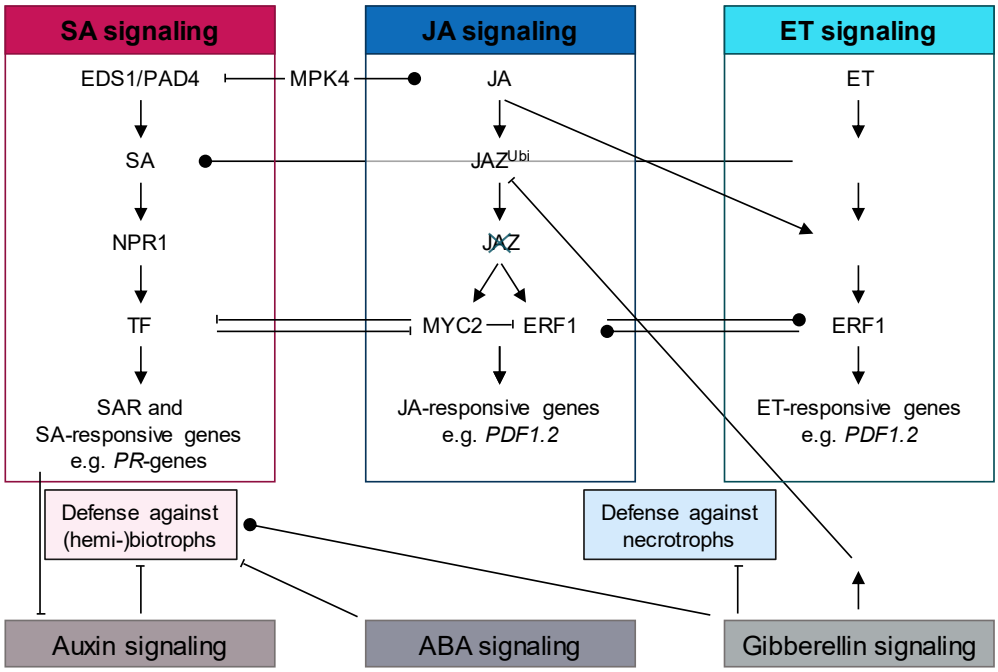

Figure 1.2: Hormone crosstalk in plant immunity with special view on SA, JA and ET. Simplified overview of the crosstalk network of the main player hormones in defense signaling. Model highlights antagonistic and positive interactions between the pathways (⊥ negative effect; ● positive effect) (modified from Pieterse et al., 2009 and added with Checker et al., 2018).

1.3 Plant proteases in immunity

Proteases are a diverse subclass of enzymes that cleave proteins by catalyzing the hydrolysis of a peptide bond. The enzymes are regulated by several stringent mechanisms and can be found in all organisms (González-Rábade et al., 2011; Schaller, 2004; van der Hoorn, 2008a). In plants, proteases are involved in almost every process including development and immunity. In comparison to other eukaryotes, plant genomes frequently encode for significantly expanded protease families, which is indicative of their crucial roles in plant biology (Balakireva & Zamyatnin, 2018; Liu et al., 2024a; van der Hoorn & Klemenčič, 2021). Proteases can be divided into catalytic “sub-subclasses”, namely cysteine proteases, serine proteases, metalloproteases and aspartic proteases (van der Hoorn, 2008b). This categorization is mainly built on the main amino acid of their active side. Thus, the active site of serine proteases (SP) contains a serine residue (Ser) in addition to aspartic acid (Asp) and histidine (His), whereas cysteine proteases possess a cysteine (Cys) instead of Ser, an asparagine (Asn) instead of Asp and His. Both serine and cysteine proteases form covalent enzyme/substrate complexes. Besides, aspartic proteases depend on an Asp residue for their catalytic activity and metalloproteases use a metal ion, mainly a zinc ion (Antão & Malcata, 2005).

While most proteases remain to be studied, the available examples indicate their crucial function in responses to biotrophic, but also hemibiotrophic and necrotrophic pathogens (Balakireva & Zamyatnin, 2018; van der Hoorn & Klemenčič, 2021). Proteases play a pivotal role in plant defense through four principal mechanisms: (1) the direct degradation of pathogen proteins, leading to the recognition and thus, execution of defense mechanisms; (2) the proteolytic activation of host immune proteins, such as hydrolases, which are essential for the initiation of immune responses; (3) the regulation of immune components stability, ensuring the optimal functioning of the immune system; and (4) the proteolytic release and degradation of immunogenic peptides, which are crucial for the initiation of an adaptive immune response (Liu et al., 2024b). A famous example for proteases acting directly on pathogen protein (1) are the secreted aspartic protease 1 and 2 (SAP1 and SAP2) from Arabidopsis. These two proteases are activated and secreted to the apoplast upon the infection of *P. syringae* and target the bacterial protein MucD. MucD itself is a protease and required for bacterial growth (Wang et al., 2019).

The apoplastic PLCP Rcr3 in tomato has an essential function in the resistance of tomato towards the fungal pathogen *C. fulvum* and is known to activate host immune proteins (2). Interestingly, its role is independent of its proteolytic activity but depends on the interaction between Rcr3 and Avr2, which is a secreted protease inhibitor by *C. fulvum*. In a first step, the autoinhibitory prodomain of Rcr3 is removed by the subtilase P69B. Rcr3 forms a complex with Avr2 and this is recognized by the cell-surface receptor-like protein Cf-2, which results in the initiation of the plant's immune signaling pathway and the development of the hypersensitive response (Paulus et al., 2020). In Arabidopsis, RBOHD is endocytosed to the vacuole for degradation by the PLCP Xylem Cysteine Protease 1 (XCP1) in the absence of an infection. However, upon pathogen recognition, XCP1 is inhibited by Cytokinase 6 (CYS6) to stabilize RBOHD, thereby promoting ROS production (3) (Liu et al., 2024). The release and degradation of immunogenic peptides (4) is a crucial part in plant-microbe interactions. On the one hand, peptides positively affect plant immunity, like plant elicitor peptides (PEPs), which are recognized by PRRs and induce PTI-like responses. PROPEPs are cleaved in Arabidopsis by METACASPASE 4 (MC4) and other type-II metacaspases (MC5 to MC9) for PEP1 release (Hander et al., 2019; Shen et al., 2019). On the other hand, pathogens can use proteases to degrade immunogenic peptides. For example, the extracellular subtilase SBT5.2 of *Nicotiana benthamiana* was shown to release the flg22 epitope but also inactivates flagellin and flg22 immunogenicity by cleaving within the flg22 epitope. Furthermore, SBT5.2 cleaves the immunogenic csp22 epitope of cold-shock proteins (CSPs) of the bacterial pathogen *P. syringae.* This cleavage renders these peptides instable and has a severe impact on the recognition of potential pathogens. This indicates that the subtilase SBT5.2 can be used by potential pathogens to avoid detection and circumvent plant immunity (Buscaill et al., 2024; Chen et al., 2024).

1.3.1 The role of serine proteases in plant immunity

Serine proteases are part of the family of serine hydrolases, which includes next to proteases also lipases, esterases, and transferases. Serine proteases represent a diverse group of enzymes that are classified into various structural categories and perform a range of essential biochemical functions (Kaschani et al., 2009). Some decades ago, serine proteases were thought to be less abundant compared to other protease families in plants. In the last 30 years, however, several serine proteases have been isolated and characterized in various plant species and has now become the largest class of proteases (Antão & Malcata, 2005; Godson & van der Hoorn, 2021). The terms serine proteases and serine peptidases are often used synonymously as they are essentially equivalent in terms of their chemical features. However, they can be distinguished primarily by the size of the peptide chains they utilize as substrates (Antão & Malcata, 2005).

In plants, serine proteases are classified into nine evolutionary distinct clans, which are divided into 14 families and each family in subfamilies. One of the largest clans is the clan SC with the name-giving clan type peptidase serine carboxypeptidase D of the common wheat (*Triticum aestivum*). This serine carboxypeptidase (SCP), as well as all other SCPs, are part of the subfamily S10 in the peptidase database MEROPS. SCP differs from most other serine protease families as these are only active at acidic pH (Godson & van der Hoorn, 2021; Rawlings et al., 2018).

Subtilisin-like proteases (subtilases, SBT) represent another subfamily of serine proteases and can be found in S8A. Members of this subfamily are mainly secreted into the apoplast and fulfill many important regulatory functions (Rawlings et al., 2018). Besides general proteolysis, protein turnover or post-translational modifications, SBTs were reported to be involved in biotic interactions and immune signaling (Schaller et al., 2018). The subtilase P69B of tomato was initially described as P69 and as PR protein (PR-7). As the expression and accumulation were significantly enhanced upon pathogen infection, a role in pathogen defense was assumed (Purwar et al., 2024a). Later, it was found that the initially described P69 consists of six different subtilases (P69A to P69F) that all have a size of about 69 kDa (Jordá et al., 1999; Jordá et al., 2000b; Pablo Tornero et al., 1997). Furthermore, the role of the subtilases P69B and P69C was confirmed as

they are coordinately and systemically activated by pathogen infection and salicylic acid treatment (Jordá et al., 2000a; Jordá & Vera, 2000b). In 2020, the interplay of Rcr3 with the protein inhibitor Avr2 and the PRR Cf-2 was discovered (Paulus et al., 2020). P69C was found to process an extracellular matrix-associated leucine-rich repeat protein (LRP), which was postulated to mediate molecular recognition to initiate immune signaling in tomato (Purwar et al., 2024b). Later, this hypothesis was confirmed through its orthologue AtSBT3.3 Arabidopsis (Ramírez et al., 2016; Pablo Tornero et al., 1996). Also, phytaspases (plant aspartate-specific protease) belong to the group of SBTs and are involved in programmed cell death (PCD). Phytaspases have a strict aspartate specificity of hydrolysis (Chichkova et al., 2010). The involvement of phytaspases in PCD was studied and shown by gain- and loss-of-function studies in *Nicotiana tabacum* (Chichkova et al., 2004, 2010). PCD is induced by the re-transport of proteolytic active phytaspases from the apoplast back to the cytoplasm and involves clathrin-mediated endocytosis (Chichkova et al., 2010; Trusova et al., 2019). SBTs are also involved in the release of signaling peptides and phytocytokines e.g. the SCOOPs (serine-rich endogenous peptide12) in Arabidopsis (Yang et al., 2023). This group of phytocytokines harbors several different peptides. A recent study showed that their expression is induced during stress, especially biotic interaction (Hou, Liu, Huang, et al., 2021). Different SBTs are responsible for the release of different SCOOPs. AtSBT3.5 cleaves PROSCOOP12 at the ‘RRLM’ motif, while PROSCOOP20 can be cleaved by SBT3.6, SBT3.8 and SBT3.9. Interestingly, PROSCOOP20 does not contain an ‘RxLx/RxxL’ motif but is hydrolyzed at the ‘VWD’ motif (Yang et al., 2023).

While numerous examples of SBTs involved in plant regulatory processes, including plant immunity, have been documented, only a limited number of biologically relevant substrates have been identified so far. Moreover, our understanding of the effect of SBTs and more general serine protease on other proteins remains largely unknown (Schaller et al., 2018).

1.3.2 The role of papain-like cysteine proteases in plant immunity

PLCPs are cysteine proteases and are the most abundant proteases in the apoplast besides subtilases. Due to their structural similarities to papain, PLCPs are found in the MEROPS database in the protease subfamily C1A. The subfamily C1A is part of the clan CA, which contains several families of cysteine peptidases (Grosse-Holz et al., 2018; Misas-Villamil et al., 2016; Rawlings et al., 2018; Sueldo et al., 2014). PLCPs are further classified in subfamilies, separated by functional and structural characteristics, also depending on their target peptide. The motif KDEL for localization in the endoplasmic reticulum (ER), is for example one criterium, but also the signal peptide for secretion in the apoplast (Richau et al., 2012). Besides the ER and apoplast, PLCPs can also be found in the vacuole and lysosomes (Grosse-Holz et al., 2018).

Apoplastic PLCPs play crucial roles in the first contact with pathogens like the smut fungus *Ustilago maydis*. Thus, they are often targeted by several effector proteins. For example, the *U. maydis* effector Pit2 is secreted into the apoplast upon penetration and crucial for successful infection. Pit2 mimics a substrate of PLCPs and binds irreversible to the active sites thereby inhibiting PLCPs. A knock-out mutant of UmPit2 in *U. maydis* revealed a significant reduction in virulence compared to the wild-type strain (Misas-Villamil et al., 2016; Misas Villamil et al., 2019). Also, mutualistic microorganisms interfere with PLCP-mediated plant defenses to maintain endophytic colonization. *Epichloë cfestucae* forms mutualistic associations with the cool season grass *Lolium perenne* and inhibits PLCP activity during endophytic interactions. The detailed interactions of this regulation are not fully understood yet, but additional inhibitors secreted by *E. festucae* might be involved (Passarge et al., 2021).

Furthermore, it was shown that the presence of SA influences PLCP activity. An activation of apoplastic PLCPs was detected 24 hours after the SA treatment (Ziemann et al., 2018). The maize genome contains the genetic information for 52 PLCPs (Schulze Hüynck et al., 2019). Of those PLCPs, seven are known to be apoplastic and five were shown to be specifically activated in response to SA, namely, CP1A and CP1B, CP2, XCP and CathB (van der Linde, Hemetsberger, et al., 2012; Ziemann et al., 2018). Until now, the mechanism of how SA activates PLCPs is not known. It might be possible that PLCPs

are activated by previously activated subtilases in maize as reported previously for tomato (Paulus et al., 2020).

1.4 Phytocytokines – release, regulation and signaling in immunity

Phytocytokines are small plant endogenous signaling peptides that have a high sequence diversity and are encoded by various different genes. They play a critical role in regulating of plant development, reproduction, immunity and adaptation to environmental stresses (Hou, Liu, & He, 2021). In the past, phytocytokines were classified as DAMPs, but subsequent research has revealed significant distinctions between phytocytokines and classical DAMPs. DAMPs, e.g. eATP or oligogalacturonides, are primarily released passively e.g. by dying cells or upon damage (Choi & Klessig, 2016; Gust et al., 2017). On the contrary, the release of phytocytokines is strictly regulated and includes proteolytic cleavage of a propeptide and post-translational modifications (Gust et al., 2017; Koenig et al., 2023). Previously, several studies demonstrated that the maturation and release of phytocytokines is promoted as a consequence of pathogen infection or other environmental stressors (Butenko et al., 2003; Hou et al., 2014; Hou, Zhang, & He, 2021; Huffaker et al., 2006). In contrast to phytohormones, which have conserved functions across the plant kingdom, phytocytokines are gene products with a high functional specificity across plant species (Hou, Liu, & He, 2021; Takahashi et al., 2019). For example, Zip1 was only found in *Z. mays* and its ancestor teosinte and is released into the apoplast upon exogenous SA application (Depotter et al., 2022b; Ziemann et al., 2018). In contrast, there are phytocytokines which are conserved among most plant species, like plant elicitor peptides (PEPs) and PAMP-induced secreted peptide 1 (PIP1) and PIP2. These peptides were first identified in Arabidopsis, but later also found in many other mono- and eudicots like maize and soybean (Hou et al., 2014; Huffaker et al., 2006, 2011; Yamaguchi et al., 2011). Phytocytokines can be divided into two main classes depending on whether the propeptide contains a signal peptide or not. To date, the majority of the identified phytocytokines possess a signal peptide and thus, are secreted (Hou, Liu, & He, 2021; Koenig et al., 2023). Examples for this category are PIP1 and PIP2 (Hou et al., 2014), hydroxyproline-rich systemins (HypSys) (Chen et al., 2008), phytosulfokines (PSKs) (Amano et al., 2007), serine-rich endogenous peptide 12

(SCOOP12) (Gully et al., 2019), plant peptide containing sulfated tyrosine 1 (PSY1) (Amano et al., 2007), immune-related peptide (IRP) (Wang et al., 2020) and rapid alkalization factors (RALFs) (Stegmann et al., 2017). Systemin (McGurl et al., 1992), PEPs (Huffaker et al., 2006, 2011; Nakaminami et al., 2018; Yamaguchi et al., 2011) and Zip1 (Ziemann et al., 2018) are examples for phytocytokines that do not harbor a signal peptide.

The processing and release of phytocytokines needs to be strictly regulated as low concentrations can already be recognized by the cell. After transcription, the phytocytokine precursors possessing a signal peptide enter the canonical ER – Golgi secretory pathway. Before biologically active mature phytocytokines are secreted from the secretory pathway into the apoplast, the propeptide needs to be processed to remove the signal peptide and prodomain. Furthermore, post-translational modifications such as tyrosine sulfation, proline hydroxylation, hydroxyproline arabinosylation, and intramolecular disulfide bond formation occur (Hou, Liu, & He, 2021; Olsson et al., 2019). For instance, the signal peptide containing precursor protein PRORALF23 moves to the ER where the prodomain is removed by the ER-localized subtilase SITE-1 PROTEASE (S1P) and subsequently, the mature RALF23 is released (Stegmann et al., 2017). For other signal peptide containing precursor proteins, like IDA, PIP1 and PIP2 or SCOOP12, the cellular compartment in which the cleavage takes place is unknown (Hou, Liu, & He, 2021). Phytocytokine precursors without a signal peptide do not enter the canonical ER-Golgi secretory pathway but are thought to be released into the extracellular compartment either through an unconventional secretory pathway or upon cellular damage (Ding et al., 2012). The essential processing for phytocytokine maturation takes place in the cytosol or the apoplast (Ding et al., 2012; S. Hou, Liu, & He, 2021). For example, PROPEP1, the precursor protein of PEP1, which does not possess a canonical N-terminal signal sequence and is tethered on the cytosolic side of the tonoplasts, is cleaved in Arabidopsis by MC4 and two other type-II metacaspases (MC5 to MC9) for PEP1 release (Hander et al., 2019; Shen et al., 2019).

Similar to DAMPs and MAMPs, mature and biologically active phytocytokines are perceived by plasma membrane-residing PRRs. Many PRRs that have been shown to perceive phytocytokines belong to the group of receptor-like kinases (RLKs) that contain

an extracellular domain, a transmembrane (TM) region, and a cytoplasmic kinase domain (Ngou et al., 2024). These RLKs are often leucine-rich repeat (LRR) receptor kinases (Hou, Liu, & He, 2021; Yamaguchi et al., 2006). The LRR-RLK receptors PEPR1/2, MALE DISCOVERER 1-INTERACTING RECEPTOR-LIKE KINASE 2 (MIK2), RGF1 INSENSITIVE (RGI) and PSKR form heterodimers with the LRR-RLKs BRASSINOSTEROID INSENSITIVE 1 (BRI1)-ASSOCIATED RECEPTOR KINASE 1 (BAK1) and/or SOMATIC EMBRYOGENESIS RECEPTOR-LIKE KINASE (SERK4) upon perception of PEPS, SCOOPs, GOLVENs (GLV) and PSKs, respectively (Fig 1.3). The heterodimer consisting of either PEPR1/2 and BAK1/SERK4 or MIK2 and BAK1/SERK4 induce the phosphorylation of the RLCK *BOTRYTIS*-INDUCED KINASE 1 (BIK1) and subsequently, induce BIK1-depdendent immune responses, whereas GLVs seem to induce BIK1 independent immune responses (Hou et al., 2014; Z. Liu et al., 2013). Similar to MAMPs, the perception of phytocytokines lead to the generation of ROS, influx of calcium ions, activation of the MAPK signaling cascade, activation of TFs and subsequently, transcriptional reprogramming (Fig. 1.3) (Hou, Liu, & He, 2021). Notably, phytocytokines cannot only activate plant immunity but also act as a negative regulator of immune responses. RALF23 perception by FERONIA (FER) suppresses the ligand-induced EFR/FLS2-BAK1 complex formation and consequently, suppresses PTI responses, whereas RALF17 promotes ROS production via FER and acts positively on the complex formation and stabilization (Hou, Liu, & He, 2021; Stegmann et al., 2017).

In general, these findings show that phytocytokines play an important role in the activation and regulation of plant immunity. Although numerous diverse phytocytokines have been identified, their maturation and mechanism of action are poorly understood. Thus, the identification of further phytocytokines as well as their release mechanism needs to be further investigated.

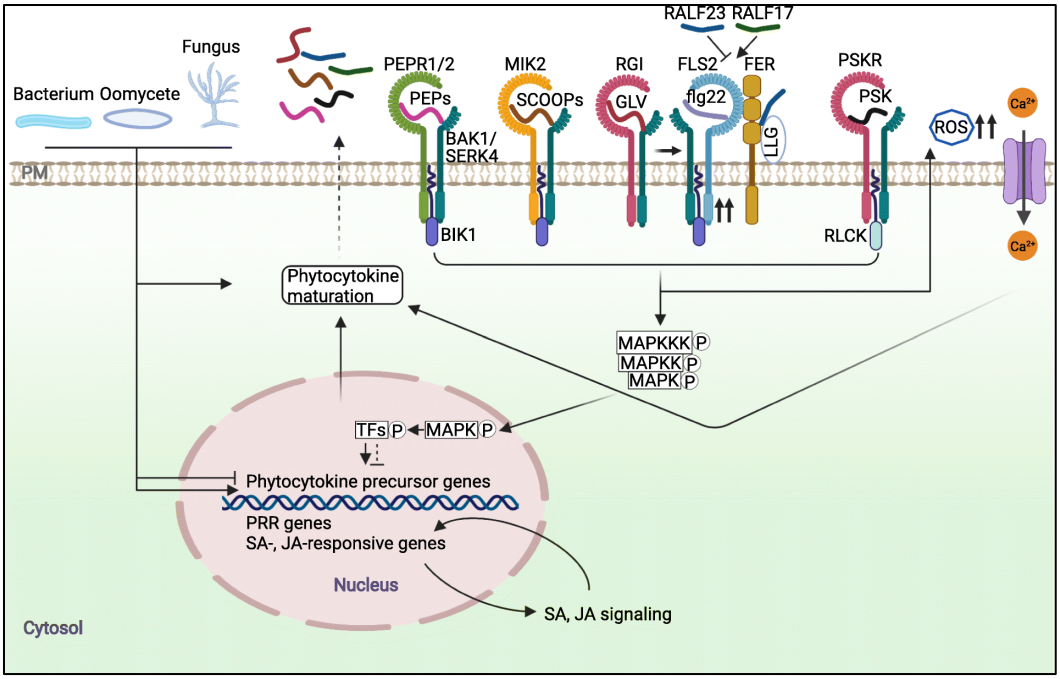

Figure 1.3: Simplified overview of the phytocytokine network upon the perception of pathogen infection. The perception of pathogens induces or inhibits the expression of phytocytokine precursor genes or directly promotes phytocytokine maturation. Once released into the apoplast, phytocytokines are detected by their corresponding receptors and co-receptors. This leads to the generation of ROS, influx of Ca^{2+} ions, which may promote phytocytokine maturation, and the phosphorylation of MAP kinase kinase kinases (MAPKKKs), which is mediated by BIK1 and/or related RLCKs. Upon activated MAPKs, TFs are phosphorylated and induce the up- or down-regulation of phytocytokine precursor gene expression. Additionally, PRR genes and SA- and/or JA-responsive genes are induced which amplifies immunity. Next to direct perception of phytocytokines by PRRs, PRR complex stability may also be influenced by phytocytokines. For instance, the complex formation between FLS2 and RGI, which is induced by flg22, results in increased FLS2 abundance. Furthermore, RALF17 or RALF23 promotes or inhibits the association between FER, FLS2, and BAK1, and regulates PTI therefore positively or negatively, respectively. (Hou, Liu, & He, 2021).

1.5 Aim of this study

In the past it has been shown that SA induces PLCP activity (Ziemann et al., 2018), however, it has not been revealed how PLCPs are activated. A recent study revealed a proteolytic cascade in tomato where the PLCP Rcr3 is activated by the subtilase P69B (Paulus et al., 2020). In maize, research on the activity of subtilases is limited particularly with regard to the activity of subtilases in response to SA. To test whether subtilases are involved in the response to SA and to identify a potential proteolytic cascade in maize, one objective of this study was to monitor the activity of subtilases in a time course within the first 24 hours after SA treatment. If subtilases are activated, the activated subtilases will be identified. Previously, it has been shown that proteolytic activity results in the release of peptides which act as signaling peptides and phytocytokines which play an important role in the plantimmune system (Del Corpo et al., 2024; Hou, Liu, & He, 2021). So far, only a few phytocytokines have been identified in maize. Thus, the second object is to identify novel apoplastic peptides that are released upon SA treatment and might act as phytocytokines.

In conclusion, this study aims to provide a comprehensive understanding of the proteolytic and peptide-based signaling mechanisms activated by SA, contributing to our knowledge of plant defense and stress responses.

2. Results

2.1 SA responsive serine hydrolases

2.1.1 Serine hydrolases are activated three hours upon SA treatment

Several studies have demonstrated a positive effect of SA to protease activity. For example, a higher activity of the subtilases P69 in tomato and PLCPs in maize has been shown (Jordá & Vera, 2000a; Paulus et al., 2020; Ziemann et al., 2018). In maize, the effect of SA on subtilases, particularly in earlier immune responses, has not been investigated yet. To this end, maize leaves were treated with SA and apoplastic fluid (AF) was extracted at 3, 6, 12 and 24 hpi. To monitor the activity of SHs, including subtilases, Activity Based Protein Profiling (ABPP) using the fluorescent probe FP-TAMRA was conducted. Through the covalently and irreversible binding of the probe to the active site of SHs, active SHs can be labeled and separated by size on an SDS-PAGE. To ensure specificity of the signals, AF was pre-incubated prior to labelling with the probe with the SH inhibitors PMSF and DCI to first block the active site and prevent binding of the probe. In general, eight major FP-labeled fluorescent bands (A-H) were detected in all samples independent from treatment and extraction time (Figs. 1A and S1). The bands E, F and G still showed signals in the samples with inhibitors, which indicates either unspecific binding of the probe or that the inhibitors are not able to fully inhibit the whole range of the various hydrolases labelled by the FR-TAMRA probe.

To elucidate whether the activity of SHs was influenced in response to SA, the fluorescent intensity of the individual bands (A-H) was quantified. The quantification of the signal strength of the SA treated SHs in comparison to the control revealed an increase of activity by 20 to 40% at 3hpi (Fig. 2.1B). The signal intensity of SHs within the bands C to H (molecular weight between 55 and 30 kDa) was higher after SA treatment in comparison to the control indicating that the activity has increased. The signal intensities of bands A and B did not show significant differences between the control and SA treatment. After the general increase of SH activity at 3 hpi, at 12 hpi only band G showed a higher intensity and thus, increased SH activity. In contrast, a decrease in signal intensity was observed for band A at 24 hpi. Overall, a wave effect seems to take place in the hydrolase activity after SA treatment. It commenced with a general activation of

SHs, which was followed by a decrease in activity levels below those observed in the control group.

The higher fluorescence intensities at 3 hpi after SA treatment indicates a rapid activation of SHs in response to SA. Which SHs are activated, and the consequences of this activation remain to be elucidated.

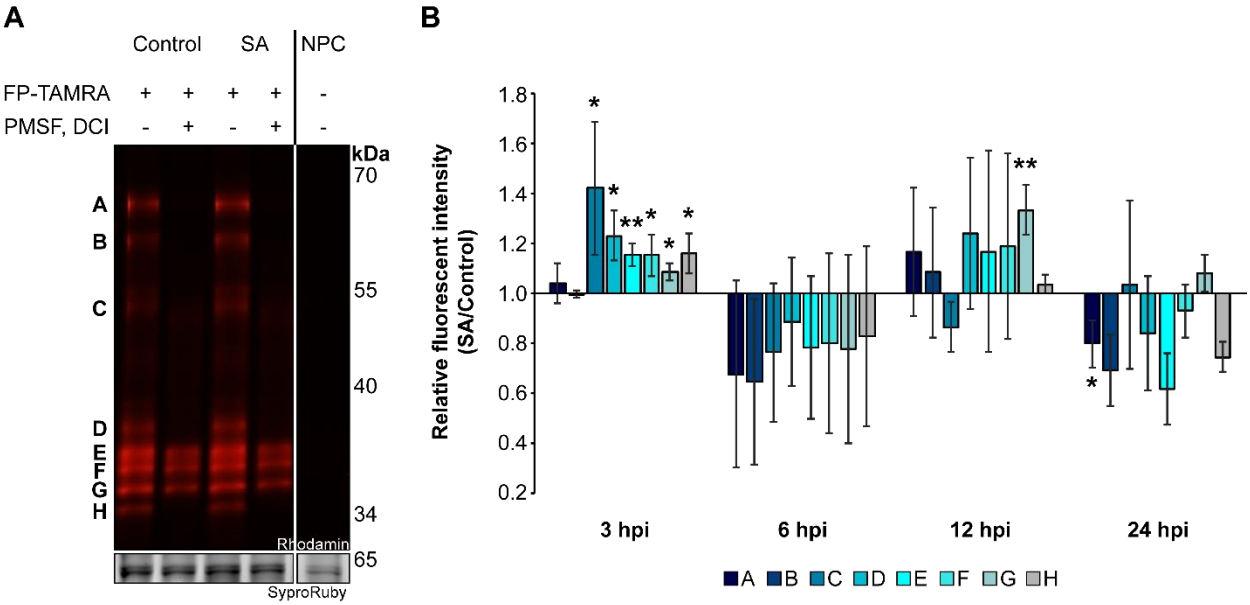

Figure 2.1: Activity-based protein profiling (ABPP) of SH after SA-treatment. Second leaves of 8-days old maize plants were detached and vacuum infiltrated with 2 mM SA and 1% DMSO as control. Apoplastic fluid was extracted at 3, 6, 12 and 24 hpi. Active SHs were labelled using 1 µM FP-TAMRA. Pre-incubation was performed with a mixture of the SH inhibitors PMSF (100µM) and DCI (10 µM) to monitor the specificity of the fluorescent signals. For size separation, samples were run on an SDS-PAGE and analyzed via fluorescence scanning (Rhodamin filter). The no-probe control (NPC) shows potential background signals. The gel is a representative figure from three biological replicates. (A). For quantification analysis, the gels were stained with SyproRuby as a loading control. Gel signals (A to H) were quantified, and values were normalized to the inhibitor pre-incubation as described in Passarge et al., 2022. The activity of the control was set to 1. (B) shows the difference in the fluorescent intensity of the mean with SD of three independent biological replicates between SA treated sample to the regarding control. Significant differences were calculated based on students t-test (* =p<0.05, ** =p<0.01, *** =p<0.001).

2.1.2 Identification of SHs activated by SA

To identify the SHs showing an increased activity three hours upon SA treatment, plants were again treated with 1% DMSO (control) or SA and AF was extracted at 3 hpi. An ABPP was performed using the extracted AF and the FP-Biotin probe followed by a pull-down with neutravidin beads. To identify unspecific binding of proteins to the neutravidin beads, which is not caused by the FP-Biotin probe and therefore not linked to SH activity, AF was incubated without FP-biotin and used as no-probe controls (NPCs). Subsequently, an on-bead digest (OBD) was performed, and samples were analyzed by mass spectrometry. Values with a Log_2 Intensity below 21 were imputated with Perseus 2.0.11, as their abundance were below the detection threshold.

In both treatments, 1% DMSO (control) and SA, 64 proteins were identified by MS analysis. 42 of these were also detected in the NPC and bound independent of the FP-Biotin probe to the beads. Therefore, no conclusion can be drawn regarding their activity. Out of the 22 proteins, which were only found in the samples labeled with the FP-Probe, only three proteins are significantly more abundant upon SA-treatment: The Gibberilin receptor GID1L2 (Zm00001eb038190), the Subtilisin-like protease 7 (SBT7) (Zm00001eb050140) and the Pectin acetylesterase (Zm00001eb071760) (Fig. 2.2).

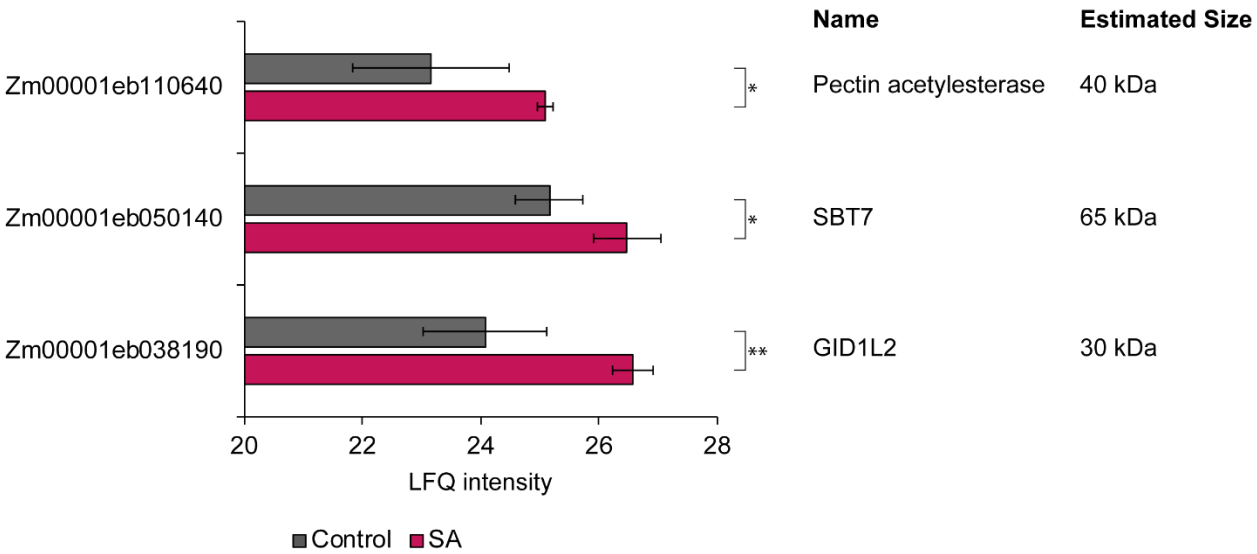

Figure 2.2: Significantly enriched apoplastic serine hydrolases upon SA treatment. AF was extracted from 8-days old plants treated with 2 mM SA or 1% DMSO (control/mock). Three hours upon treatment active serine hydrolases were labeled with FP-Biotin. The pull-down was performed with Pierce™ NeutrAvidin™ Agarose beads. Proteins were identified by MS using on-bead digestion. Results were analyzed und imputated with Perseus 2.0.11. Significant differences were calculated based on students t-test (* =p<0.05, ** =p<0.01) of four biological replicates. Shown are identified serine proteases, which are significantly more active upon SA treatment and found to be present in not more than one replicate of the NPC. The estimated size was calculated by the amino acid sequence without signal peptide and potential inhibitor domain.

In grapevine, studies with the serine protease inhibitor PMSF have shown increased infection rates by the biotrophic oomycete *Plasmopara viticola*, underscoring the pivotal role of PMSF-sensitive serine proteases in defense against biotrophic pathogens (Gindro et al., 2012). Adapting this to the approach to identify SHs that are activated three hours following SA-treatment and to ascertain the sensitivity of PMSF, the ABPP with FP-Biotin, followed by pull-down, OBD, and MS, was conducted once more and extended with PMSF treatments. Besides the 2 mM SA and the control (1% DMSO) treatments, 2 mM SA with 100 µM PMSF and the same amount of 1% DMSO was infiltrated in second leaves of eight days old plants and the AF was extracted at 3 hpi. Following by ABBP, pull-down, OBD and MS as previously described.

In all treatments a total number 873 different proteins were detected. Nearly 98% of these proteins were also found to be present in the NPC indicating unspecific binding of proteins to the beads. Since the abundance of these proteins cannot be linked to a specific binding to the FP-Biotin probe, a conclusion about the activity cannot be drawn. Nevertheless, 19 SHs were identified in the FP-probe sample but not in the NPC, indicating their activity.

The abundance of the previously detected subtilase SBT7 (Zm00001eb050140) did not significantly differ between the SA- and control-treated samples although it shows a tendency of activation after the SA treatment. Besides, three SHs were significantly more abundant in SA-treated samples compared to control-treated samples (Fig. 2.3). Two of the three identified SHs are subtilisin like protases (SBTs), namely SBT1.9 (Zm00001eb082810) and SBT4 (Zm00001eb314120). The significant decrease of abundance of detected SBTs in the presence of PMSF, indicates PMSF sensitivity thus, specific protease activity as the active site seems to be blocked by PMSF. Furthermore, SBT4 is mainly present after SA-treatment, as the abundance in the NPC (except for replicate 3) and control with PMSF was below the detection limit. The third SH is a carboxypeptidase (Zm00001eb229790), which seems not to be affected by PMSF, as the abundance of the peptidase does not alter in the presence of PMSF.

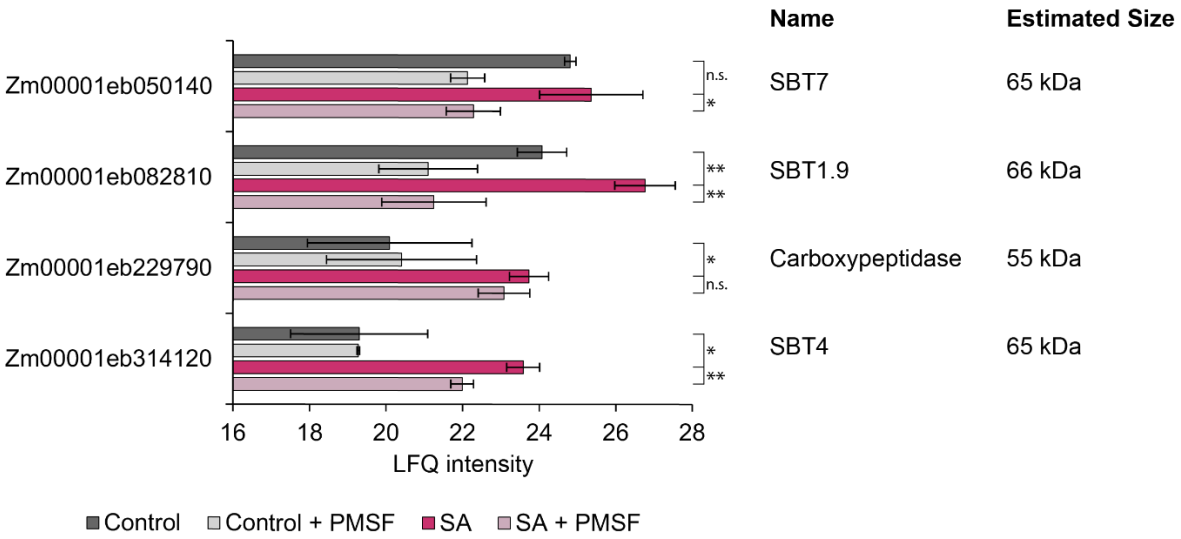

Figure 2.3: Significantly active apoplastic serine proteases upon SA treatment. Second leaves of 8-days old plant, that were treated with 2 mM SA and 2 mM SA with 100 µM PMSF and as control, 1% DMSO and 1% DMSO with 100 µM PMSF. AF was extracted three hours upon treatment and active serine hydrolases were labeled with FP-Biotin. The pull-down was performed with Pierce™ NeutrAvidin™ Agarose beads. Attached proteins were identified by On-bead digestion and a following MS. Results were analyzed und imputated with Perseus 2.0.11. Significant differences were calculated based on students t-test (* =p<0.05, ** =p<0.01, n.s. = not significant) of three biological replicates. Shown are all serine proteases, which are significantly more active upon SA treatment and found to be present in not more than one replicate of the NPC. SBT7 was added, as it was found to be more abundant three hours after SA-treatment in the previous MS. The size was calculated by the amino acid sequence without signal peptide and potential inhibitor domain.

In general, as most proteins were found to be bound to the beads independent to the activity-based probe, the washing during the pull-down was not stringent enough to remove unspecific bound proteins from the beads. Nevertheless, the four identified serine proteases are good candidates for further analysis of their role in SA related responses.
Sequence analysis of ZmSBT7 revealed that the end of the inhibitor domain is in close proximity to the active site (Hou et al., 2023). This suggests that ZmSBT7 might undergo self-cleavage and self-activation, a mechanism that has been observed in other subtilases such as the barley subtilase BAJ93208 and Arabidopsis AtSBT3.3 (Plattner et al., 2014; Ramírez et al., 2013). To explore this hypothesis, ZmSBT7 as well as a potentially catalytic-inactive mutant (ZmSBT7 S540A, where the catalytic Ser residue was substituted with Ala) was overexpressed, in *Nicotiana benthamiana*. A size difference of approximately 10 kDa was observed between the wild-type and mutant proteins in the SDS PAGE (Fig. S1). This reduction in size likely results from autocatalytic cleavage of the inhibitor domain, which is approximately 9 kDa in size (Hou et al., 2023). Additionally, another reduction of size was detected upon treatment with Protein Deglycosylation Mix II, which removes all types of protein glycosylation and thus, suggests that ZmSBT7 is glycosylated (Fig. S2). Subtilases secreted to the apoplast are typically glycosylated, which serves as protection in the harsh apoplastic environment (Figueiredo et al., 2014). The predicted molecular weight of ZmSBT7 including the inhibitor domain and signal peptide is approximately 80 kDa. However, the deglycosylated ZmSBT7 was still larger than its predicted size, suggesting the presence of additional post-translational modifications. Due to the inability to demonstrate enzyme activity, further investigations were not conducted (Fig. S1).

2.1.3 Phylogenetic tree of SBTs and SCPs

To investigate the structure-based relation of the serine peptidases found in the previous MS analysis and for better functional characterization, a phylogenetic tree of SBTs and SCPs was generated. In the MEROPS database the SBTs are associated to the clan of subtilisin (SB), as the catalytic residues within the sequence are in the following order: Asp, His, Ser. SCPs contain the catalytic residues in the order Ser, Asp, His in their sequence and form therefore another clan (Rawlings et al., 2018). Sequence alignments

of SBTs and SCPs present in the MEROPS database compared with the MaizeGDB database revealed 84 serine proteases, which are associated to the two clans where a specific ZmID (*Zea mays* identification number) can be associated. The SBTs are found in the family S8 (subtilisin family) of the clan SB, whereas the SCPs are associated to the families S9 (prolyl oligopeptidase family), S10 (SCPs) and S28 (Exopeptidases) of the SCP clan. The sequences were aligned using the package Biopython and the programs MAFFT (multiple alignment using fast Fourier transform) and RAxML (Randomized Axelerated Maximum Likelihood) (Cock et al., 2009; Rozewicki et al., 2019; Stamatakis, 2014). Additionally, an analysis by the online tool TargetP was used to predict a signal peptide which would indicate secretion into the apoplast. The tree was calculated with MEGAX and visualization was performed with the online tool iTOL (Kumar et al., 2018; Letunic & Bork, 2024).

The phylogenetic tree splits into two groups which consist mainly of the two families S10 of SCPs and S8, the subtilisin family. Surprisingly, some members of the families S9 and S28 are associated with the S8 family. Two peptidases of the S9 family and two of the S28 family show more sequence similarities to the subtilisin family S8 of a different clan than to the S10 family of the same clan. About half of all peptidases (49%) is predicted to be secreted to the apoplast (Fig. 2.4, marked with orange dot). Only one SCP (Zm00001eb420820) is predicted to translocate into chloroplasts and two to the mitochondria (Zm00001eb014640(S9), Zm00001eb249900 (S8)) (Fig. 2.4, marked with blue or green dot, respectively). Interestingly, the two peptidases predicted to be located to mitochondria are part of different clans, but show high sequence similarity, as they cluster next to each other.

The three SBTs, which were found to be significantly more active upon SA treatment in the previous MS analysis (Zm00001eb050140 (SBT7), Zm00001eb082810 (SBT1.9) and Zm00001eb314120 (SBT4)), can be found in a S8 clade consisting of 13 peptidases (Fig. 2.4; light gray; identified proteases are marked with a violet dot). Except for one member (Zm00001eb076400), all proteases of this clade are predicted to possess a signal peptide that enables the secretion into the apoplast. The structural similarity and secretion in the apoplast indicate a close relationship between the SBTs, suggesting that they may be involved in similar responses.

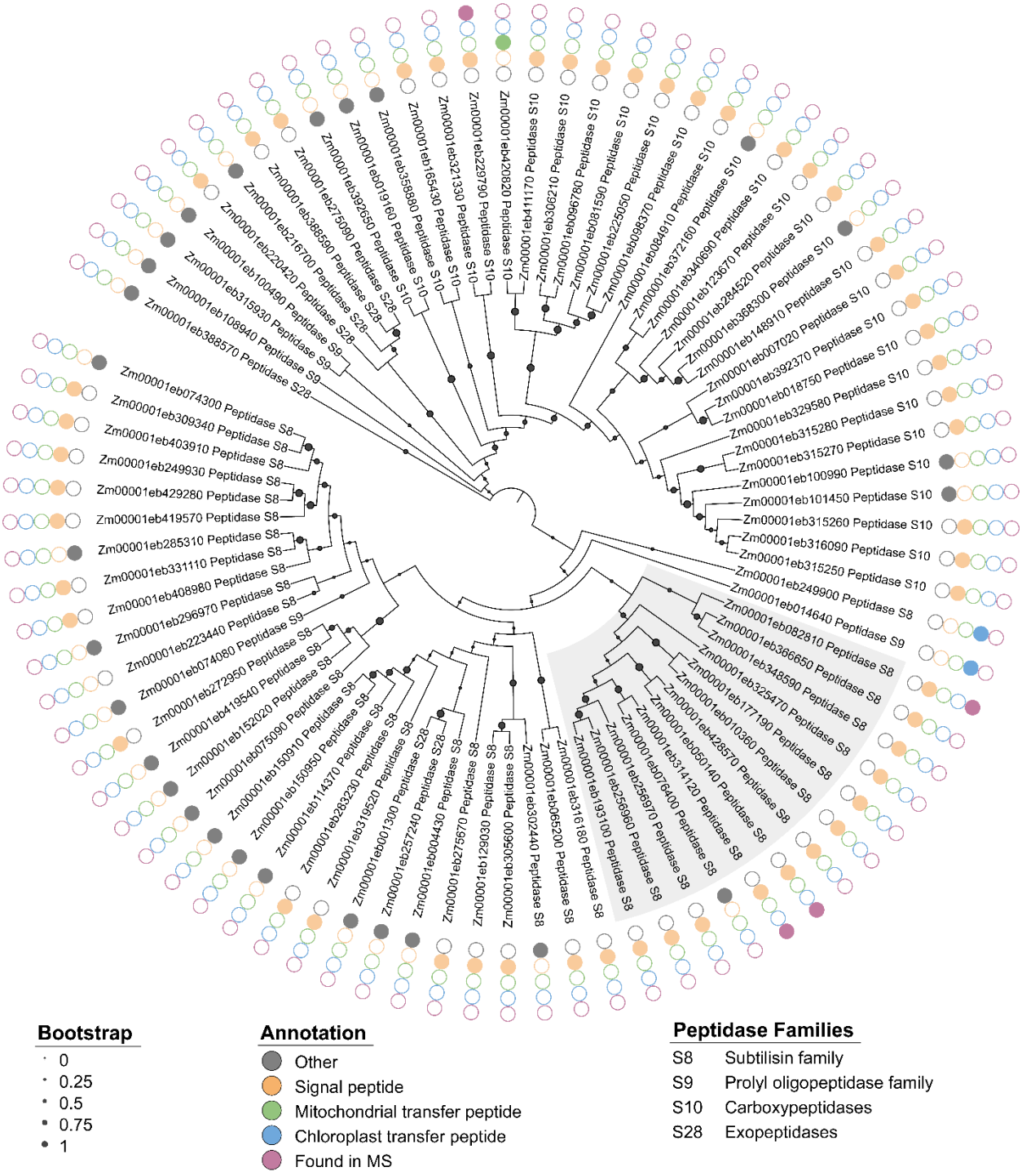

Figure 2.4: Phylogenetic tree of SBTs and SCPs in *Zea mays*. 84 serine peptidases were found to be associated to the clans of subtilisin with the family S8 and SCPs with the families S9, S10 and S28 by combining information of the MEROPS database and MaizeGDB. The sequences of these peptidases were aligned using the package Biopython and the programs MAFFT (multiple alignment using fast Fourier transform) and RAxML (Randomized Axelerated Maximum Likelihood). Phylogenic relation was calculated based on these sequence alignments with maximum likelihood by MEGA-X. As substitution model Jones-Taylor-Thornton (JTT) model with uniform rates was used. Visualization was done with iTOL and annotation information were received from TargetP. In purple serine proteases are marked, which were found in the previous MS analysis.

2.2 Identification of Phytocytokines involved in SA signaling

2.2.1 Apoplastic peptide fraction from SA-treated plants induce *PR*-gene expression

Previous studies have shown that the apoplastic peptide fraction (APF) extracted 24 hours after SA treatment contains peptides that are smaller than 10 kDa and are able to induce *PR*-genes, which are commonly used as marker for SA signaling (Cao et al., 1994; van der Linde, Hemetsberger, et al., 2012; Ziemann et al., 2018). In order to test the hypothesis that signalling peptides are generated shortly after SA treatment in the apoplast, an extraction of AF was performed from plants that had been treated with either SA or a control solution (1% DMSO) at 3, 6, 12 and 24 hpi. Subsequently, the AF was filtered through a concentration column with a cutoff of 10 kDa. The flow-through was employed as APF, comprising of peptides below 10 kDa. Afterwards, the APF was re-infiltrated into 8-day old plants, and *PR*-gene expression was analyzed at 24 hpi via qRT-PCR. To confirm the efficacy of the initial SA treatment, *PR*-gene expression of treated leaves was assessed at 24 hpi. Additionally, the expression of *CC9* was analysed to exclude the potential involvement of JA and/or wounding (Fig. 2.5) (van der Linde, Mueller, et al., 2012).

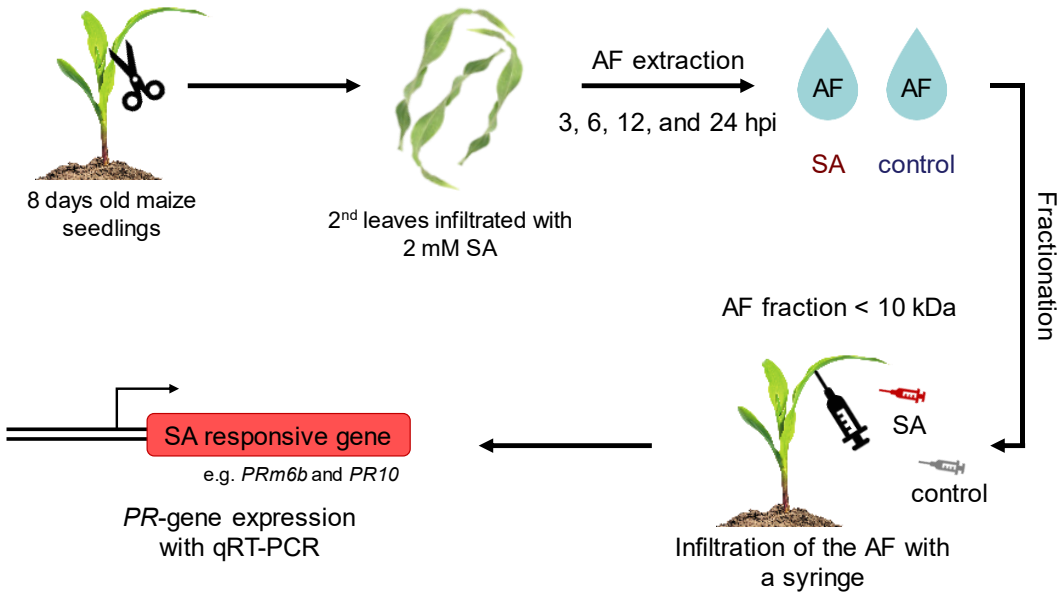

Figure 2.5: Experimental procedure of testing APF for SA responsive *PR*-genes. Second leaves from 8-day old maize plants were vacuum infiltrated with 2 mM SA in 1% DMSO or with 1% DMSO (Control) and AF was extracted at 3, 6,12 and 24 hpi. The AF was filtered with a Vivaspin 10 kDa filter and the flow-through was reinfiltrated with a syringe into second leaves of 8-day old plants. Expression of *PR*-genes and *CC9* was determined 24 hours after SA infiltration.

Expression analysis via qRT-PCR of the *PR*-genes *PR3*, *PR5*, *PRm6b* and *PR10* from plants infiltrated with SA or the control solution at 24 hpi revealed that the expression of all tested *PR*-genes was induced in SA-treated leaves compared to control treated leaves, while *CC9* was not induced, indicating no wounding responses were activated during the treatments (Fig. 2.5A).

Re-infiltration of leaves with APF extracted from plants three hours after treated with SA lead to a significant induction of *PR3*, *PR5* and *PRm6b* expression in comparison to plants that were infiltrated with APF extracted from control treated plants (Fig. 2.5B). Only *PR10* was not significantly induced (Fig. 2.5B). The expression of the tested *PR*-genes did not change upon treatment with APF harvested at 6 hpi, while only the expression of *PR10* or *Prm6b* was significantly induced upon treatment with APF extracted from 12 or 24 hpi, respectively, compared to plants that were infiltrated with APF extracted from control treated plants (Fig. 2.5B). Expression of the JA marker *CC9* was not induced upon APF extracted at any time point excluding that wounding or JA induced the expression of the tested genes.

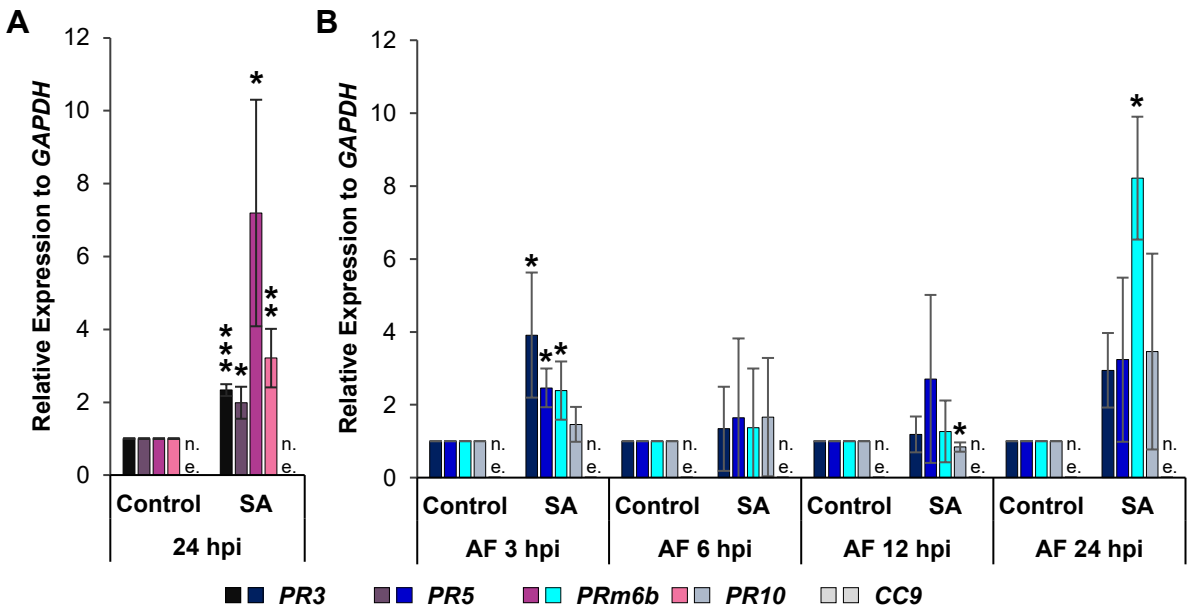

Figure 2.6: Re-infiltration of APF extracted three hours upon SA treatment induces *PR*-gene expression. Second leaves from 8-day old maize plants were vacuum infiltrated with 2 mM SA in 1% DMSO or with 1% DMSO (Control) and AF was extracted at 3, 6,12 and 24 hpi. The AF was filtered with a 10 kDa cut-off column and the flow-through was reinfiltrated into second leaves of 8-day old native plants using a syringe without needle. Expression of *PR*-genes and *CC9* was determined 24 hours after SA (A) or APF fraction re-infiltration (B). *CC9* was not expressed (n.e.). The expression was set relative to GAPDH and the corresponding control. Significant differences were calculated based on students t-test (* =p<0.05, ** =p<0.01, *** =p<0.001).

2.2.2 Peptides within the APF induce *PR*-gene expression

Besides peptides, the APF could contain RNA or DNA which might have been released by damage during the treatment. The released RNA or DNA could be recognized by the plant as DAMP and induce *PR*-gene expression. To test whether the induced *PR*-gene expression is the result of transferred RNA, DNA or peptides, the APF extracted from leaves three hours after SA treatment was incubated either with trypsin, RNase, or DNase to cleave potential peptides, RNA or DNA, respectively. To remove the added enzymes (trypsin, RNase and DNase), the APF was filtered again with a 10 kDa filter (Fig. S3). To demonstrate that the signaling capacity of the APF is not influenced by the incubation, the APF of the control and SA treated leaves without any enzyme were the same. Afterwards, the treated APF was re-infiltrated into leaves of 8-days old maize plants and the expression of *PRm6b* was analyzed using qRT-PCR (Fig. 2.5A). The SA treated APF, which was not treated with an enzyme, still induces the expression of *PRm6b*, whereas the control APF did not. Thus, the signal transduction through the APF was still present.

RNase and DNase treatments of either the APF from SA treated or control treated plants did not alter the effect of the APF (Fig. 2.7A). In contrast, trypsin treatments destroys the signaling capacity of the APF extracted upon SA treatment (Fig. 2.7 A). Thus, trypsin was the only tested enzyme altering the effect of the APF significantly on *PRm6b* expression suggesting that the APF contains peptides which have signaling capacity. Notably, the expression of *Prm6b* was slightly increased in response to APF treated with trypsin and RNase compared to untreated APF (Fig. 2.7). Gel analysis revealed that small amounts of RNase and trypsin still remain in the APF upon filtering (Figure S2). It might be possible that maize plants are able to perceive the presence of those enzymes leading to the induction of PRm6b.

The phytocytokine Zip1 was shown to be involved in the SA response in the crop plant maize. Upon SA-infiltration, Zip1 is released from PROZIP1 and induces the expression of *PR*-genes (Koenig et al., 2023; Ziemann et al., 2018). The maize inbred line Ky21 does not contain PROZIP1 and thus, Zip1 is not present in Ky21 APF (Depotter et al., 2022a; Koenig et al., 2024). To exclude that Zip1 is present in the APF extracted at 3 h upon SA treatment from B73 and causes the observed *PR*-gene induction, Ky21 was treated with SA and at 3 hpi APF was extracted. The extracted APF was re-infiltrated into leaves of native B73 plants and *PR*-gene expression was analyzed. Besides this, *PR*-gene expression of Ky21 upon SA-treatment was analyzed using qRT-PCR. The SA-treatment in Ky21 induced the expression of *PR5* and *PRm6b* (Fig. 2.7, SA treatment). Additionally, the re-infiltration of APF extracted three hours after the SA-treatment from Ky21 induce *PR5* and *PRm6b* expression in B73 leaves (Fig. 2.7B), which demonstrates that other peptides than Zip1 must be present in the APF which induce *PR*-gene expression.

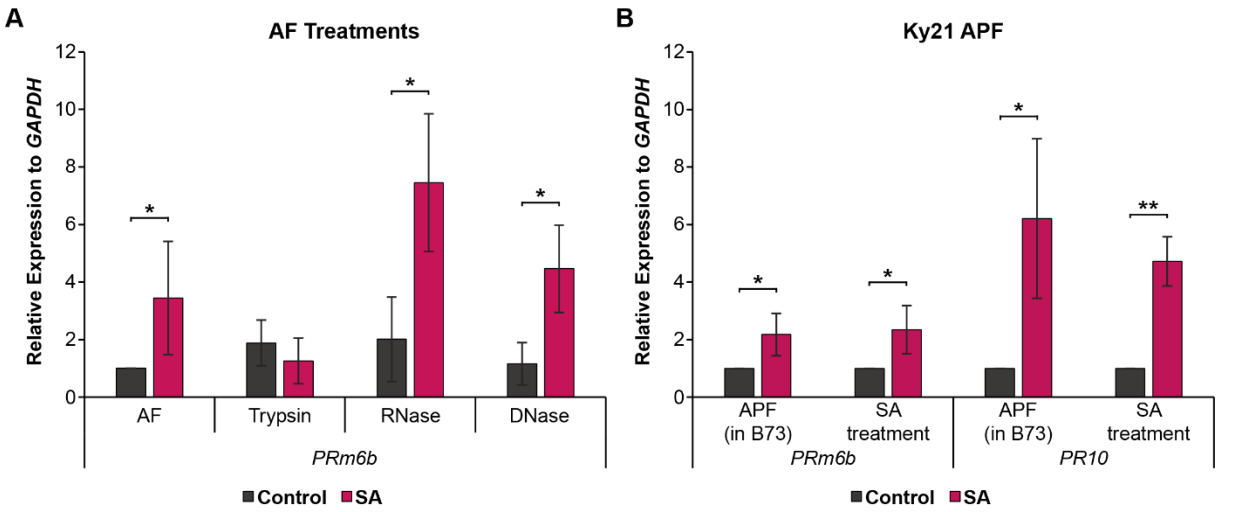

Figure 2.7: *PR*-gene expression is induced by re-infiltrated peptides and is independent of Zip1. Maize leaves (line B73 (A) and Ky21 *(B)*) were infiltrated with 2 mM SA in 1% DMSO or with 1% DMSO (Control) via vacuum infiltration. AF was extracted at 3 hpi and filtered with a 10 kDa filter. The flow through containing peptides smaller 10 kDa was incubated with Trypsin, RNase and DNase, respectively, for one hour. Afterwards the AF was filtered again to remove the Trypsin, RNase and DNase and reinfiltrated into native B73 plants by syringe (A). The APF of Ky21 was reinfiltrated into native B73 plants by syringe (B). *PR*-gene expression was determined via qRT-PCR 24 hours after SA or AF re-infiltration. The expression was set relative to *GAPDH* and the corresponding control. Significant differences were calculated based on students t-test (* =p<0.05, ** =p<0.01, *** =p<0.001).

2.2.3 The APF peptidome changes in response to SA

In order to identify the peptides that induce *PR*-gene expression, a mass spectrometry analysis of the APF was conducted. Therefore, the preceding treatments and preparation of the APF were repeated. Following the confirmation of the induction of *PR*-gene expression by the SA treatment, the APF was examined by MS analysis. Samples were loaded and washed on C18-stage tips followed by elution of the peptides. Samples were directly analyzed by MS without a prior digest.

A Principal Component Analysis (PCA) was prepared to identify groupings or clusters in the data and visualize the distribution and variability of the peptides in the APF. The PCA plot shows that the peptide composition of the APF is markedly altered in response to SA (Fig. 2.8). In total, the peptidomics analysis revealed 4876 peptides in the APF after both treatments. Most peptides (about 92%) are not significantly influenced and are equally present in both treatments. Following SA treatment, 200 peptides were significantly enriched, with 189 peptides deemed unique in comparison to the control. 185 peptides were found to be significantly more abundant in the APF of the control group, while 178

of these were exclusively present in the control. The abundance of these peptides may be negatively influenced by the SA treatment. The peptides being more abundant or only identified in the APF upon SA-treatment might include promising phytocytokine candidates (PC), which could transduce the SA response. The stability of peptides and their presence over time may affect the immune responses potentially elicited by these peptides.

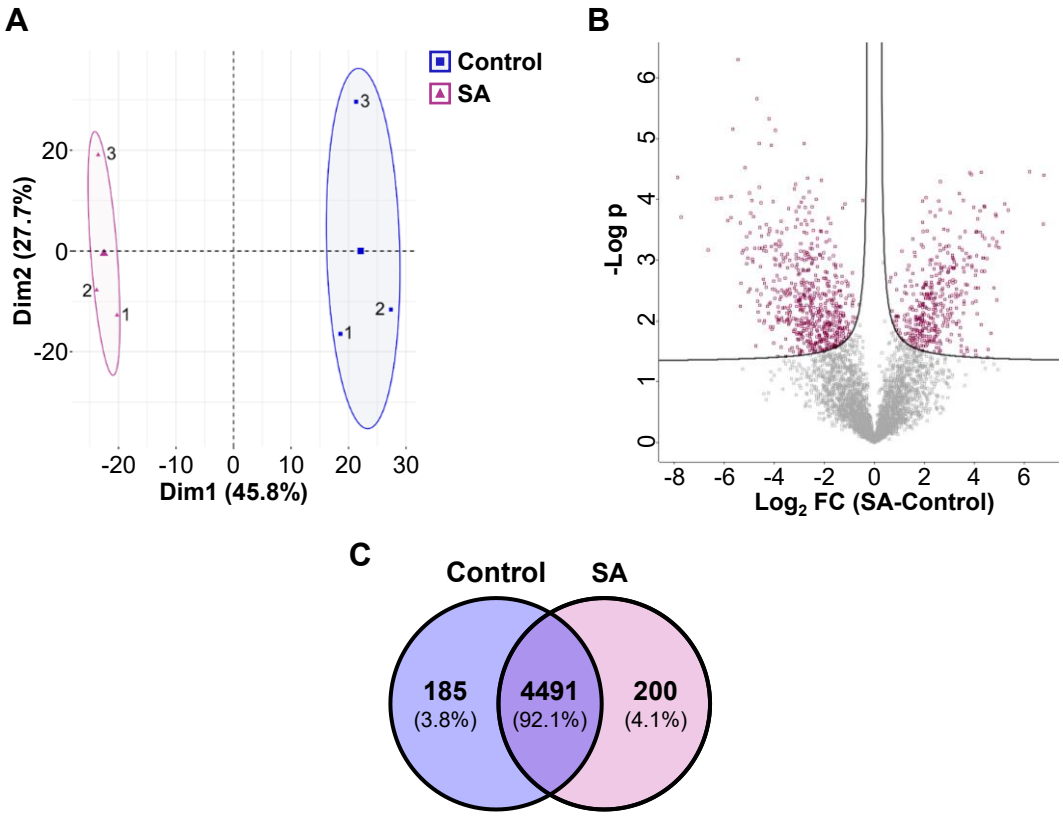

Figure 2.8: SA treatment alters peptide abundance at 3 hpi. Second leaves from 8-day old maize plants were infiltrated with 2 mM SA in 1% DMSO or with 1% DMSO (Control) via vacuum infiltration and AF was extracted at 3 hpi. The AF was filtered with a 10 kDa filter and the flow-through was used for peptidome MS analysis. (A) PCA plot of the SA/control depicting the distribution of proteomic samples. Raw values were used for the calculation of the contributions of the PCs. (B) Volcano plot of proteomic samples illustrating the distribution of the peptides within the treatments. Purple squares indicate significant differences in either direction (p-value <0.05, FDR <0.05). (C) Venn-diagram of identified peptides, visualizing the number of peptides, which are found to be significant upon the SA-treatment, in the control APF or the abundance di not differ between the treatment.

To investigate the peptide composition and stability over time, AF was extracted at 6, 9 and 12 hpi from leaves infiltrated with SA or control solution and filtered through a 10 kDa cut-off column. Subsequently, the peptidome of the APF was analyzed via MS. The PCA of the APF from SA or control treated plants at different time points depicts the distribution and change in the peptidome profile. While the peptidome of control treated leaves only showed minimal variation over time, the peptidome from APF from SA treated plants showed a discernible change in the samples over time (Fig. 2.9A). At 6 hpi 6487 peptides were identified of which 1837 (28%) were significantly enriched in response to the SA-treatment (Fig. 2.9B). Three hours later, at 9 hpi, 6668 peptides were found of which 2337 (35%) were enriched in response to SA. At 12 hpi, a total of 6741 peptides were identified of which 2481 (37%) were significantly enriched in the SA treatment. Only 10% (440 peptides) of all significant enriched peptides upon SA-treatment were identified to persist at all analyzed time points (Fig. 2.9B). At 6 hpi 610 peptides (14%) are significantly enriched, which are only found at 6 hpi. At 9 hpi 855 peptides (19%) were identified to be unique for 9 hpi and at 12 hpi the most peptides, were found to be unique (1186 peptides, 27%). At 6 and 9 hpi 488 peptides (11%) are shared between the two time points and may persist in the apoplast, or peak in between these measuring points. 555 peptides (13%) were already present at 9 hpi upon SA-treatment but were also detected at 12 hpi. 300 peptiedes (7%) were detected and significantly more abundant upon SA-treatment at 6 and 12 hpi but absent at 9 hpi (Fig. 2.9B). To compare the results of the SA-treatment peptidomics analysis over time, taking all analyzed time points into consideration, the change in peptide abundance was visualized with each line representing one peptide (Fig. 2.9C). Therefore, only peptides were considered, which were significantly more abundant upon SA treatment at 3 hpi and detected in all four time points in at least three replicates each. About two thirds of the peptides stay more abundant over all four tested time points although their abundance slightly differs over time. A group of about 15 peptides was more abundant in the first MS at 3 hpi upon SA-treatment compared to the control, but was found to be less abundant in the following time points (6, 9 and 12 hpi) of the second MS. This analysis helps to identify and further characterize potential PCs.

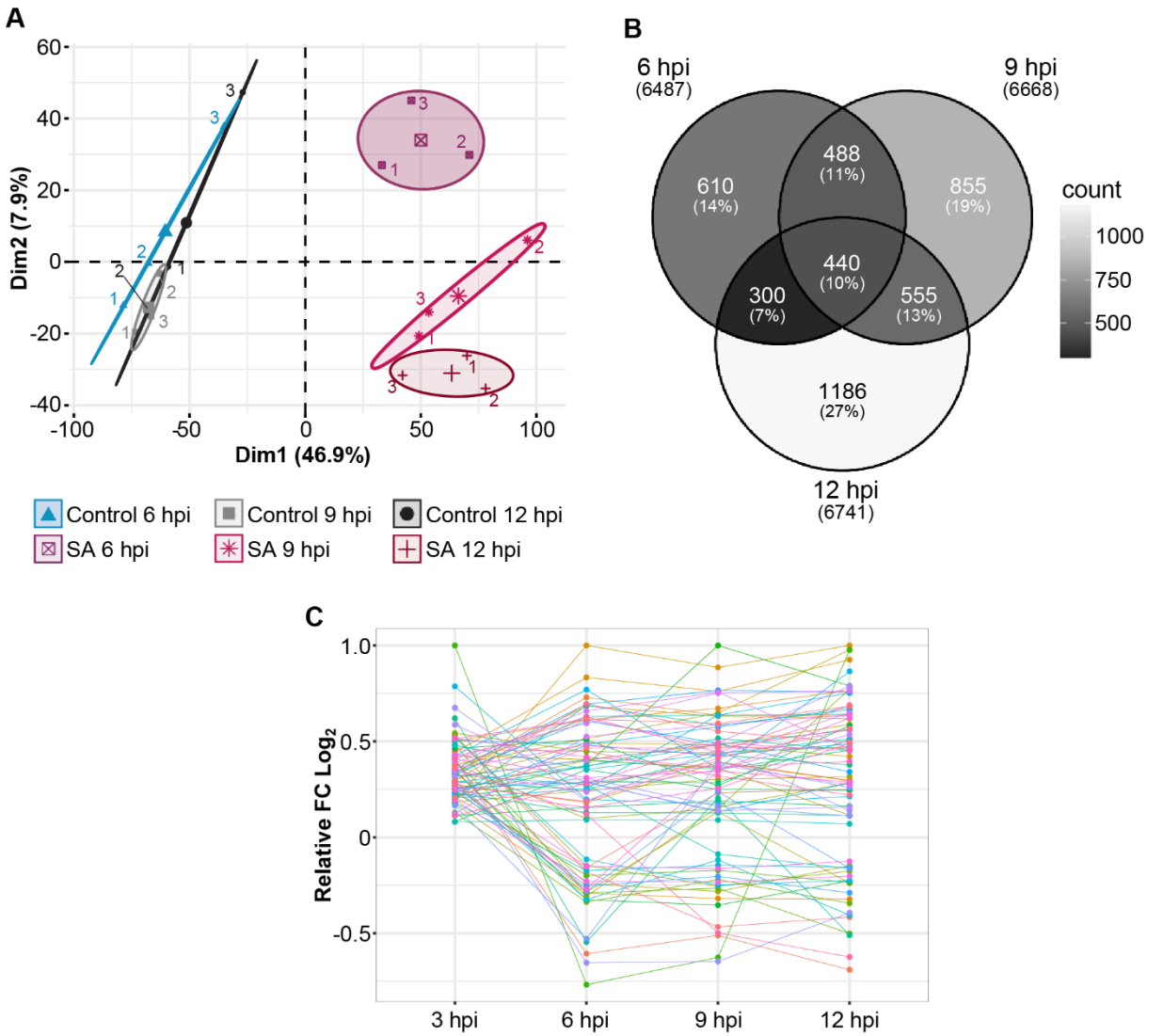

Figure 2.9: Peptide abundance over time after SA treatment. Peptides found via MS analysis in the APF of SA- or control treated maize plants at 6, 9 and 12 hpi. (A) PCA plot of the SA/control depicting the distribution and change of the peptidome over time. (B) Venn diagram of peptides found to be significant after SA treatment at the corresponding time point. For significance students t-test with a permutation-based FDR calculation was performed. The total number of detected peptides for each time point is indicated below each time point (C) Change of abundance of selected peptides over time. Visualized is the relative FC Log_2 of the peptides relative to the highest value. Selected were all peptides, which were significantly more abundant at 3 hpi after SA treatment. Significant differences were calculated based on students t-test.

A list of several hundred phytocytokine candidates was obtained from the peptidome analysis. To reduce the number of candidates, the following criteria were employed: The selected peptides must be present in at least three of the four replicates following SA treatment and should be significantly more abundant upon treatment with SA than with control. Moreover, the peptides should be distinctive, allowing for their association to a

single razor protein. As several peptides are released upon protein degradation, with no specific manner for the single peptide, the selected peptides should be the only peptide found from a specific protein suggesting a specific peptide release. Additionally, the length of the peptide should not extend 25 amino acids. Peptides that are part of universal regions of proteins, like signal peptides, were excluded. After these criteria have been applied, 14 phytocytokine candidates, namely PC1 to PC14, were selected for further analysis (Table 2.1).

PC1 to PC9 and PC14 were exclusively found in at least three replicates upon SA treatment and were absent in the control sample. The first nine PCs (PC1 to PC9) were selected primarily as they had the highest abundance in the first MS of the APF at 3 hpi, while also matching all other criteria mentioned. PC10 and PC13 were selected as their proproteins were already related to stress in previous studies. The proprotein of PC10 is a survival protein SurE-like phosphatase/nucleotidase (Zm00001eb361250). This metal ion-dependent phosphatase is distributed among eubacteria, archaea, and eukaryotes, but apart from activities as nucleotidase and exopolyphosphatase in *E. coli,* there is no detailed information on the biological role of this protein (Iwasaki & Miki, 2007). In the Uniprot database the protein in maize is inferred from homology. The proprotein of PC13 is the stress associated protein homolog 7 (SAP7) and consists of two zinc-finger domains (ZNF), AN1 and A20. In plants the role of SAPs is poorly understood, but it is shown that in several plant species SAPs are involved in many stress responses including biotic stress (Kang et al., 2017). In mammals, it is known that the two ZNF domains need to dissociate for function. The AN1 domain facilitates a functional interaction with the tumor necrosis factor receptor-associated factor 2, while the A20 domain plays a crucial role in regulating the activation of the nuclear factor kappaB (Chang et al., 2011). PC13 constitutes a component of the linker chain that connects the two domains and the release of PC13 would consequently result in the dissociation of the domains. The proproteins of PC11 and PC12 are yet totally unknown. PC14 was found to be continuously present in the APF up to 12 hpi only after SA treatment. With respect to the sequence of the peptide, PC14 was named SIGGI. The Proprotein of SIGGI is mostly known from mammals as Macrophage migration Inhibitory Factor (MIF) where it acts as a proinflammatory cytokine with tautomerase activity (Sumaiya et al., 2022). Structural comparisons of human MIF

with the orthologous MIF/D-DT-like (MDL) proteins of Arabidopsis revealed a high three-dimensional similarity. The available experimental evidence suggests that the tautomerase activity of MDLs is significantly diminished in comparison to that of human MIF (Spiller et al., 2023). The first isoleucine in the SIGGI peptide is part of the catalytic site of the potential tautomerase activity.

Table 2.1: Selected peptides from MS analysis of APF. Peptides were selected fulfilling all selected criteria, namely abundance in at least three replicates, significance after SA treatment, unique peptides, smaller than 25 amino acids, being not part of signal peptides or other specific domains. The selected peptides are numbered and named phytocytokine candidate 1 (PC1) to PC14.

PC#	Sequence	Length [AA]	Leading razor protein	Information (Pfam ID, GO Terms, etc.)
1	FDGEKPEPA	9	Zm00001eb250790	chloroplast thylakoid membrane - Protein binding
2	VTVAESKPRREF	12	Zm00001eb328390	RNA recognition motif (PF00076)
3	EAGGEKKHHF	10	Zm00001eb407710	aasr1 - abscisic acid stress ripening1
4	AYKVTIEHGGESRVV	15	Zm00001eb052650	2Fe-2S iron-sulfur cluster binding domain (PF001111)
5	AAAGAGRHPHDVQ	13	Zm00001eb335590	PB1 domain (PF00564) - protein binding
6	SLHSQGEQEKKEDTS	15	Zm00001eb010400	Ubiquitin interaction motif (PF02809) - proteasome complex
7	TVDVDANGRKGK	12	Zm00001eb171230	Photosystem II 10 kDa polypeptide PsbR (PF04725)
8	VDSESKKKQDASIPRVG	17	Zm00001eb056930	Aluminium induced protein (PF12481)
9	APAPSTGVPKKA	12	Zm00001eb160340	Ribosomal protein L19e (PF01280) - RNA binding
10	QLGKDASAAGAA	12	Zm00001eb361250	Survival protein SurE (PF01975) - peptide in exposed helix
11	STKSKELSGHDIFADHEDPKPN	22	Zm00001eb392390	Protein of unknown function (DUF4057)
12	DAPAAAPAPEEAESKAEEKADKEVS	25	Zm00001eb136750	Protein of unknown function (DUF538)
13	IDSIVNGGDGGKGPVIA	17	Zm00001eb236360	A20 and AN1 domain-containing SAP 7
14/ SIGGI	VSIGGIGPGVN	11	Zm00001eb226780	Macrophage Migration Inhibitory Factor 1

2.2.4 Active SHs may release potential phytocytokines

The previously conducted peptidomics analysis of this study demonstrated that SA-treatments result in alterations in peptide abundance and the appearance of new peptides at 3 hpi. Furthermore, a higher SH activity was observed at the same time point, which may lead to the release of peptides. To investigate if peptide release requires subtilase activity, the peptide abundance was investigated in response to SA was co-infiltrated with the SH inhibitor PMSF. Therefore, the second leaves of 8-day old maize plants were infiltrated with either SA or a control solution with or without PMSF. After 3 hpi, AF was extracted and filtrated through a 10 kDa cut-off column filter to obtain the APF which was subsequently analyzed by MS. In total, nearly 6,000 peptides were detected in all four treatments. In the APF of plants treated with the control solution, 2093 peptides were detected in at least three replicates. With the addition of PMSF this number increases by approximately 3% to 2186 peptides. There is no alteration in the abundance of peptides caused by the addition of PMSF, as the cluster of control and control with PMSF overlapped in the PCA (Fig. 2.10 A). The APF extracted from plants that were treated with SA harbors more peptides than the control, in total 3643. The addition of PMSF to the SA treatment resulted in an equivalent increase in the number of peptides (about 3 %) as observed in the control group. Nevertheless, the addition of PMSF to the SA-treatment appeared to exert a more pronounced influence on the individual peptides than in the control and control with PMSF as the treatments of SA and SA with PMSF differ significantly. A comparison of the identified peptides upon treatment with SA and SA with PMSF revealed that approximately 25% of the detected peptides were unique to each treatment.

From the selected phytocytokine candidates, three were significantly more abundant upon SA treatment, namely PC1, PC7 and SIGGI (PC14), confirming previous results. The peptides PC3 to PC10 were also found in this peptidomics analysis, but not significantly enriched upon SA treatment. PC2, PC11, PC12 and PC13 were not found in this experiment. One explanation could be that the accumulation is not only SA dependent or that the peptide release in the apoplast happened this time earlier or later than 3 hpi. The peptide SIGGI was exclusively present upon SA treatment and absent upon co-infiltration of SA and PMSF indicating that SIGGI might be released from its proprotein

(MIF, Zm00001eb226780) through the activity of serine hydrolases. To further show that subtilases are involved in the direct cleavage of the proprotein MIF, recombinantly produced MIF linked to His (MIF-His) was incubated with either AF extracted from leaves treated with SA for 3 h or AF extracted from leaves treated with SA for 3h and PMSF. Incubation of the AF from SA treated plants with MIF-His revealed processing of MIF, while the addition of PMSF inhibited this processing (Fig. S4). This result demonstrates that MIF-His is cleaved by PMSF-sensitive apoplastic serine proteases. The question whether the SIGGI peptide is released by the observed cleavage and the identity of the serine proteases responsible must be addressed in future experiments.

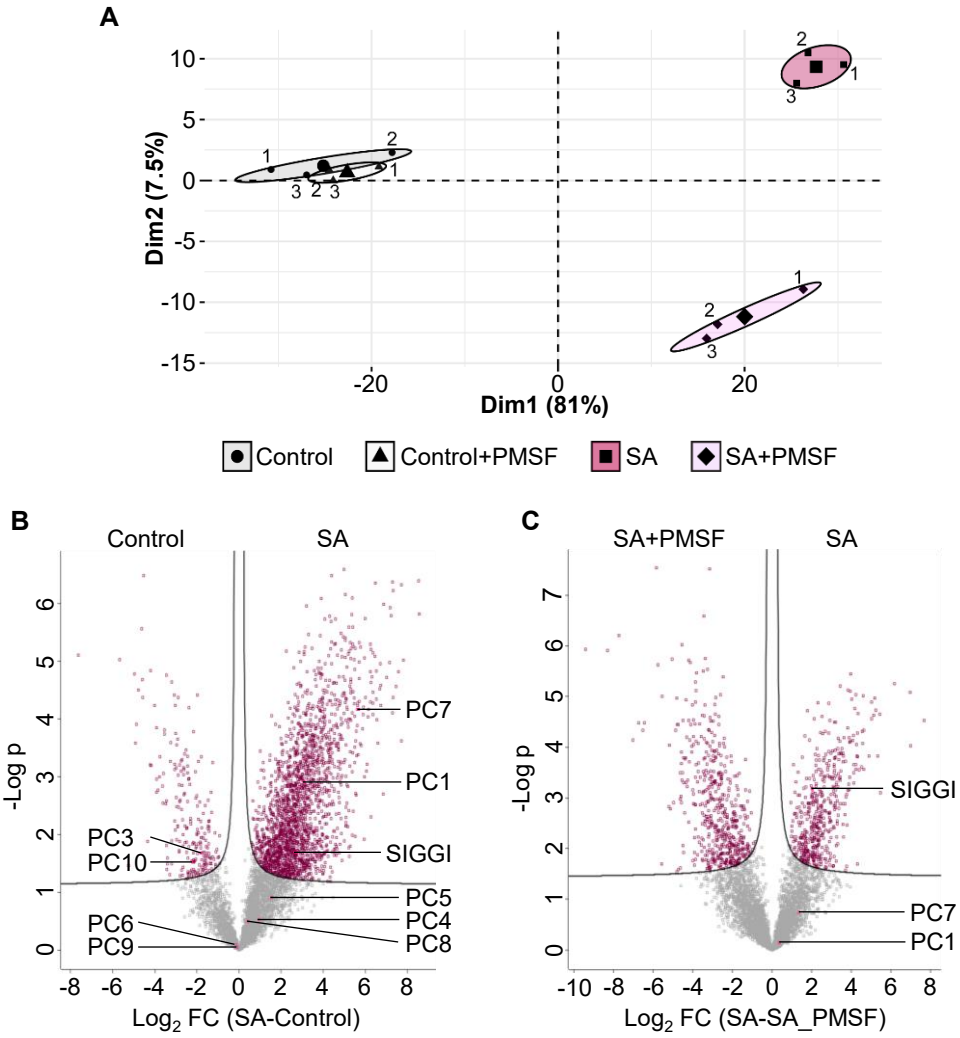

Figure 2.10: Peptidome analysis of APF three hours upon SA and PMSF treatments. Second leaves of 8-days old plants were treated with 2 mM SA, 2 mM SA with 100 µM PMSF (SA + PMSF), a control solution containing 1% DMSO (control) and 1% DMSO with 100 µM PMSF (control + PMSF). AF was extracted three hours upon treatment and filtered with a 10 kDa cut-off column. Flow through was loaded on stage tips and peptides without digestion were detected in MS. Analysis and imputation values were done in Perseus 2.0.11. Significant differences were calculated based on students t-test (p-value <0.05, FDR <0.05) of three biological replicates. (A) The PCA plot demonstrates the alteration of peptide abundance when PMSF is co-infiltrated with SA, in comparison to SA alone and the absence of SA or both. (B/C) The volcano plots illustrate the degree of significance in peptide abundance between the various treatments. The peptides exhibiting a statistically significant difference in abundance are highlighted in purple. On the right of the volcano plots are shown peptides that are significantly more abundant following the SA treatment in comparison to the control (B) or the control with PMSF (C). Detected PCs are marked and significantly most abundant in SA indicated in pink.

2.2.5 Six of the selected PCs induce expression of *PRm6b* and *PR10*

To analyze whether the selected PCs are able to induce *PR*-gene expression, the fourteen selected peptides were synthesized by Davids Biotechnologie GmbH and syringe infiltrated into the second leave of 8-day old maize plants. Expression analysis of *PRm6b* and *PR10* was performed at 24 hpi as these genes were shown to be SA induced at 24 hpi (van der Linde, Hemetsberger, et al., 2012; Ziemann et al., 2018). As a negative control, MAP1, an apoplastic peptide found in previous analysis and does not induce *PR*-gene expression, was used (Ziemann et al., 2018). As a positive control, the known phytocytokine Zip1 was included (Koenig et al., 2023; Ziemann et al., 2018). Besides Zip1, six PCs significantly induced the two tested *PR*-genes (PC1, PC10, PC11, PC12, PC13 and PC14 (SIGGI)) indicating that they might play a role in the activation of immune responses. Thus, these six candidates were selected for further analysis.

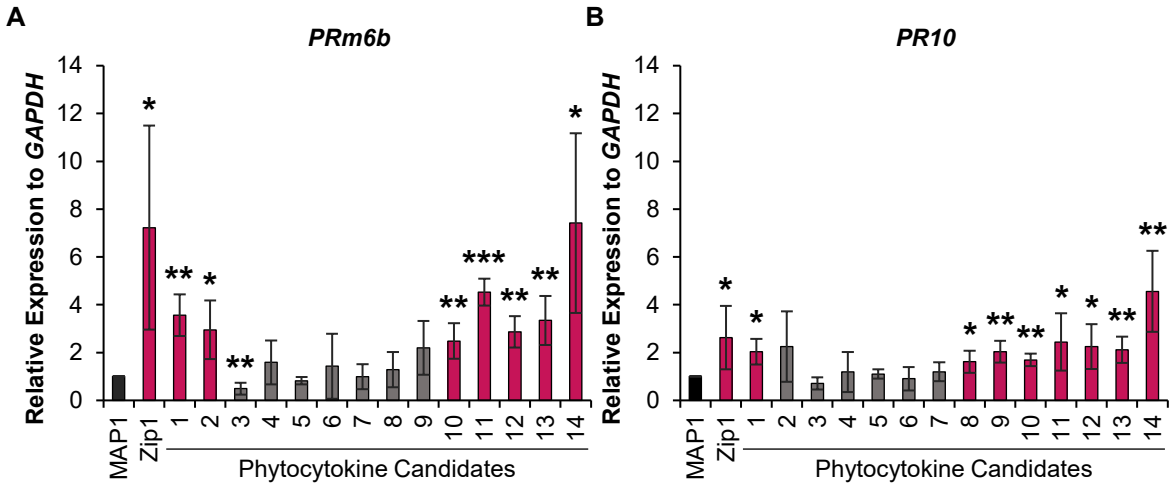

Figure 2.11: Six phytocytokine candidates (PC) induce *PRm6b* and *PR10* expression. Synthesized PCs (4 µM) were syringe infiltrated into maize leaves. As negative control, the peptide MAP1 was used (black bar) whereas Zip1 was included as positive control. At 24 hpi, samples were taken, RNA was extracted and expression of *PRm6b* (A) and *PR10* (B) were analyzed via qRT-PCR. *GAPDH* was used as a housekeeping gene and the relative expression of *PRm6b* and *PR10* was normalized to *GAPDH* expression. The purple color of the bar indicates PCs that induce significantly the expression of the tested genes or in grey PCs that did not significantly increase the expression. Significant differences were calculated based on students t-test (* =p<0.05, ** =p<0.01, *** =p<0.001).

2.2.6 SIGGI and PC13 influence *U. maydis* virulence

The smut fungus *U. maydis* is a biotrophic pathogen of maize and infects all aerial maize organs including leaves. During infection, it secretes several effectors into the apoplast in order to promote its virulence. *U. maydis* virulence can be evaluated based on the induction of chlorosis, tumor formation and tumor sizes. It is noteworthy that *U. maydis* can be employed as a biotechnological tool to facilitate the delivery of plant peptides into the leaf apoplast during the infection which enables the assessment of the impact of peptides on the virulence phenotype (van der Linde et al., 2018a; Ziemann et al., 2018). In order to elucidate the influence of PCs on the virulence of *U. maydis*, five PCs were examined: PC1, PC10, PC11, PC13 and SIGGI were recombinantly expressed in *U. maydis*, which secretes these peptides in the maize apoplast during infection. 7-day old maize plants were infected with the generated *U. maydis* strains and disease symptoms were monitored at 12 dpi. As a control, the solo-pathogenic strain SG200 was used. Here, the disease symptoms were scored on a scale of zero to ten with zero indicating no symptoms and ten indicating death of the infected plant. This scoring system was used to calculate the disease index relative to the solo-pathogenic SG200 strain. The virulence phenotype of *U. maydis* strains secreting either PC1, PC10 or PC11 was not significantly different from the SG200 control (Fig 12A). This indicates that the presence of these PCs did not alter the virulence of *U. maydis* and thus, do not influence the infection. In contrast, SIGGI and PC13 showed a significant change in the virulence of *U. maydis* compared to the SG200 control. The disease index increases when maize plants were infected with *U. maydis* secreting SIGGI (Fig. 2.12). The number of chlorosis and small tumors decreases, whereas more heavy tumors were detected in comparison to SG200 (Fig. 2.12B). In contrast, the virulence phenotype of *U. maydis* secreting PC13 seems to be reduced compared to SG200. The number of heavy tumors is decreased, while more small tumors can be observed compared to plants infected with SG200. If the peptides directly influence the fungus viability or if the virulence phenotype is due to an activation of immune responses is unclear. Nevertheless, both peptides influence the interaction of the plant and a biotrophic pathogen in a contrasting manner. Therefore, they might be newly identified phytocytokines.

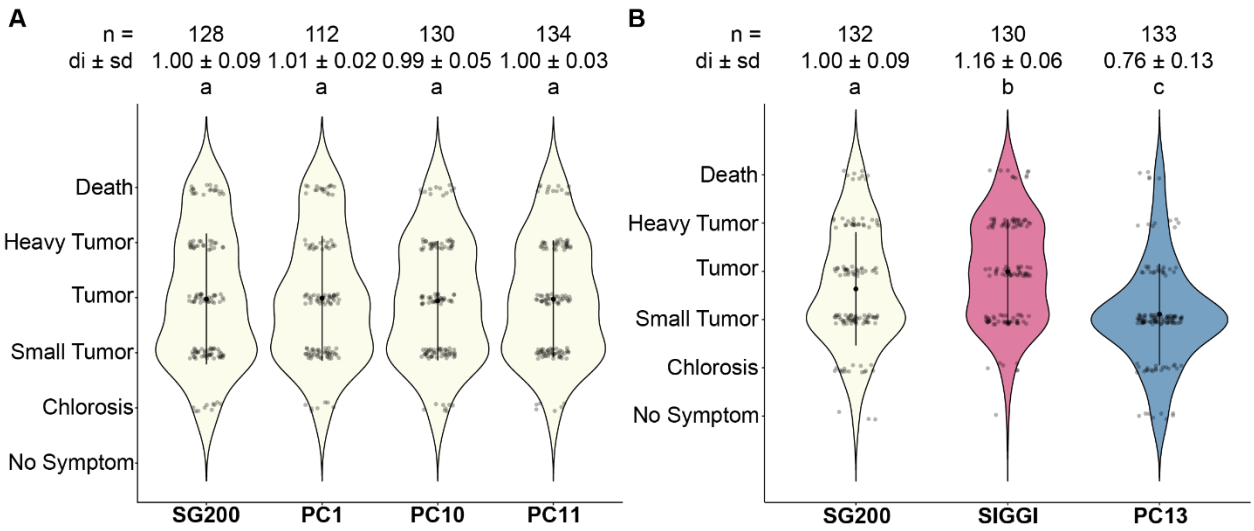

Figure 2.12: SIGGI and PC13 influence virulence of biotrophic fungal pathogen *U. maydis*. Seven-days old maize seedlings were infected with the solo-pathogenic strain SG200 and the transgenic SG200, which express and secrete either PC1, PC10, PC11, PC13 or SIGGI under the control of the *pit2* promotor. The severity of the disease symptoms was quantified at 12 days' post-infection (dpi). The disease index (di) displays the mean relative to the wild-type strain SG200. The mean was calculated regarding to the symptoms, which were associated to numbers from 0 (no symptoms) to 10 (death). The data were subjected to statistical analysis using a one-way ANOVA followed by the Tukey HSD (Honestly Significant Difference) and the plots were colored regarding to the statistical groups. The number of tested plants is indicated by n. The results presented here are based on three independent biological replicates.

2.2.7 RNA-seq analysis upon peptide treatment

PC13 and SIGGI have been shown to activate immune responses. However, they also display a differential virulence phenotype in *U. maydis* infection suggesting that they activate distinct immune pathways. To examine the impact of the two promising phytocytokine candidates on plant gene expression, an RNA-seq analysis was conducted. Therefore, 4 µM peptide solution was infiltrated in the second leaf of 8-days old maize seedlings. At 2, 6, 12 and 24 hpi samples were taken. As samples, the part of the leaf was chosen where the peptide solution was infiltrated but no wounding caused by the syringe infiltration was detected. From the frozen material, RNA was extracted and sent to Novogene for sequencing. As controls, the known phytocytokine Zip1 and MAP1 were included (Koenig et al., 2023; Ziemann et al., 2018).

A PCA was preformed to visualize the transcriptional changes in response to the different treatment at the different time points. The distance of data points demonstrates the difference between the visualized samples. The closer the data points are to each other, the more similar is the expression pattern . A clustering regarding the different tested time

points is clearly visible and follows the chronological order of the time points (Fig. 2.14A). The cluster of 24 hpi is closer to 2 hpi than to 12 hpi, which indicates a strong influence of the daytime to the gene expression. Furthermore, the different treatments show the highest distance between each other at 2 hpi and overlap more and more overtime. An indistinguishable overlay has already formed at 12 hpi. The distances indicate that the expressional responses to all peptides differ the most at two hours after the treatment and have the highest impact on gene expression (Fig. 2.14A). MAP1 formed an out group compared to the other treated peptides. PC13 lays intermediate between Zip1 and SIGGI. At 6 hpi, the differences between the peptides are still visible but vanish 12 hours after the treatments and fully disappeared at 24 hpi. The strongest peptide specific influence on gene expression is within the first six hours after infiltration, which indicates fast responses to the peptides.

The differences in the responses to the respective peptides become more obvious by plotting the number of differentially expressed genes (deg) in comparison to MAP1. SIGGI infiltration changes the expression pattern of more than 8,500 genes at 2 hpi of which more than 2,500 genes are significantly upregulated (p-value < 0.05; $log_2FC > 1$) and 1,200 down-regulated (p-value < 0.05; $log_2FC < -1$) (Fig. 2.14B). In comparison, the impact of PC13 and Zip1 on gene expression is much weaker. Infiltration of PC13 treatments results in 5531 deg at 2 hpi with 1491 deg being significantly upregulated (p-value < 0.05; $log_2FC > 1$) and 449 deg significantly downregulated (p-value < 0.05; $log_2FC < -1$). From the 2842 deg affected by Zip1, 648 are significantly up- (p-value < 0.05; $log_2FC > 1$) and 127 are down-regulated (p-value < 0.05; $log_2FC < -1$). The number of deg is lower for all peptides at 6 hpi compared to 2 hpi and is further reduced at 12 hpi. Interestingly, the number of up-regulated genes increases again for all peptides between 12 and 24 hpi (Fig. 2.14B).

A comparative analysis was conducted to identify the genes that are either up- or down-regulated by the peptides. Therefore, all genes that exhibited significant up- or down-regulation in comparison to MAP1 (p-value < 0.05; up: $log_2FC > 1$, down: $log_2FC < -1$) were compared for every time point. This comparison revealed several genes specifically up-regulated upon certain peptide treatments and indicates peptide specific responses. At 2 hpi about 45% (1174 genes) of the significant up-regulated genes

upon SIGGI treatment were found to be only up-regulated upon SIGGI treatment but not in response to Ziü1 or PC13 at 2 hpi (Fig. 2.14C). Specificity for PC13 is only found for 7% (106 genes) of the significant up-regulated genes upon PC13 treatment. 56% of the genes induced by PC13 are also found to be up-regulated by SIGGI (842 genes). Zip1 induced the lowest number of genes (648) of which the most (80%) are commonly shared with SIGGI and PC13 (517 genes). Only 9% of the Zip1 induced genes are Zip1 specific (56 genes). Also, for the significantly down-regulated genes SIGGI demonstrates the strongest influence on gene expression (SIGGI: 1200 genes, PC13: 449 genes, Zip1 127 genes). Nearly three quarters (73%, 871 genes) of the significantly down-regulated genes upon SIGGI treatment are specifically down-regulated after SIGGI treatment at 2 hpi. About 27% (261 genes) of the down-regulated genes upon PC13 treatment are specifically found to be down-regulated upon PC13 treatment. Similar to the up-regulated genes, PC13 also demonstrates a high coverage of 58% (261 genes), which are down-regulated upon PC13 and SIGGI treatments. From the 127 down-regulated genes upon Zip1 treatment, about one third (43 genes) are specific for Zip1. 52 genes are shared by all three peptides. At 6 hpi most of the genes are still influenced by SIGGI (449 up-, 498 down-regulated). About 75% (346 genes) of the up-regulated genes and about 66% (332 genes) of the 498 down-regulated genes upon SIGGI treatment are specific for SIGGI. About three times more genes compared to 2 hpi are specifically up-regulated at 6 hpi by Zip1 (151 genes) and about 50% of the 131 down-regulated genes upon Zip1 treatment are Zip1 specific (63 genes). 25 genes are commonly up- and 24 genes are commonly down-regulated by the three peptides. At 12 hpi less than 100 genes are up- or down-regulated for every peptide. 53 genes are specific upon SIGGI treatments up- and 47 down-regulated. PC13 treatment leads to 68 up- and 71 down-regulated genes. Upon Zip1 treatments 30 genes are specifically up- and 60 down-regulated. Only three genes are up- and only seven are down-regulated by all three peptides. At 24 hpi the number of genes being up-regulated by the peptides increased again between 12 and 18 times compared to 12 hpi. 258 genes are specifically up-regulated upon SIGGI treatment, and 409 genes are specifically up-regulated upon PC13 treatment. Upon Zip1 treatment 262 genes are specifically up-regulated. 384 genes are up-regulated by all three peptides. The number of genes down-regulated by the peptides doubles at 24 hpi compared to

12 hpi. SIGGI treatment causes a down-regulation of 116 genes and 139 genes are down-regulated upon PC13 treatment. Zip1 specifically down-regulated the expression of 115 genes. 19 genes are down-regulated by all three peptides. In conclusion, SIGGI seems to have the biggest impact on gene expression as it modulates the expression of the most genes of the tested peptides. In general, the gene expression pattern is in line with the PCA, as the most differences between the peptides are found at 2 hpi.

Interestingly, the expression of the proproteins of SIGGI (Zm00001eb361250, MIF) and PC13 (Zm00001eb226780, SAP7) was neither significantly up-regulated nor down-regulated in response to any peptide at any of the tested time points. This indicates that the peptides do not induce a feedback loop in which the proproteins are expressed.

The peptide treatments showed the strongest impact on gene expression in the first two hours upon treatment. The SIGGI peptide had the highest influence on gene expression at 2 and the highest specificity in gene regulation at 6 hpi. The treatment with PC13 showed a substantial overlap with SIGGI and Zip1 responses. At 24 hpi the majority of genes are specifically up- or down-regulated upon PC13 treatment.

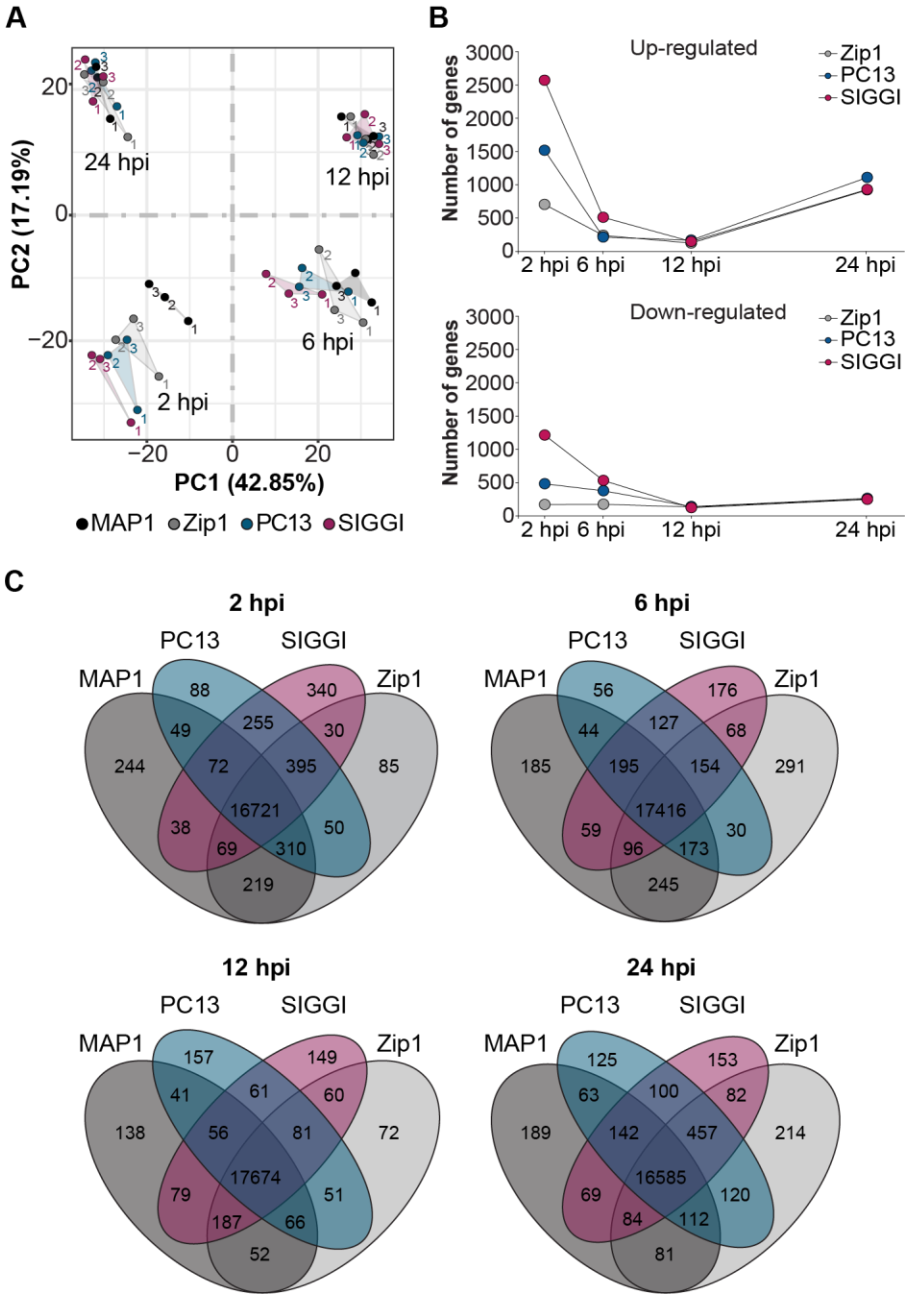

Figure 2.13: RNAseq analysis reveals early responses to peptide treatments. 7-days old maize leaves were syringe infiltrated with 4 µM of the synthetic peptides. The area between the infiltration site was marked and harvested at 2, 6, 12 and 24 hpi. RNA sequencing and analysis was performed by Novogene. The PCA plot illustrates the variation of gene expression between the treatments and the different time-points (A). Graphical illustration of number of differential expressed genes (deg), which are significantly up- or downregulated upon PC13, SIGGI or Zip1 in comparison to MAP1 (B). Venn-diagrams show differentially or shared gene expression upon the different treatments. Used were significantly up- or downregulated genes upon PC13, SIGGI or Zip1 in comparison to MAP1 (C). Significant differences were calculated based on students' t-test p-value < 0.05. A cut off for log_2FC was set for up: > 1, down: < -1.

The Gene Ontology (GO) enrichment analysis of differential genes is a major bioinformatics classification system to unify the presentation of gene properties and assists in the functional classification of differential expressed genes. Generally, the GO terms are divided regarding the molecular function of the gene, the cellular component, where the encoded protein localizes or the biological process (BP), that is influenced by the genes. To obtain an overview of biological processes that are affected by the three peptides, a GO Term analysis was conducted. The GO enrichment analysis was performed by Novogene and significant upregulated genes upon the specific peptide treatment in comparison to MAP1 were used (p-value > 0.05; $log_2FC > 0$) and the three GO terms with respect to biological processes with the highest significance ($-Log_{10}(padj)$) are displayed.

At 2 hpi upon Zip1 treatment, the GO terms cell recognition, pollination and pollen-pistil interaction are enriched and include eight genes. These genes have a p-value of 0.037 resulting in a padj of 1 for the GO terms and consequently, in a -log10 of 0 (Fig. 2.15A). Those GO terms are also enriched after PC13 treatment (Tab. S1), however, the top three processes enriched upon PC13 at 2 hpi were metabolic and biosynthetic processes involving fatty acids and monocarboxylic acid. Treatment with SIGGI lead to the upregulation of genes which are associated to protein modification and ubiquitination at 2 hpi (Fig. 2.12A).

At 6 hpi, genes that were upregulated in response to SIGGI can be associated to the GO terms “carbohydrate metabolic process”, “response to stress” and “defense response” (Fig. 2.15B). Those genes include the *PR*-genes (*pathogenesis-related protein11* (*PRP11,* Zm00001eb167710), pathogenesis-related protein7 (*PRP7*, Zm00001eb014000)), a chitinase (Zm00001eb167720) and two genes encoding for MLO-like proteins (Zm00001eb288190, Zm00001eb271870) (Tab. S1). Similarly, the GO term “defense response” was also found upon Zip1 treatment at 6 hpi. Interestingly, both treatments induce the expression of *PRP11* (Zm00001eb167710) and the chitinase (Zm00001eb167720) suggesting and overlap in the activation of the salicylic acid pathway. Besides, the GO terms “carbon fixation” and “response to external stimulus” were identified in response to Zip1 (Fig. 2.15B). The top three GO terms associated with

PC13 treatment include four genes that encode for potassium high affinity transporters (Zm00001eb330230, Zm00001eb071150, Zm00001eb048930, Zm00001eb430810).
The GO terms enriched upon Zip1 at 12 hpi are “cellulose metabolic process”, “cellulose biosynthetic process” and “polysaccharide biosynthetic process (Fig. 2.15C). All three GO terms include the same three genes, which all encode for cellulose synthases (Zm00001eb306030, Zm00001eb303110, Zm00001eb345740) (Tab. S1). In maize plants treated with SIGGI genes associated to the GO term “proteolysis” were enriched, which includes a SBT (SBT41, Zm00001eb305600), a SCP (Zm00001eb340690) and a E3 ubiquitin-protein ligase SINA-like 10 (Zm00001eb334930). Besides, the GO terms “negative regulation of cellular metabolic process” and “negative regulation of nitrogen compound metabolic process” are upregulated at 12 hpi (Fig. 2.15C). “DNA integration” and “DNA metabolic process” as well as “mRNA processes” were the GO terms found to be mostly enriched in response to PC13 at 12 hpi. Only five of 13 genes associated to these processes have been described so far, namely three pre-mRNA-processing splicing factors (Zm00001eb271550, Zm00001eb292700, Zm00001eb375530), associated to “mRNA processes” and a nuclear pore complex protein (Zm00001eb352670) as well as a DNA topoisomerase (Zm00001eb280820) which can be categorized into the GO term “DNA metabolic process” (Fig. 2.15C and Tab. S1).
24 hours after the infiltration of Zip1 the GO terms regarding “drug catabolic process”, “carbohydrate derivative catabolic process” and “chitin metabolic process” are upregulated (Fig. 2.15D). All genes associated with these GO terms are chitinases (Tab. S1). Interestingly, those genes were also associated to two of the top three GO terms found in response to SIGGI treatment at 24 hpi, namely “carbohydrate derivative catabolic process” and “chitin metabolic process”. The third GO term found upon treatment with SIGGI was “defense response”. Six genes are associated to the GO term “defense response”, namely, *PRP3* (Zm00001eb167690), *PRP6* (Zm00001eb014010), *PRP7* (Zm00001eb014000), *PRP11* (Zm00001eb167710), a chitinase (Zm00001eb167720) and a Hevein-like preproprotein (Zm00001eb167700) (Fig. 2.15D and Tab S1). Notably, three of those genes (*PRP7* (Zm00001eb014000), *PRP11* (Zm00001eb167710), a chitinase (Zm00001eb167720) were already upregulated at

6 hpi. PC13 induces at the latest tested point many genes involved in translation and peptide biosynthesis (Fig. 2.15D).

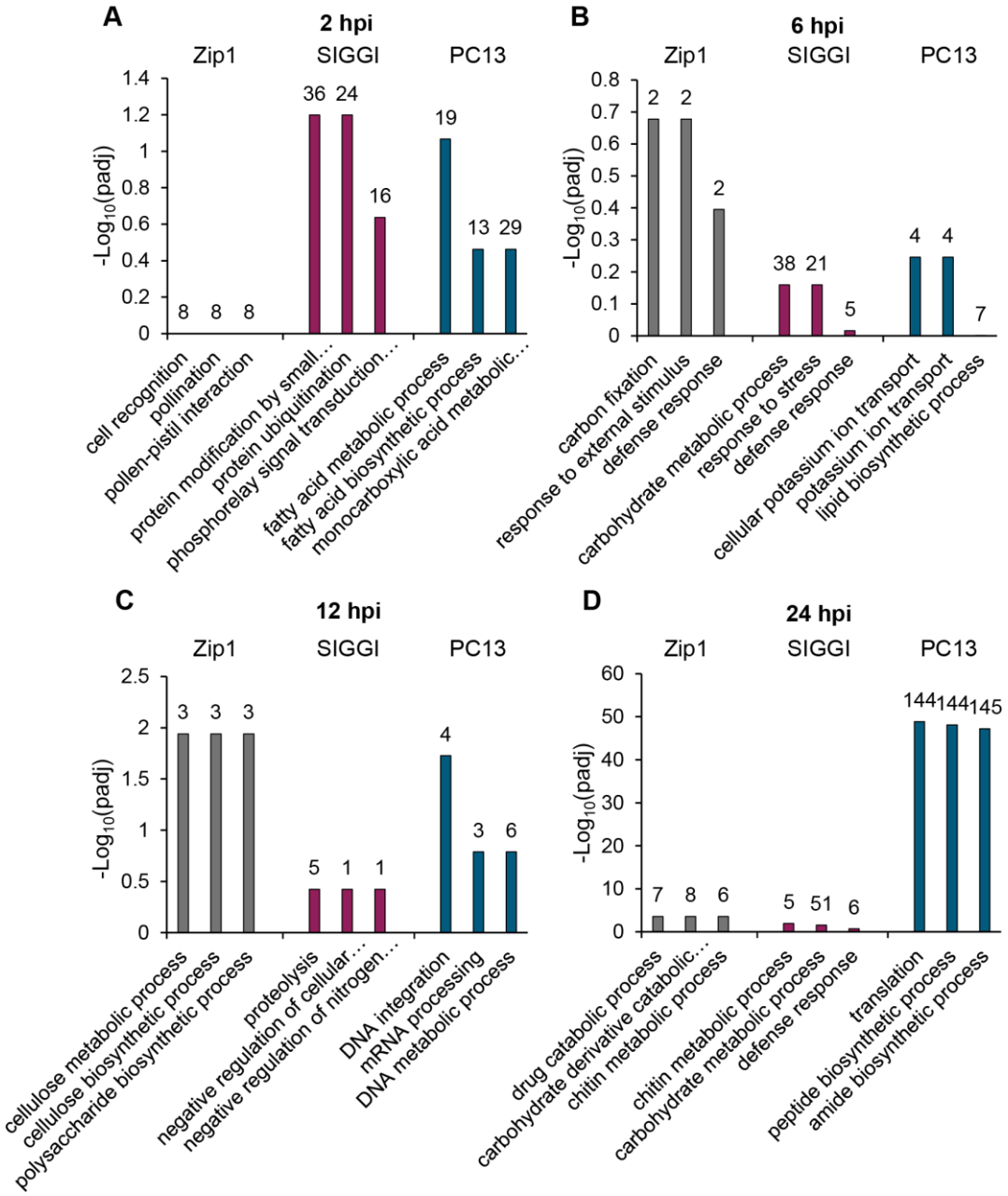

Figure 2.14: Peptide treatments induce different biological progresses. The most significant three GO Terms of the GO enrichment analysis for biological progress (provided by Novogene) are displayed (an extensive list can be found in Tab. S1). The ordinate is the significance level of GO Term enrichment, expressed as -log10 (padj). Higher values correspond to higher significance. The different colors represent the three different treatments (grey Zip1, pink SIGGI, blue PC13). Numbers above the bars represent the number of genes associated with the GO Term. Shortened GO names: 2 hpi SIGGI "protein modification by small protein conjugation or removal" and "phosphorelay signal transduction system", PC13 "monocarboxylic acid metabolic process"; 12 hpi SIGGI "negative regulation of cellular metabolic process" and "negative regulation of nitrogen compound metabolic process"; 24 hpi Zip1 "carbohydrate derivative catabolic process".

2.2.8 SIGGI specific gene expression

SIGGI was found upon exogenous application of SA and shown to induce *PR*-gene expression, which suggests its association to SA induced immunity. Also, SIGGI increases the virulence of *U. maydis*, which is counterintuitive to the induction of *PR*-genes. In order to investigate how the peptide influences gene expression over time and to reveal responses to SIGGI treatment which may be beneficial for *U. maydis* virulence, a comparative analysis was performed. Accordingly, all genes exhibiting significant up- or down-regulation for SIGGI in comparison to MAP1 (p-value < 0.05 and $Log_2FC > 1$ for up- or $Log_2FC < -1$ for down-regulation) at each time point were compared and distinguished as belonging to the same or different group, depending on whether they were identified at different time points.

At 2 hpi upon SIGGI treatment, 2582 genes were significantly upregulated in comparison to MAP1. From these the majority of genes (2101 genes) was only significantly upregulated at 2 hpi and not at any other time point (Fig. 2.16A). At 6 hpi, 449 genes are significantly higher expressed and 217 of these were unique for 6 hpi, whereas 99 are higher expressed at 2 and 6 hpi. The least number of significant upregulated genes were found at 12 hpi (73 genes), of which 47 genes are unique for 12 hpi and 4 genes are commonly upregulated at 6 hpi and 12 hpi (Tab. S2), and 14 at 2 hpi. At 24 hpi, 883 genes are significantly upregulated and 461 are only found at 24 hpi. Of those 883 genes, 53 genes were also significantly up-regulated at 12 hpi and 73 genes were also found to be significantly up-regulated at 6 hpi. Interestingly, the strongest overlap is found between 2 hpi and 24 hpi with 288 significantly upregulated genes, which are only significantly up-regulated at these two time points. For the significantly down-regulated genes a similar picture was observed, even if the total number of significantly down-regulated genes is lower compared to the number of up-regulated genes. Upon SIGGI treatment, 1200 genes are significantly down-regulated compared to MAP1 at 2 hpi, where 1144 are only significant down-regulated at 2 hpi. From 498 significant down-regulated genes at 6 hpi nearly 95% (469 genes) are only found at 6 hpi and 24 are also down-regulated at 2 hpi. At 12 hpi, 78 genes are significantly down-regulated of which one is also down-regulated at 6 hpi and two at 2 hpi, but none at all three time points. At 24 hpi, 207 genes are significantly down-regulated of which two are also down-regulated at

12 hpi, three at 6 hpi and 29 at 2 hpi. Only one gene is commonly down-regulated at 2, 6 and 24 hpi.

After excluding genes which were also found at different time points upon PC13 and Zip1 treatment, the numbers of genes being up- and downregulated reduced, but the relative distribution of genes between the time points remained largely unchanged. For example, upon SIGGI treatment 1116 genes are found which are treatment specific significantly up-regulated at 2 hpi (Fig. 2.16B). 296 genes are significantly upregulated in comparison to MAP1 and are specific upon SIGGI infiltration at 6 hpi. Gene expression of 44 genes are only induced at 12 hpi and of 207 at 24 hpi. No gene is commonly upregulated at all four tested time points, whereas at 25 genes are significantly upregulated at 2 hpi and 24 hpi and 20 genes at 6 and 24 hpi. In contrast, only four genes were found to be upregulated at the three time-points 2, 6 and 24 hpi (Tab. S2). The number of SIGGI specific genes that were significantly down-regulated in comparison to MAP1 is 851 genes at 2 hpi and 319 at 6 hpi. At both time points, 2 and 6 hpi, ten genes are found to be significantly down-regulated. Of the 76 genes, which are significantly down-regulated at 12 hpi, 46 and 30 are only down-regulated at 12 hpi and at 12 and 24 hpi, respectively. 103 genes are specifically down-regulated at 24 hpi, two at 6 and 24 hpi and nine genes at 2 and 24 hpi. Only one gene is significantly down-regulated at 2, 6 and 24 hpi. In comparison of the total number of genes, only a few genes are found to be up- or down-regulated over a longer period, so they appear at different time points. To analyze a relation between the upregulated genes, which are specific for the SIGGI treatment, and to characterize their function, a GO enrichment analysis regarding biological processes was performed using the online tool ShinyGO (Ge et al., 2020). As input, genes which are significantly up-regulated (p-value < 0.05 and $Log_2FC > 1$) in comparison to MAP1 and were only found upon SIGGI treatment at the corresponding time point were used. Enriched GO terms were only found for the first two time points, 2 hpi and 6 hpi. The GO enrichment analysis revealed that eight genes (Tab. S2) are strongly associated to the “regulation of defense response to fungus” at 2 hpi (Fig. 2.16C). Another 20 genes are associated with “Immune system processes”. Additionally, 30 genes associated with “responses to external stimulus” were are also associated to the GO terms “responses to hormone” (41 genes), “to endogenous stimulus” (41 gens)

and “to organic substance” (45 genes). These GO terms are formed mainly out of the same genes, as many of them are associated to several GO terms. The same 63 genes are associated with the GO terms “signal transduction”, “signaling” and “cell communication”. Besides these 63 genes, six additional genes are associated to “cell communication”. At 6 hpi, three genes are significantly up-regulated in comparison to MAP1 and only upon SIGGI treatment, which are involved in “salicylic acid biosynthetic processes” and their regulation, as well as “phenol-containing compound biosynthetic processes” (Zm00001eb042820, Zm00001eb125120, Zm00001eb410260) (Fig. 2.16D). Three other genes play a role in the “regulation of protein serine/threonine phosphatase activity” (Zm00001eb013990, Zm00001eb014000, Zm00001eb396710). Two of these genes (Zm00001eb013990, Zm00001eb014000) among other genes are also involved in the following responses: “response to cold” (five genes), “response to salt stress” (five genes), “response to inorganic substance” (eight genes) and “response to temperature stimulus” (seven genes) (Tab. S2/ Fig. 2.16D).

In conclusion, the SIGGI peptide induces genes in a time specific manner as most of the genes are only found to be up- or down-regulated at specific time points. The genes which are specifically and significantly up-regulated upon SIGGI treatment are involved in immune signaling and responses to external signals at 2 hpi, which is followed at 6 hpi by genes, which are involved in SA biosynthesis and responses to different stimuli and stresses. The induction of immune signaling is in line with the induction of *PR*-gene expression (Fig. 2.11), whereas the induction of gene expression involved in SA biosynthesis was unexpected with respect to the increased virulence of *U. maydis* demonstrated in this study (Fig. 2.12).

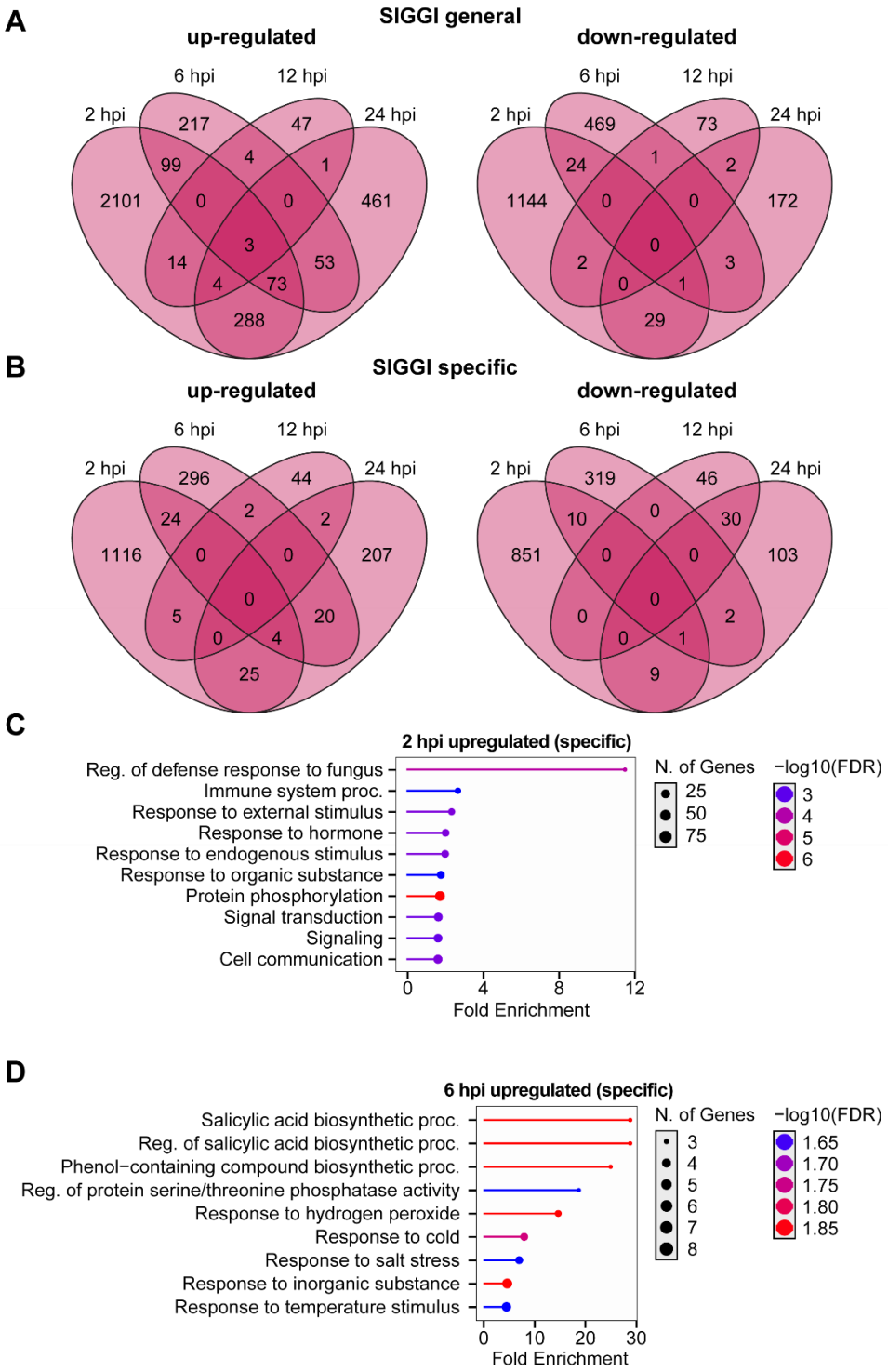

Figure 2.15: SIGGI treatment induces expression of several genes including several immune responses. For analysis only significant up- or down regulated genes upon SIGGI treatment in comparison to MAP1 were used (p-value < 0.05 and Log2FC > 1 (up) or < -1 (down)). (A) All genes of the different time points are compared and visualized, at which time point they are significantly up- or down-regulated. (B) Only genes were shown, which are exclusively for each time point significant upon SIGGI treatment. (C/D) For GO term analysis ShinyGO was used (Ge et al., 2020) and biological processes are displayed. Analyzed are the genes, which are significant up-regulated specifically upon SIGGI treatment at 2 hpi (C) and 6 hpi (D). For 12 hpi and 24 hpi "No significant enrichment found!".

2.2.9 PC13 specific gene expression

PC13 was found in the apoplast upon SA treatments and shown to induce *PR*-gene expression as well to reduce the virulence of *U. maydis*, which suggests its association to SA induced immunity. In order to investigate how the peptide influences further gene expression over time and to reveal its role in SA mediated immunity, a comparative analysis was performed. As for the SIGGI peptide, all genes exhibiting a significant up- or down-regulation in comparison to MAP1 (p-value < 0.05 and $Log_2FC > 1$ for up-regulation or $Log_2FC < -1$ for down-regulation) at each time point were compared and distinguished as belonging to the same or different group, depending on whether they were identified at different time points. At 2 hpi, 1491 genes showed a significant increase in expression compared to MAP1. Most of these genes (1230) showed significant upregulation only at 2 hpi (Fig. 2.17A). At 6 hpi, 141 genes show higher expression in response to PC13 than MAP1, with 102 genes being unique to this time point. 22 genes are common to both time points, 2 and 6 hpi. At 12 hpi, the lower number of genes is expressed (93). 69 genes are unique for 12 hpi, two are shared with 6 hpi, and seven are shared with 2 hpi. At 24 hpi, 1069 genes up-regulated of which 824 were only found at this time point. Eight genes showed significant upregulation at 12 and 24 hpi. Six genes demonstrated significant upregulation at 6 and 24 hpi. The highest number of genes exhibited significant up-regulation across both 2 and 24 hpi with a total of 222 genes. A similar pattern was seen for the significantly down-regulated genes, though fewer genes are down- than up-regulated. PC13 treatment led to a significant decrease in gene expression at 2 hpi with 449 genes being affected. Of those, 416 genes were only found to be down-regulated at 2 hpi. Out of 340 down-regulated genes at 6 hpi, 90% (305 genes) were only identified at this time point. Seven genes were identified as being down-regulated at both 2 and 6 hpi. At 12 hpi, 96 genes are significantly down-regulated, with 73 unique to this time point. Additionally, 17 genes are down-regulated at 6 hpi. At 24 hpi, 222 genes are significantly down-regulated, with 188 (81%) being unique to this time point. Additionally, two genes are down-regulated at 12 hpi, ten at 6 hpi, and 22 at 2 hpi (Fig. 2.17A).

The exclusion of genes that are also identified to be differentially expressed at distinct time points following SIGGI and Zip1 treatment reveals the number of genes, which are

specific to PC13 treatment. At 2 hpi upon PC13 treatment, 103 genes are identified as being significantly upregulated in a time point and treatment-specific manner (Fig. 2.17B). 42 genes are significantly upregulated in comparison to MAP1 and are specific to PC13 infiltration at 6 hpi. Gene expression of 66 genes is only induced at 12 hpi, and 401 genes are only induced at 24 hpi. No genes are commonly shared at all four time points. At 2 hpi and 24 hpi, three genes are significantly upregulated, and at 6 and 24 hpi, two genes are significantly upregulated (Table S3). PC13 exhibited 112 significant down-regulated genes in comparison to MAP1 at 2 hpi and 146 at 6 hpi. At both time points (2 and 6 hpi), two genes were identified as significantly down-regulated. Of the 71 genes that are significantly down-regulated at 12 hpi, 66 are only present at that time point. A total of 133 genes exhibited specific downregulation at 24 hpi. Additionally, two genes demonstrated differential expression at both 6 and 24 hpi, while three genes exhibited temporal specificity at 2 and 24 hpi. In comparison to the total number of genes, only a few genes are found to be up- or down regulated over a longer period, resulting in their appearance at different time points.

For the analysis of the upregulated genes upon PC13 treatment and to characterize their function a GO enrichment analysis was performed using the online tool ShinyGO (Ge et al., 2020). As input, significantly up-regulated genes (p-value < 0.05 and $Log_2FC > 1$) in comparison to MAP1 were analyzed. The analysis for PC13 specific genes resulted in "no significant enrichment found" and thus, the general up-regulated genes upon PC13 treatment for each time point were used. Enriched GO terms were only found for two time points, namely 2 hpi and 24 hpi. The GO enrichment analysis revealed, that six genes are strongly associated to the “programmed cell death induced by symbiont” and “plant-type hypersensitive response“ (Fig. 2.17C, Tab. S3). Eleven genes are connected to JA pathways, as they are associated with the GO terms “regulation of JA mediated signaling pathway”, “JA mediated signaling pathway”, “cellular response to jasmonic acid stimulus”. Additional to the eleven genes, one gene each is associated to “response to JA” (Zm00001eb051200) and “response to wounding” (Zm00001eb041390). 131 significantly up-regulated genes upon PC13 treatment are associated to “protein autophosphorylation” and 99 genes to “regulation of defense response”. All GO terms, which are calculated for the genes significantly up-regulated at 24 hpi upon PC13 treatment, are associated to

ribosomes. These include the “maturation of LSU-rRNA” (13 genes), “ribosomal large subunit biogenesis” (25 genes) and “ribosome assembly” (17 genes) (Fig. 2.17D). Also the biogeneses of ribosomes and the ribosomal subunit seems to be influenced by 66 genes and 14 genes, respectively. “RRNA metabolic processes” and “RRNA processing” are also induced by the same 37 genes.

To conclude, PC13 induces less genes in comparison to SIGGI, but similar to the response to SIGGI the majority of genes are found only at a certain time point to be up- or down-regulated. The genes, which are significantly up-regulated upon PC13 treatment are involved in PCD and HR at 2 hpi, as well as JA associated pathways. The JA association seems to be counterintuitive for a SA related peptide as far the association leads to a positive regulation of JA mediated signaling.

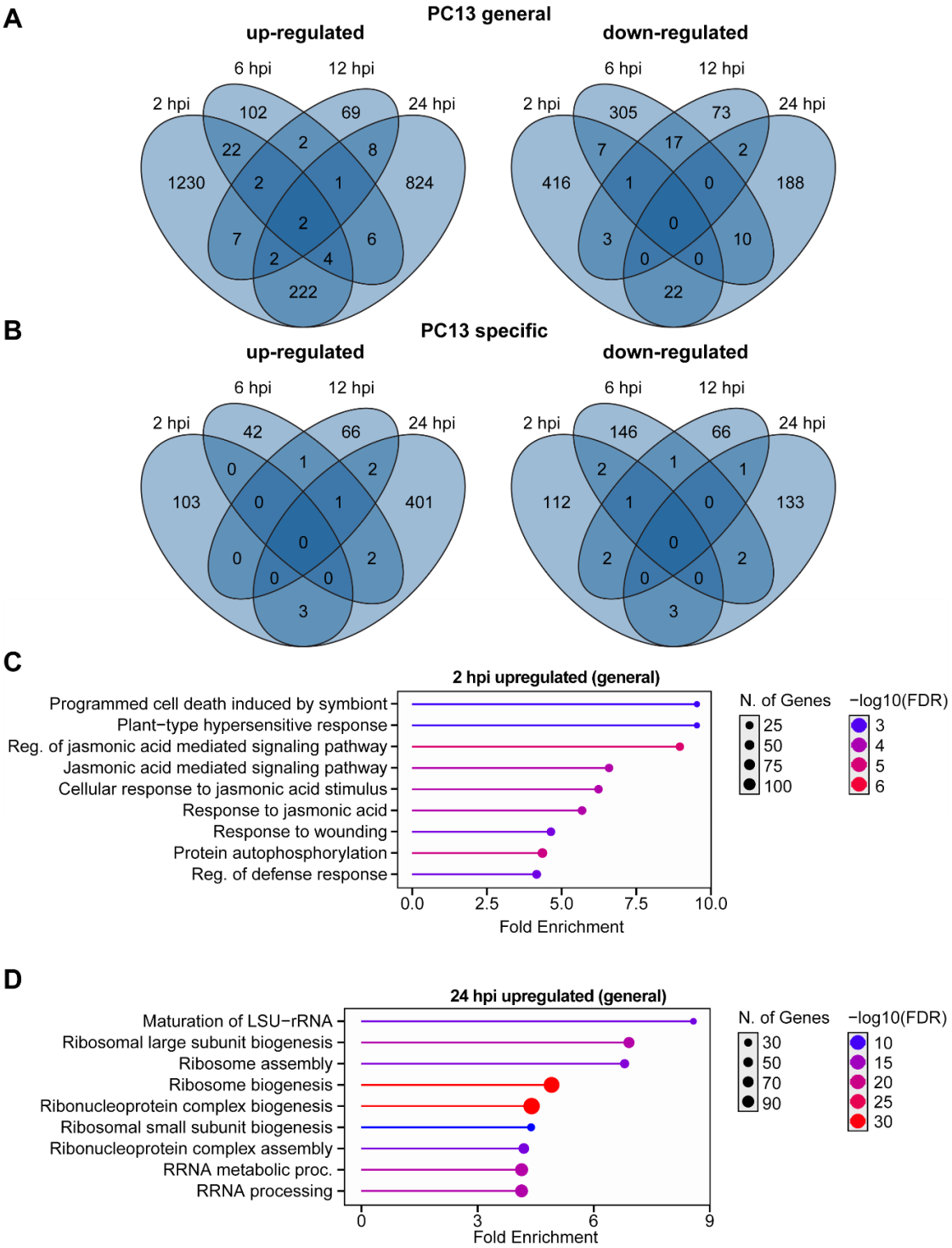

Figure 2.16: PC13 treatment alter genes expression, especially in association with PCD, HR and JA. For analysis only significant up- or down regulated genes upon PC13 treatment in comparison to MAP1 were used (p-value < 0.05 and Log2FC > 1 (up) or < -1 (down)). (A) The significant up- or down-regulation of all genes at different time points is compared and visualized. (B) Only genes exclusively for each time point significant upon PC13 treatment are shown (C/D) For GO term analysis ShinyGO was used (Ge et al., 2020) and biological processes are displayed. Analyzed are all genes, which are significantly regulated upon PC13 treatment at 2 hpi (C) and 24 hpi (D). For 6 hpi and 12 hpi "No significant enrichment found".

2.2.10 Activity and expression of PLCP upon peptide treatments

To monitor immune activity in maize, mainly the expression of *PR*-genes and the activity of PLCPs is determined. Especially apoplastic PLCPs are important in the defense against pathogens such as the smut fungus *U. maydis* (Misas-Villamil et al., 2016). Notably, inhibition of PLCPs results in a loss of induction of *PR*-gene expression upon SA treatments (van der Linde, Hemetsberger, et al., 2012). The induction of *PR*-gene expression caused by SIGGI and PC13 was demonstrated in this study (Fig. 2.18). To test if SIGGI and PC13 activate PLCPs and thus, play crucial roles in maize immunity, an ABPP was performed. Therefore, 4 µM peptide solution of SIGGI or PC13 was infiltrated into 8-days old maize leaves and the PLCP activity was detected at 24 hpi in the total leave extract with the probe DCG04-Cy5 via ABPP. Infiltration of MAP1 serves as negative control and reflects the overall activity of PLCPs, while Zip1 was shown to be able to activate PLCPs and was used as positive control (Ziemann et al., 2018). Pre-incubation with the PLCP inhibitor E64 prior to incubation with the probe demonstrates the specificity of the signals, as the inhibitor blocks the active site of active PLCP by binding covalently and irreversibly, so the probe is not able to bind anymore. Thus, only signals which are present without E64, but not present after pre-incubation with E64 are specific to PLCP activity. Three bands containing active PLCPs were observed (A, B and C) and quantified (Fig. 2.18A). Treatment with Zip1 resulted in a significant increase in the fluorescence of the upper (A) and the lower band (C), while band B showed no change in fluorescence intensity compared to the negative control MAP1. This indicates that Zip1 activates PLCPs present in band A and C (Fig. 2.18B) which is in accordance to published results (Ziemann et al., 2018). PC13 does not change PLCP activity significantly in comparison to MAP1. Interestingly, the fluorescence intensity in response to SIGGI only increases for band A but decreases for band B and C compared to MAP1 (Fig. 2.18B) leading to the conclusion that SIGGI treatments differentially modulate PLCP activity. Moreover, the bands A and C upon SIGGI treatment demonstrate also significant differences in comparison to Zip1 (Fig. 2.18).

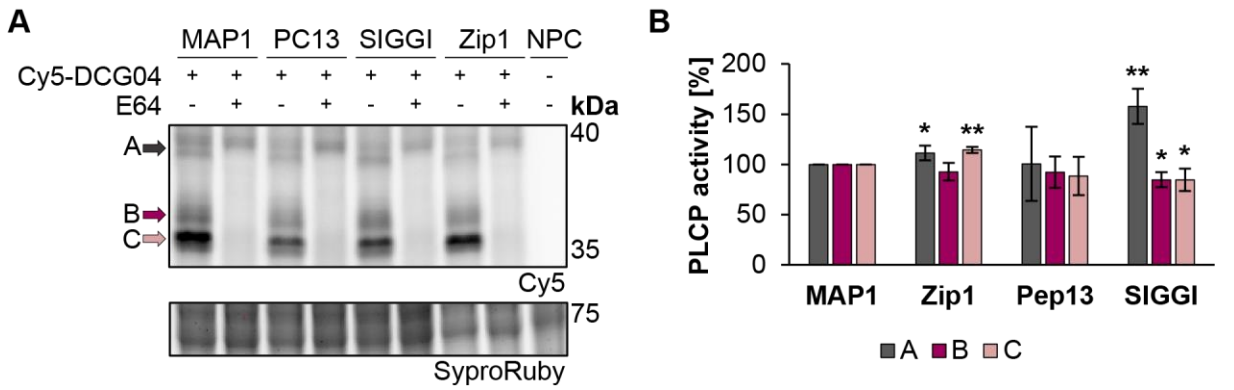

Figure 2.17: Zip1 and SIGGI differentially modulate PLCP activity. Activity-based protein profiling (ABPP) of maize leaves infiltrated with 4 µM of the synthetic peptides MAP1 (negative control), Zip1 (phytocytokine and positive control) and SIGGI. Leaves were syringe infiltrated, and samples were taken at 24 hpi. Total protein extract was prepared from whole leaves using a protein extraction buffer (pH=6). Active PLCPs were labelled using 1 µM Cy5-DCG04. Pre-incubation was performed with 40 µM of the PLCP inhibitor E-64. Samples were run on an SDS-PAGE and analyzed via fluorescence scanning (Cy5 filter). The gels were then stained with SyproRuby as loading control. The no-probe control (NPC) shows potential background signals. Shown is a representative Figure. (A). For quantification analysis gel signals (A, B and C) were quantified and values were normalized to the E-64 pre-incubation and the activity of the mock control was set to 100%. Shown is the mean and SEM of the fluorescence intensity of three biological replicates (B). Significant differences were calculated based on students t-test (* = $p<0.05$, ** = $p<0.01$, *** = $p<0.001$).

As Zip1 and SIGGI treatments demonstrate an influence on PLCP activity, expression analysis of *PLCP* genes upon treatments with SIGGI, PC13 and Zip1 was performed. Although PLCPs are mainly activated by posttranscriptional processing (Misas-Villamil et al., 2016), a recent study in maize revealed an upregulation of the expression of *Corn Cysteine Protease 1* (*CCP1*) upon virus infection (Yuan et al., 2024). To visualize the expression in a heatmap, the Log_2FC of each PLCP gene, comparing the treatments with MAP1, were normalized from 1 (the highest) to -1 (the lowest) for all treatments and time points. The color scale indicates in red the highest Log_2FC of the gene and the lowest in blue. If the gene was not expressed, the field is colored grey. Overall, neither the treatment with PC13 nor with SIGGI did yield in a general increase of *PLCP* expression (Fig. 2.19). The expression patterns of most PLCPs are more time- than treatment-dependent, but do not demonstrate significant differences in expression levels in comparison to MAP1. For example, the expression levels of *SAG12* (Zm00001eb418570) and *XCP1* (Zm00001eb375740) upon SIGGI, PC13 or Zip1 treatment do not differ significantly from treatments with MAP1 but expression is not detected at all after 6 hpi for all treatments. The expression of the gene encoding for *CP1A* (Zm00001eb068400) is significantly induced at 2 hpi by all three peptides in comparison to MAP1. In contrast,

CP1B (Zm00001eb432170) expression is only significantly induced by SIGGI treatment at 2 hpi. At 6 hpi upon SIGGI treatment the *PLCP* gene expression of Zm00001eb100260 and *CCP9* (Zm00001eb326570) is significantly down regulated (Fig. 2.19). On the contrary, PC13 induces the expression of *CCP9* significantly. At 24 hpi, the expression of *CCP35* (Zm00001eb039650) and one of the *RD21B-like* (Zm00001eb273440) are significantly upregulated while the expression of *CCP18* (Zm00001eb169010) is significantly downregulated in response to PC13. Zip1 treatment results in a significant upregulation of both *RD21B-like* genes (Zm00001eb113940 and Zm00001eb273440) at 24 hpi. In summary, a general up- or downregulation of genes encoding PLCPs was not observed, however, the expression of a few PLCPs was affected by the three different peptides in comparison to MAP1.

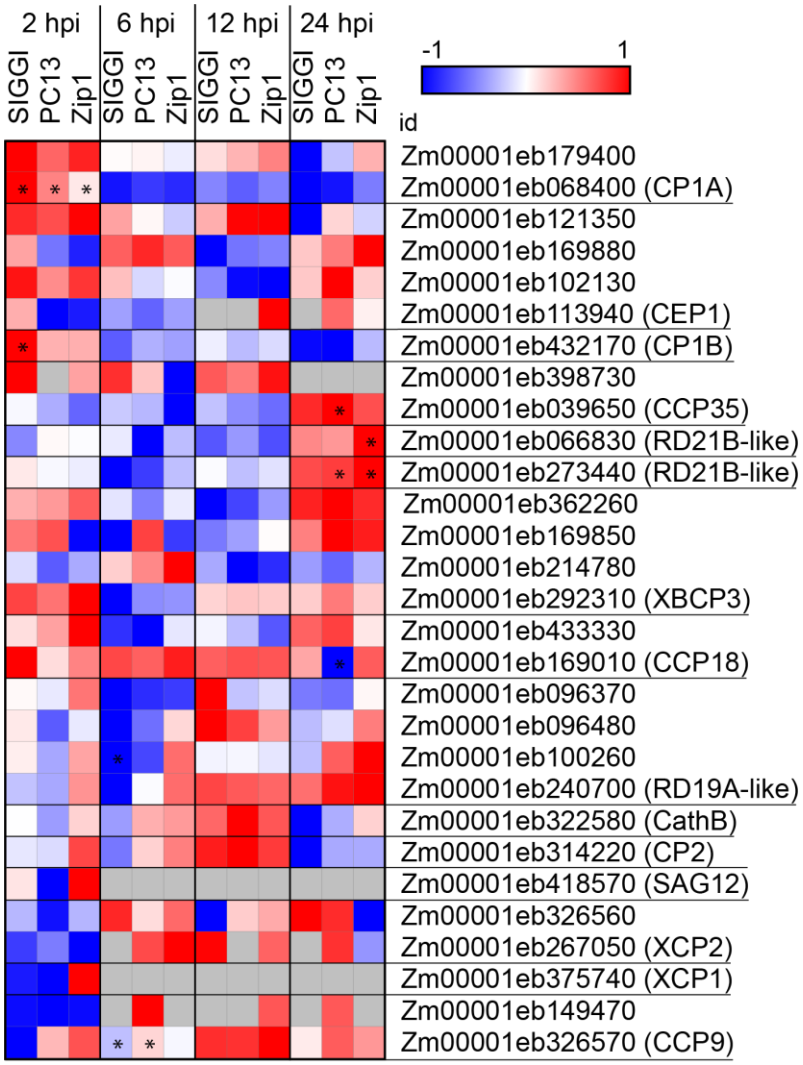

Figure 2.18: Peptides induce various PLCP expressions at different time points. Log_2FC of PLCPs in response to the indicated peptide. Shown are degs of PLCPs after different peptide treatments in comparison to MAP1. Log_2FC is normalized from 1 to -1 per gene (per row), with 1 (red) strongest up-regulation to -1 (blue) strongest down-regulation and grey not detected at all. PLCP names are added regarding to Barghahn et al., 2023 and van der Linde et al., 2012. Heatmap was created with Morpheus (clue.io/Morpheus; Subramanian et al., 2017). Asterisks indicate significance in comparison to MAP1 (p-value < 0.05, Log_2FC > 1 or < -1 respectively).

3. Discussion

Serine proteases (subtilases, SBTs) have been shown to play pivotal roles in plant immunity. They directly target the pathogen, like the apoplastic NbSBT5.2, which releases and degrades flagellin resulting in the induction immune responses (Buscaill et al., 2024). Furthermore, different SBTs were shown to be responsible for the release of signaling peptides, like SCOOPs, and for the transduction of immune responses (Buscaill et al., 2024; Chen et al., 2024; Yang et al., 2023). A substantial number of serine proteases have already been identified in Arabidopsis and several examples have been also documented in tomato and *N. benthamiana* (Paulus et al., 2020; Schaller et al., 2018; van der Hoorn & Klemenčič, 2021). Even though maize is an important crop, the responses and interactions of subtilases in maize immunity are still poorly understood. Thus, this study investigates the early activity of serine proteases in maize, within the first 24 hours, upon SA treatment, which is an important phytohormone in immunity. Further, the release of peptides was analyzed with the focus on signaling peptides to find potential yet undiscovered phytocytokines.

3.1 SA treatment leads to an increase in subtilase activity

Serine proteases, and in particular subtilases (subtilisin-like proteases), have been shown to play crucial roles in growth, development and plant immunity (Schaller et al., 2018). In this study an increase in serine hydrolase activity in maize 3 hours after SA infiltration was demonstrated indicating that SHs are involved in the rapid response to this phytohormone. Similarly in *Arabidopsis* the subtilase SBT3.3 has been shown to be activated during pathogenic attacks which is linked to SA-dependent responses (Gil et al., 2005; Schaller et al., 2018). Besides, in tomato, the subtilisin-like protease P69B has been shown to be induced by SA treatments (Filippova et al., 2019; Tornero et al., 1996). A distinct pattern of timing is not mentioned in these studies. Nevertheless, it would be interesting to figure out if there are differences and commonalities in timing and response of SHs between different plant species.

Three subtilases, namely ZmSBT7 (Zm00001eb050140), ZmSBT1.9 (Zm00001eb082810), and ZmSBT4 (Zm00001eb314120), were enriched after SA treatment compared to the control suggesting a higher activity, as increased abundance

might correlate with higher enzymatic activity. Interestingly, the activity of these subtilases was reduced when the serine protease inhibitor PMSF was co-infiltrated with SA indicating their potential function as active proteases upon SA treatments. Unfortunately, the pull-down assay using the FP-probe did not directly lead to the identification of active SA-responsive SHs as most proteins were also unspecifically bound to the beads in the NPC. In grapevine varieties, the use of the serine protease inhibitor PMSF was shown to increase infection rates by the biotrophic oomycete *Plasmopara viticola* highlighting the importance of PMSF-sensitive subtilases in defense responses to biotrophic pathogens (Gindro et al., 2012). This leads to the suggestion that also in maize PMSF sensitive subtilases might play a significant role in immunity and the plant's response to biotrophic pathogens. All these subtilases contain the SBT typical peptidase S8 domain, which features a conserved α/β-fold structure that supports the subtilase typical Asp/His/Ser catalytic triad and stabilizes the active site, which is important as S8 are mainly secreted to the harsh environment of the apoplast (Hou et al., 2023; Rawlings et al., 2018). In addition, they possess a Protease Associated (PA) domain which is typically found as an insert in various proteases and functions as a lid-like structure that shields the active site of the protease. They also feature a fibronectin type III (Fn3)-like domain which may enhance the enzyme's flexibility enabling it to bind to a broad range of substrates and cell receptors (Hou et al., 2023; Luo & Hofmann, 2001; Siritapetawee et al., 2022). Furthermore, all three subtilases contain an inhibitor I9 domain, which must be cleaved to activate the protease (Hohl et al., 2017; Hou et al., 2023).

A direct link between the identified subtilases and the previously demonstrated PLCP activity at 24 hpi in the apoplast seems unlikely due to the temporal distance. The subtilases described in this study are already active three hours after SA treatment, and the general increased activity of SHs is already gone at 6 hpi. Nevertheless, individual subtilases may be active at later stages of SA treatment, as the resolution of the ABPP does not allow to quantify the activity of single SHs. In addition, individual PLCPs may be active at earlier stages than 24 hpi after SA treatment. Further experiments may reveal a potential proteolytic cascade. Thus, a direct connection between subtilases and PLCP, as in tomato for P69B and Rcr3 (Paulus et al., 2020), can neither be proven, nor excluded.

Interestingly, the release of SIGGI from its precursor protein MIF is dependent on PMSF-sensitive proteases since the co-infiltration of SA with PMSF did not yield in apoplastic SIGGI, while SIGGI was present in the apoplast at 3 hpi upon SA infiltration. This is also in line with the increased activity of SH at 3 hpi upon SA treatment. In an initial experiment it was shown that recombinant MIF is cleaved by apoplastic proteases, where the most proteases are inhibited by an inhibitor mix, excluding PMSF and other SBT inhibitors. The addition of PMSF resulted in the stability of MIF. This experiment indicates that MIF is directly targeted by PMSF-sensitive proteases. However, to prove that SIGGI is released through the action of PMSF-sensitive proteases, additional experiments are needed. Nevertheless, transcription analysis revealed that SIGGI induces the gene expression of the PLCPs CP1A and CP1B at 2 hpi. An increase in expression does not directly lead to an increase in protease activity as the transcript needs to be translated into a protein. Furthermore, proteases are translated as proproteases (zymogens) and need to be cleaved to be activated (Richau et al., 2012). However, an increase in gene expression indicates that SIGGI might be responsible for an increased PLCP activity before 24 hpi. This might be indicative of a link to PLCP activation 24 hours upon SA treatment through the activity of SBTs.

3.1.1 Three apoplastic subtilases are activated upon SA-treatment

During the course of this project, the three subtilases, ZmSBT7, ZmSBT1.9, and ZmSBT4, have been identified as being more abundant upon SA treatment. These subtilases cluster in a group containing 13 members within the subtilase family demonstrating their close phylogenetic relationship but also indicating potential similarities in their roles in immunity. This group of 13 SBTs can also be found in previously published phylogenetic analyses which compared maize SBTs with those from rice and Arabidopsis based on their structural features (Hou et al., 2023). The phylogenetic relationship of subtilases can provide insights into their fundamental functions particularly when considering the annotation of orthologous sequences. Moreover, this cluster contains additional candidates that may be involved in SA and pathogen-related responses.

The subtilisin-like protease ZmSBT7 (Zm00001eb050140) was identified as one of the three subtilases with significantly increased activity three hours after treatment with SA. So far, neither the function, the regulatory role nor the substrate of ZmSBT7 are known. The orthologue of ZmSBT7 in Arabidopsis is AtSBT1.7. AtSBT1.7 has been shown to release the flg22 epitope from flagellin, which is then perceived by the plant through the PRR FLS2 (Matsui et al., 2024). Additionally, AtSBT1.7 is involved in the processing of the CLE40 signaling peptide, a key regulator of stem cell differentiation in Arabidopsis (Stührwohldt et al., 2020). In the wild tomato *Solanum chilense*, the orthologue SchSDD1-like has been implicated in stomatal development and regulation of stomatal opening. Regulation of stomatal opening and closure is an important aspect of plant immunity as stomata represent a natural opening and could allow pathogens to overcome the plant cell wall and colonize the plant apoplast (Hou et al., 2023; Morales-Navarro et al., 2018; Zeng et al., 2010). The activation of ZmSBT7 upon SA treatment and the functional roles of its orthologues in Arabidopsis and wild tomato suggest a potential link to immunity and release of peptides.

Second, the subtilase ZmSBT4 (Zm00001eb314120) was found to be more abundant in maize at 3 hpi following SA treatment compared to mock treatment. Furthermore, its activity was reduced in response to co-infiltration of SA and PMSF compared to infiltration of SA alone indicating that ZmSBT4 is sensitive towards PMSF. Sensitivity towards PMSF is a characteristic of subtilases (Rawlings et al., 2018). In maize, ZmSBT4 is also known as ZmSPS8.1.4 and ZmSBT43, and the expression was reported to be downregulated under drought stress conditions (Cui et al., 2023; Hou et al., 2023). The Arabidopsis orthologue of ZmSBT4 is AtSBT1.8, and has been shown to be involved in the processing of the peptide regulator Twisted Seed 1 (TWS1), which plays a role in embryonic cuticle formation (Hou et al., 2023; Royek et al., 2022). Another orthologue in pineapple (*Ananas comosus*), AcoSBT1.12, was shown to negatively influence flowering (Hou et al., 2023; Jin et al., 2021). Specifically, AcoSBT1.12 is expressed in pineapple leaves and flowers and its overexpression in Arabidopsis leads to a delayed flowering phenotype. Furthermore, transient expression of AcoSBT1.12 in tobacco revealed its localization in the plasma membrane (Jin et al., 2021). While the function of ZmSBT4 or its orthologues in SA-regulated immune responses has not yet been demonstrated, the observed

changes in its abundance upon SA treatment suggest a potential involvement in immunity and release of signaling peptides. Further experiments are needed to clarify whether ZmSBT4's activation in response to SA treatment is specifically related to immunity and how it may contribute to the regulation of stress and defense mechanisms in maize.

ZmSBT1.9 (Zm00001eb082810) is the third subtilase, which was found to be more abundant upon SA treatment in comparison to the control. Until now, the function of ZmSBT1.9 has not been described maize. However, the ortholog in wheat (*Triticum aestivum*), namely TaSBT1.7, was shown to be involved in stripe rust resistance, which is caused by the biotrophic fungus *Puccinia striiformis* f. sp. *tritici*. Overexpression of TaSBT1.7 in *N. benthamiana* resulted in necrotic cell death, whereas knocking down *TaSBT1.7* in wheat using virus-induced gene silencing compromised the HR and resistance against *P. striiformis* f. sp. *tritici*, (Hou et al., 2023; Yang et al., 2020). Furthermore, the expression of *TaSBT1.7* is induced in wheat leaves by chitin and flg22, indicating that this SBT might not only play a role in responses to fungal pathogens but also to bacteria. It might be possible that ZmSBT1.9 has a comparable role in mediating defense responses against biotrophic pathogens as TaSBT1.7. Further research will be necessary to show whether ZmSBT1.9 contributes to resistance against biotrophic pathogens.

The phylogenetic analysis revealed that ZmSBT1.9 is closely related to ZmSBT49 (Zm00001eb366650) and ZmSBT48 (Zm00001eb348590). The orthologue of ZmSBT49 in tomato (*Solanum lycopersicum*), SlSBT3, has been shown to regulate pectin methylesterases. Moreover, SlSBT3 was found in its active form in the gut of insects feeding on tomato plants suggesting a role in defense against insect feeding (Cedzich et al., 2009; Hou et al., 2023; Ribeiro et al., 1995). The overexpression of three orthologous genes (SlPhyts3/4/5) of ZmSBT48 in tomato leaves resulted in cell death under oxidative conditions (Hou et al., 2023; Reichardt et al., 2018). These findings suggest that further comparison and phylogenetic analysis of apoplastic subtilases in maize may uncover additional candidates involved in SA-mediated responses to biotrophic pathogens.

3.2 Number of SA specific apoplastic peptides underline importance of peptides in SA signaling

Several apoplastic peptides were found within this work to be enriched upon SA-treatments compared to the control, making many of them potential phytocytokine candidates. The presence of these peptides in the APF demonstrates the relevance of apoplastic communication in the activation of signaling responses which we monitored by the expression of *PR*-genes associated with SA responses. It has been shown that several phytocytokines induced *PR*-gene expression or other SA marker genes, such as ZmZip1, ZmIRP, ZmPSK1e and ZmPIP1 in maize (Koenig et al., 2023). Also, in different plant species many phytocytokines were found in SA related responses like the PIPs and RALFs in Arabidopsis or Systemin in Tomato (Hou et al., 2014; Huffaker et al., 2006; McGurl et al., 1992; Yamaguchi et al., 2011). This broad range of known phytocytokines indicates the potential of unknown peptides in the APF. Therefore, 14 candidates (PC1-PC13 and SIGGI) representing potentially novel phytocytokines were synthesized and tested them for their implication in triggering *PR*-gene expression and their modulation of the virulence of a biotrophic fungus.

3.2.1 Four apoplastic peptides induce *PR*-gene expression but do not alter virulence of *U. maydis*

From the 14 tested PCs, six (PC1, PC10, PC11, PC12, PC13 and SIGGI) induced SA-associated *PR*-gene expression. This suggests that these peptides play a role in transducing SA-related signals during plant immunity (Goodluck et al., 2022). PC1, PC10 and PC11 were also tested in the trojan horse approach which is an *in vivo* delivery system of peptides in the apoplast during infection with recombinant *U. maydis* strains. Using this system, a direct effect of peptides can be tested in plant responses on the biotrophic fungus (Koenig et al., 2023; van der Linde et al., 2018b). In this approach the three tested peptides PC1, PC10 and PC11 did not alter the virulence of *U. maydis* in comparison to the solopathogenic strain SG200. Therefore, these peptides have a signaling function, as they induce *PR*-gene expression, but do not alter *U. maydis* infection. As *U. maydis* secrets during infection a wide range of effectors to suppress and overcome host immunity, it is also possible, that the responses induced by these peptides

is directly targeted by *U. maydis* effectors (Brefort et al., 2009; Hemetsberger et al., 2012; Misas Villamil et al., 2019). Further investigations of these peptides may elucidate their mechanisms of activation of immunity. Since they do not alter the virulence of *U. maydis*, I focused on the two peptides SIGGI and PC13 which showed an alteration of the virulence of *U. maydis*.

3.2.2 SIGGI acts as pro-life signal and increases virulence of the biotrophic pathogen *U. maydis*

Upon treatments with SIGGI an upregulation of *PR*-gene expression was shown indicating its role in plant immunity. However, the *in vivo* delivery of SIGGI using *U. maydis* resulted in a significant increase in virulence of this biotrophic fungus. This phenotype is a completely new finding as so far peptide expressing *U. maydis* strains led either to no change or a reduced virulence in comparison to SG200, like the maize phytocytokines Zip1, ZmPSK1, ZmPRP1, and ZmIRP (Koenig et al., 2023; Ziemann et al., 2018). The peptide SIGGI is derived from the proprotein Macrophage Migration Inhibitory Factor (MIF). MIF was initially discovered in vertebrates including humans and is a pleiotropic pro-inflammatory cytokine, which has since been implicated in a wide range of inflammatory processes (Bloom & Bennett, 1966; Sumaiya et al., 2022; Weiser et al., 1991). In humans, MIF is predominantly localized to the cytoplasm where it is induced by various pro-inflammatory factors, including lipopolysaccharide (LPS), tumor necrosis factor (TNF)-α, hypoxia, hydrogen peroxide (H_2O_2) and thrombosis. Also, glucocorticoids (GCs) acting as a GC counter-regulator to modulate inflammation and immunity induce MIF (Leng et al., 2009; Sun et al., 2013). Furthermore, the expression of MIF is tightly regulated by many TFs, like Nuclear factor kappa B (NF-κB) (Zeng et al., 2024). MIF has been shown to promote the activation of macrophages and T-cells, as well as to contribute to cell death with a nucleic acid enzymatic activity (Lue et al., 2002; Zeng et al., 2024). In addition, MIF plays a vital role in promoting inflammatory responses including the chemo-attractive effect on immune cells, the production of proinflammatory cytokines and stress molecules (Kong et al., 2022; Lue et al., 2002; Sumaiya et al., 2022). For example, MIF regulates LPS-mediated host responses, which are induced by Lipopolysaccharides (LPS) of Gram-negative bacteria, in an autocrine manner by

upregulating the Toll-like receptor 4/myeloid differentiation factor 2 (TLR4-MD2) expression (Roger et al., 2001, 2003). Also, MAPK are activated by MIF thereby promoting the release of interleukin (IL)-6, IL-1β, and TNF-α in cancers, renal inflammation, and neuroinflammation (Zeng et al., 2024).

Although homologs of MIF have been identified in plants, its function in plants remains unclear (Zhao et al., 2021). In wheat (*Triticum aestivum*), TaMIF1 exhibited tautomerase activity which was comparable to the activity of MIF from *Mus musculus* in *in vitro* experiments (Zhao et al., 2021). The BCL2-associated X (Bax) protein from mammals has been shown to induce programmed cell death (PCD) when expressed in plants. Co-expression of Bax with TaMIF1 in *N. benthamiana* did not result in cell death, indicating that the cell death induced by Bax was successfully suppressed by TaMIF1. The mechanism of the suppression of cell-death and if the tautomerase activity of TaMIF1 is crucial for this phenotype remains to be elucidated (Zhao et al., 2021). Until now, it is not known whether ZmMIF1 also possesses tautomerase activity. Based on sequence homology, one of SIGGIs isoleucine residues is part of the catalytic site in the human MIF and thus, it would be interesting to investigate whether is possess tautomerase activity (Spiller et al., 2023). It is tempting to speculate that the release of SIGGI from ZmMIF in maize may disrupt a potential tautomerase activity. Also, ZmMIF1 and TaMIF1 show high sequence similarities and also the SIGGI peptide identified in maize can be found in TaMIF1 with the exchange of the second isoleucine to leucin. If the suppression of PCD by TaMIF1 is related to the release of a SIGGI-like peptide, a suppression of cell-death in maize caused by SIGGI would be conceivable. This could also be an explanation of the increased virulence of *U. maydis* strain secreting SIGGI. During initial infection of *U. maydis*, a small fraction of epidermal cells was observed to undergo cell death indicating that not all hyphae were capable of establishing a biotrophic interaction (Doehlemann et al., 2008). A cell-death suppression by SIGGI would be beneficial for these hyphae and positively affect the establishment of the biotrophic interaction. As a consequence, more hyphae would be able to successfully infect the cell which, in turn, would result in an increased virulence of *U. maydis*. However, the function of ZmMIF and its potential tautomerase activity remains to be elucidated and requires further investigation. Future experiments may reveal the ability of SIGGI to suppress PCD.

In recent studies three MIF orthologs (MIF/D-DT-like proteins, MDLs) in Arabidopsis were found and shown to be involved in flowering time and innate immunity. The details of how these two processes interacted with these three proteins are not yet understood (Gruner et al., 2021). Here, SIGGI was shown to induce SA biosynthesis related genes. As the peptide SIGGI was found in the apoplast upon SA treatment, it seems likely that the peptide is part of the downstream responses induced by SA. At 6 hpi upon SIGGI treatment, three genes (Zm00001eb042820, Zm00001eb125120, Zm00001eb410260) are found to be up-regulated which are associated with SA biosynthesis. The three genes encode for the transcription factor SAR DEFICIENT 1 (SARD1) and two structurally related proteins. SARD TFs were shown to induce the expression of isochorismate synthase (ICS) genes in Arabidopsis (Zhang & Li, 2019). ICSs are important regulators of pathogen-induced SA accumulation and SAR (Wang et al., 2011). They catalyze the conversion of chorismate to isochorismate which is then converted to SA (Strawn et al., 2007). Loss of ICS1 in Arabidopsis is sufficient to abolish pathogen-induced SA accumulation and SAR (Wildermuth et al., 2001). This indicates that SIGGI might induce the biosynthesis of SA and therefore might form a positive feedback loop. The accumulation of phytohormones in response to other phytocytokines was described in previous studies. The maize specific phytocytokine Zip1 activates SA signaling pathways and induces the accumulation of SA (Ziemann et al., 2018). Notably, the genes encoding for SARD1 are also up-regulated in response to Zip1, at 24 hpi further supporting the hypothesis that SIGGI might induce SA biosynthesis. Besides, Arabidopsis PIP1 promotes the expression of genes involved in SA biosynthesis including SARD1 (Hou et al., 2019). The phytocytokine AtPep1 has been shown to activate both SA and ET/JA signaling pathways, thereby promoting plant resistance to biotrophic and necrotrophic pathogens (Liu et al., 2013; Yamaguchi et al., 2010). In contrast, PSK, PSY1, and RALF have been shown to activate the JA signaling pathway in Arabidopsis, thereby enhancing plant resistance to necrotrophic pathogens and/or compromising plant resistance to hemibiotrophic pathogens (Guo et al., 2018; Mosher et al., 2013). The potential induction of SA biosynthesis upon SIGGI treatment is in contrast to the observed increased virulence of *U. maydis* in the presence of SIGGI, as SA is a key regulator of plant immunity particularly in defense against biotrophic pathogens like *U. maydis* (Brefort et al., 2009;

Misas Villamil et al., 2019; Pieterse et al., 2012). SA typically promotes immune responses by activating various defense mechanisms such as the expression of *PR*-genes and the reinforcement of plant cell walls, which should ideally limit pathogen growth and reduce virulence (Kahmann & Kämper, 2004; Pieterse et al., 2012; Spoel & Dong, 2024a). Therefore, one might expect that enhanced SA production would result in a stronger defense response leading to decreased pathogen virulence. The observation of enhanced virulence suggests that the mechanisms *U. maydis* has evolved to evade and suppress the host's SA-mediated immune responses are sufficient to overcome the SIGGI induced responses. *U. maydis* secretes effector proteins that can interfere with host immune signaling including the SA pathway and consequently, facilitate infection. One example is the effector chorismate mutase 1 (UmCmu1) which is taken up by the plant cell. The presence of UmCmu1 leads to a reduced SA level as it modifies chorismate homeostasis (Djamei et al., 2011). The activity of plant peroxidases and thereby generation of ROS is suppressed by the *U. maydis* effector essential during penetration-1 (UmPep1) (Doehlemann et al., 2009; Hemetsberger et al., 2012). This ability of *U. maydis* to overcome SA-mediated immunity highlights a complex interaction between the plant and a well-adapted biotrophic pathogen.

In addition to the interference with the SA pathway and ROS production, *U. maydis* needs to decrease PLCP activity to facilitate infection (Misas Villamil et al., 2019; Mueller et al., 2013). Therefore, *U. maydis* secretes effectors such as UmPit2 which have been demonstrated to inhibit PLCPs. The negative impact of SIGGI on PLCP activity in conjunction with UmPit2 could result in enhanced PLCP inhibition and consequently, contribute to the enhanced virulence phenotype. Interestingly, treatments with Zip1, ZmIRP, ZmPSK, and ZmPIP1 resulted in enhanced activity of various PLCPs and *U. maydis* strains expressing these peptides show an reduced virulence (Koenig et al., 2023; Ziemann et al., 2018). Upon SIGGI treatments the upregulation of the PLCP inhibitor genes *Corn Cystatin 6* (*CC6*) and *CC7* at 24 hpi and *CC9* at 12 hpi was shown. As infections with an *U. maydis* strain expressing CC9 did not alter the virulence in comparison to the solopathogenic strain SG200 (van der Linde, 2011), it is possible that CC6 and CC7 may target different PLCPs than CC9 and UmPit2, and therefore take a part in the increased virulence. To verify whether PLCP activity is further decreased in

the presence of SIGGI, PLCP activity should be tested in maize plants infected with SG200 and SG200 expressing SIGGI.

Although the activity of PLCPs upon SIGGI treatment is decreased at 24 hpi, the RNASeq analysis revealed that SIGGI treatments causes an increased expression of the genes encoding for the PLCPs *CP1A* and *CP1B* at 2 hpi. An increase in expression does not directly lead to an increase in protease activity as the transcript needs to be translated into a protein. Furthermore, proteases are translated as proproteases (zymogens) and need to be cleaved to be activated (Richau et al., 2012). However, an increase in gene expression might indicate another important role of PLCPs in the downstream response of SIGGI like proteolysis. GO-Term analysis showed that many genes associated with ubiquitination were upregulated two hours after SIGGI treatment followed by proteolysis at 12 hpi. The up-regulated genes at 2 hpi are mainly E3 ubiquitin ligases. Those enzymes are the most abundant ubiquitin enzymes in plants and transfer the ubiquitin protein to the target protein which is degraded (Craig et al., 2009). They can be classified according to their mechanism of action and the presence of specific domains in different classes, including RING (Really Interesting New Gene), HECT (Homologous to E6-associated protein C-Terminus), F-box and U-box (Yee & Goring, 2009). Following SIGGI treatment, two main types were identified as being up-regulated, namely E3 ligases with either a U-box domain (e.g. pub61 (Zm00001eb385250), pub45 (Zm00001eb425310), pub83 (Zm00001eb371590)) or a RING domain (e.g. arm6 (Zm00001eb190130), arm15 (Zm00001eb149420) or arm16 (Zm00001eb368740)). The specific functions of the identified E3 ubiquitin ligases are not known. In general, the U-box family is associated with a wide range of functions in plants including self-incompatibility, hormone responses, defense mechanisms and abiotic stress responses (Mao et al., 2022). For instance, Arabidopsis is predicted to have 64 plant U-box (PUB) proteins and the biological roles of many of these remain to be elucidated (Mao et al., 2022; Yee & Goring, 2009). U-Box proteins contain a domain for substrate recognition such as armadillo (ARM) repeat domains, which are located at the C-terminus (Craig et al., 2009). The RING and U-box proteins are structurally related. Sequence and predicted secondary structure analyses revealed that the U-box is a modified RING-finger domain, although the scaffold-stabilizing, zinc-chelating cysteine and histidine residues are lacking which are

characteristically conserved in the RING domain (Yee & Goring, 2009). Both, U-Box and RING domain, utilize zinc chelation and hydrogen bonds/salt bridges to facilitate the transfer of ubiquitin to the target (Yee & Goring, 2009). In recent years, it has been revealed that ubiquitination of proteins plays a critical role in the regulation of plant immunity (Gao et al., 2022). Ubiquitination of immune receptors and RLCKs is important to maintain the immune signals at a certain threshold (Gao et al., 2022). In Arabidopsis, the U-box E3 ubiquitin ligases AtPUB12 and AtPUB13 are involved in the polyubiquitination of AtFLS2 which results in its degradation in response to flagellin perception. Notably, *atpub12* and *atpub13* mutants displayed increased immune responses to flagellin treatment (Lu et al., 2011). Also, the protein level of the well-characterized NLR SUPPRESSOR OF npr1-1 CONSTITUTIVE 1 (SNC1) in Arabidopsis is regulated by ubiquitination and proteasomal degradation. A mutation in the E3 Ubiquitin Ligase CONSTITUTIVE EXPRESSOR OF PR GENES 1 (CRP1) leads to an accumulation of SNC1 and an autoimmune phenotype (Thulasi Devendrakumar et al., 2019). RLCK activation frequently results in the influx of Ca^{2+}, production of ROS and the activation of MAPK cascades. These processes signal downstream components and suppress pathogen growth. A strict regulation of immune responses and downstream signaling is important to restore normal growth and function after successfully defending against pathogens and maintaining a balance between defense and growth. These initial immune responses can be precisely calibrated through ubiquitination. For example, it was shown that ubiquitination can modulate ROS burst by regulating the stability of the plasma membrane-localized NADPH oxidase RbohD (DongHyuk Lee et al., 2020). Furthermore, a negative regulator of plant immunity in potato, namely potato putative K-homology RNA-binding protein StKH17, is turned over by the potato E3 ligase StPUB17 upon infection with *Phytophthora infestans* (McLellan et al., 2020).

Interestingly, many genes associated with the GO term proteolysis are upregulated at 12 hpi. This is in accordance with the finding that genes associated with ubiquitination are upregulated at 2 hpi as ubiquitinated proteins undergo proteolysis, a process in which proteins are degraded to peptides or amino acids (Yanan Liu et al., 2024b). One carboxypeptidase and the subtilase SBT41 are among those genes associated to proteolysis. The function of both proteases including their substrates has not yet been

described in maize. In Arabidopsis, the SBT41 ortholog SBT5.2 was shown to cleave and release flg22 from flagellin similar to the tobacco subtilase NbSBT5.2 (Buscaill et al., 2024; Hou et al., 2023; Matsui et al., 2024). Besides, the expression of the E3 ubiquitin-protein ligase Seven in absentia (SINA)-like 10 is upregulated. So far, the role of SINA-like 10 has not been described in maize. However, SINA E3 ubiquitin ligases were shown in the past to have different functions in various plants. In rice, OsDIS1 acts as a negative regulator of the response to drought stress (Ning et al., 2011). SINA3 of tomato plays a negative role in plant responses to *Pseudomonas* infection as it ubiquitinates NAC1 and promotes its degradation. NAC1 is a transcription factor, which is involved in plant defense responses and is upregulated upon pathogen infection (Miao et al., 2016). In Arabidopsis, SINA2 functions as a positive regulator of the ABA-dependent stress signaling pathway, whereas ABA signaling has a negative influence on SA signaling cascades (Bao et al., 2014; Chen et al., 2018; Pieterse et al., 2009). Although the exact function of the genes up-regulated in response to SIGGI is not known, it seems that SIGGI has an influence on ubiquitination and proteolysis which may in turn regulate immune responses.

This study suggests that SIGGI acts as a pro-life signal as it might inhibit cell death as observed for TaMIF1 and induce innate immunity through the upregulation of SA biosynthesis. As a pro-life signal SIGGI would also be beneficial for *U. maydis* infection as it would reduce cell death in response to the biotrophic fungus. It seems that PLCP activity is tightly regulated by transcription and expression of PLCP inhibitors e.g. CC6, CC7 and CC9, which also correlates with the upregulation of ubiquitination and proteolysis associated genes. Future investigations will help to understand the mechanisms and illuminate these interactions.

3.2.3 PC13 proprotein is likely to be involved in SA mediated stress responses

PC13 is part of the maize proprotein ZmSAP7. ZmSAP7 is part of SAP family proteins of which 10 have been identified in maize (Fu et al., 2022). They contribute to responses to various abiotic and biotic stimuli in plants (Fu et al., 2022; Su et al., 2022). Two recent studies investigated the expression of ZmSAP7 in response to different stresses and obtained contradictory results. In response to salt treatments, ZmSAP7 was shown to be

down-regulated in the study of Fu et al., while it was shown to be up-regulated by Su et al. The different growth conditions used in the two studies might explain the contradictory results. However, both studies predict cis-acting elements in the promoter region of ZmSAP7. These cis-acting elements are associated with stress responses as well as SA and MeJA responses (Fu et al., 2022; Su et al., 2022).

In plants, OsSAP1 from rice was first identified as an A20/AN1 zinc finger protein. This protein has been shown to accumulate upon various stresses including low temperatures, desiccation, salt, submergence and exposure to heavy metals as well as injury (Mukhopadhyay et al., 2004). Using a sequence similarity approach with OsSAP1 as a reference, 18 *SAP* genes in rice (*OsSAPs*) and 14 *SAP* genes in Arabidopsis (*AtSAPs*) were found (Vij & Tyagi, 2006). Expression analysis of most of these *OsSAPs* and *AtSAPs* revealed an induction of those genes by abiotic stress such as drought, salt and temperature (Hozain et al., 2012; Huang et al., 2008; Kang et al., 2011; Kanneganti & Gupta, 2008; Ströher et al., 2009). Besides rice and Arabidopsis, SAPs were found in nearly all plants including e.g. tobacco, banana, potato or *Medicago truncatula* (Charrier et al., 2013; Duceppe et al., 2012; Giri et al., 2013; Kanneganti & Gupta, 2008; Lloret et al., 2017). Interestingly, it was demonstrated that the activity of PaPha13, a homolog of AtSAP5 in orchid (*Phalaenopsis aphrodite*), was positively influenced by SA. Additionally, both homologs PaPha13 and AtSAP5 are involved in the induction of *NPR1* expression (Ben Saad et al., 2024; Chang et al., 2018). NPR1 binds SA and serves as a transcriptional co-activator and influence the activity of TFs which regulate the transcription of SA responsive genes (Fan & Dong, 2002). Interestingly, the transcriptome analysis upon PC13 treatment revealed the upregulation of the regulatory protein NPR1 (Zm00001eb121040). Furthermore, NPR1 is also recruited to JA-responsive promoter regions and inhibits transcriptional activation of JA-responsive genes by the transcription factor MYC2. Thus, NPR1 also acts as a repressor of JA-responsive MYC2 (Wu et al., 2012; Zavaliev & Dong, 2024). Upon PC13 treatment the expression of genes associated to the regulation of JA mediated signaling pathway as well as cellular responses to JA stimulus and responses to JA and wounding is induced. Next to NPR1, all these genes encode for Zinc finger protein expressed in Inflorescence Meristem (ZIM)-TF which have recently been renamed regarding their conserved core

motif TIF[F/Y]XG to TIFY (Singh & Mukhopadhyay, 2021; Zhang et al., 2023). TIFY-TFs regulate various biological processes including responses to stress, defense mechanisms and hormonal signaling (Zhang et al., 2023). In maize, one subfamily of TIFY-TF are JAZ proteins, which inhibit crucial TFs of the JA pathway and therefore act as repressors of the JA signaling pathway (Ghorbel et al., 2021b; Sun et al., 2021). The JAZ subfamily also orchestrates the cross talks between other phytohormones like SA and ethylene, as they inhibit the TFs MYC and ERF (Ghorbel et al., 2021b; Singh & Mukhopadhyay, 2021). The upregulation of genes by PC13 that are known to be involved in the repression of the JA-signaling pathway suggests that PC13 is a possible negative regulator of JA responses and JA mediated signaling pathways. Furthermore, PC13 was shown to induce the expression of the activator of SA-signaling NPR1. This is in accordance with the finding that PC13 was found upon SA treatments and that SA and JA pathways act antagonistically (Pieterse et al., 2012; Wasternack & Song, 2017). Upon infections with biotrophic pathogens like *U. maydis*, SA signaling including NPR1 gets activated and the antagonistic JA pathways get repressed (Barna et al., 2012; Doehlemann & Hemetsberger, 2013; Pieterse et al., 2009).

SAPs were first discovered in humans and the african clawed frog (*Xenopus laevis*) and demonstrated to play key roles in innate immunity and cell death (Lee et al., 2000; Opipari Jr et al., 1990). The ZNF216 protein, which is the structural equivalent in humans to plant SAPs, was shown to be an inhibitor of NFκB activity (Huang et al., 2004). The transcription factor NFκB plays critical roles in regulating the immune system inducing inflammatory responses and preventing apoptosis. NFκB is activated by IκB kinase, a complex consisting of two catalytic subunits, namely IKKα and IKKβ, and a non-enzymatic regulatory subunit, namely IKKγ, which is inhibited by the ZnF-A20 domain of ZNF216 (Huang et al., 2004). The ZnF-AN1 domain is a ubiquitin-like domain and interacts with E3-ligase tumor necrosis factor-6 (TRAF6), which targets the Transforming growth factor-β activated kinase-1 (TAK1). The ubiquitination leads to the degradation of TAK1 and therefore prevents the activation of NF-κB (Huang et al., 2004; Landström, 2010; Linnen et al., 1993). Both domains, ZnF-A20 and ZnF-AN1, are structurally related in ZmSAP7 (Fu et al., 2022; Su et al., 2022) suggesting a similar activating role in cell death in maize. In accordance to this, the transcriptome analysis revealed that PC13 induced the

expression of six genes associated to PCR and HR at 2 hpi. Four of these genes (Zm00001eb153200, Zm00001eb180480, Zm00001eb241040, Zm00001eb267380) encode for proteins possessing a membrane-attack complex/Perforin (MACP) domain. In total, nine genes encoding for proteins harboring a MACP domain have been identified in maize (Yu et al., 2020). Unfortunately, their expression pattern and their functions remain to be elucidated. Overexpression of AtMACP2 in Arabidopsis suggests that the protein induces PCD, bacterial pathogen resistance, and necrotrophic fungal pathogen sensitivity as necrotic lesions were increased in the overexpression lines upon pathogenic infections. Furthermore, it seems to promote pathogen resistance by activating SA signaling (Zhang et al., 2022). In mammals, the MAC domain is known to create oligomeric pore structures on the cell surface during pathogen infection and subsequently, cause cell death and inflammatory responses (Morgan, 2016). This function and molecular mechanism of MACP proteins in plants is not described yet (Zhang et al., 2022). The other two genes Zm00001eb272020 and Zm00001eb313140 encode for the LAZARUS 1 (LAZ1) protein and a yet uncharacterized gene, respectively. In Arabidopsis, AtLAZ1 has previously been shown to modulate PCD (Malinovsky et al., 2010). Additionally, it was revealed that the gene *AtSARD6* actually encodes for AtLAZ1 and was found to be a positive regulator of biosynthesis genes of SA and N-hydroxypipecolic acid (NHP), which are two key signaling molecules in SAR (Chen et al., 2024). Furthermore, overexpression of either AtLAZ1 or the respective homologs from *N. benthamiana* and potato in *N. benthamiana* resulted in an enhanced resistance against *Phytophthora* pathogens (Chen et al., 2024). Although an up-regulation of PCD and HR related genes was detected upon PC13 treatment, no macroscopic cell death in response to PC13 treatment was observed. The transcription of a gene does not subsequently lead to an active protein. It might be possible that another trigger or another component is necessary to induce PCD or HR. The missing zinc-finger domains A20 and AN1 may play an important role in the induction of cell death responses as it was demonstrated in human. The two ZnF domains A20 and AN1 are connected in one protein but need to dissociate from each other to enroll their function and the inhibition of NF-κB (Huang et al., 2004; Donghoon Lee et al., 2023). Due to the presence of ZnF-AN1 and ZnF-A20 in ZmSAP7, it is tempting to speculate that ZmSAP7, similarly to ZNF216

from humans, might also be involved in the inhibition of a transcription factor, which is associated with cell death responses. PC13 is part of the linker of these two domains in plants and the release of PC13 from its proprotein would consequently cause the dissociation of the two domains. The released peptide PC13 might then directly fulfill a signaling task and act as phytocytokine in the apoplast. This hypothesis is underlined by a blast research based on the peptide sequence, which revealed a strong conservation for the peptide in monocotyledons with maximum one amino acid exchange. Conservation of structures or sequences correlates mostly with conserved functions.

Taken together, one can conclude that PC13 might act as pro-death signal as it induces genes associated to the GO Terms PCD and HR. Even though a cell death phenotype was not observed, the association of the proprotein SAP7 underlines the hypothesis as well the reduced virulence of *U. maydis* in presence of PC13 might be explained with induced PCD.

3.3 Future perspective of the project

During the course of this project, a general activation of SHs at 3 hpi upon SA treatment was observed which decreased again at 6 hpi. In order to obtain a deeper insight into the activity of SHs in SA signaling, the activity of SHs in response to exogenous application of SA should be analyzed between 1 and 5 hpi. In combination with an improved protocol for the pulldown e.g. more washing steps or using more harsh chemicals for washing to reduce the number of unspecifically bound proteins, the exact determination of the time point of the highest activity could also help to reveal the identity of the activated SHs in another MS analysis.

The role of the three identified SBTs in SA signaling could not be elucidated in this work. The heterologous expression of ZmSBT7 did not yield in an active protease which might be explained with the lack of a certain trigger like SA. To test this hypothesis, *N. benthamiana* leaves expressing ZmSBT7 could be treated with SA 3h prior purification. If the purified ZmSBT7 is active upon SA-treatment, it can be concluded that the activity of ZmSBT7 is dependent on SA. If ZmSBT7 is not active, it might be possible that a molecular component for activation is needed which is present in maize but not *N. benthamiana*. ZmSBT7 is predicted to have an autoinhibitory domain and the inactive

mutant ZmSBT8 S540A shows a higher molecular weight than ZmSBT7 in Western Blot. To test whether the inactive mutant is not able to cleave the inhibitory domain, mass spectrometry of the purified protein could be conducted. Besides ZmSBT7, the two other identified subtilases should be characterized including their cleavage pattern. Therefore, the proteomic identification of protease cleavage sites (PICS) method could be used which uses a proteome-derived library and followed by mass spectrometry to identify preferred cleavage sites. This might help to identify potential targets of the SBTs.

In tomato, a proteolytic cascade in which PLCPs are activated by a serine protease was identified. A similar cascade for maize could not be identified in this project. In order to test whether the early activation of SHs leads to a subsequent activation of PLCPs, leaves of maize plants could be co-infiltrated with SA and PMSF and activity of PLCPs should be tested with an ABPP using the fluorescent probe DCG-04-Cy5. The absence of PLCP induction would indicate that PMSF-sensitive SHs induce PLCPs.

The identified phytocytokines PC13 and SIGGI are thought to act as pro-death and pro-life signal, respectively. TaMIF is able to suppress Bax-induced cell death (Zhao et al., 2021). One approach to test their potential involvement in cell death could be to test whether PC13 and SIGGI are able to influence of Bax-induced phenotype in *N. benthamiana*. Additionally, their ability to induce cell death could be investigated by infiltrating maize leaves with the respective peptide with a syringe. The observation of cell death upon syringe infiltration of PC13 would be in accordance with an upregulation of genes associated to cell death and HR. To test the involvement of the two ZnF domain AN1 and A20 of SAP7 in PCD and if these domains are necessary to induce PCD with PC13, both domains could be expressed in *N. benthamiana* and the peptide PC13 could be infiltrated exogenously.

The analysis of the influence of SIGGI and PC13 on the virulence of necrotrophic pathogens represents another interesting aspect. Previously it was shown that Zip1, ZmIRP, ZmPSK1, and ZmPIP1 affect the virulence of *Botrytis cinerea* (Koenig et al., 2023). To test whether the two newly identified phytocytokines influence the virulence of a necrotrophic pathogen, maize leaves could be first treated with the respective peptide and at 24 hpi infected with droplets of conidia spores of *B. cinerea*. By quantifying the

lesion size, the influence of the peptides on infection with the necrotic fungus could be elucidated.

So far, it has not been elucidated how PC13 and SIGGI are released from their respective proproteins. As both peptides are found at 3 hpi and an increase of SH activity was observed at 3 hpi, it is tempting to speculate that both are released through SHs. To test this hypothesis, the respective proproteins could be incubated with the SHs that were shown to be activated upon SA treatment. A subsequent mass spectrometry analysis would reveal whether the proproteins were cleaved and the respective peptide released or not.

Overall, the proposed future analysis would explore the dynamic regulation of SHs and the functional characterization of peptides PC13 and SIGGI, what could reveal new insights into how maize orchestrates immune signaling in response to pathogens. It may lead to an explanation of how the variety of peptides with specific responses and may partially contradictory regulations coordinate in specialized and precise responses.

3.4 Conclusion

This study investigated early SA responses in the apoplast with regard to SH activity and phytocytokine release. Upon SA treatment, an increase in SH activity was demonstrated and three active subtilases, namely ZmSBT7, ZmSBT1.9, ZmSBT4, were identified (Fig. 2.3). Moreover, the accumulation of various peptides, including SIGGI and PC13, was detected. It is conceivable to speculate that the active SHs cleave proproteins resulting in the release of phytocytokines. The proprotein of SIGGI, MIF, was shown to be cleaved by apoplastic SBTs that might lead to the release of SIGGI. In the presence of SIGGI, genes associated to SA-biosynthesis e.g. *SARD1*, PLCPs and further defense related genes were induced (Fig. 2.17). Furthermore, *U. maydis* expressing SIGGI exhibits increased virulence that might be explained with a suppression of cell death. Taken together, this could indicate that SIGGI acts as a pro-survival signal (Fig. 3.1). Besides MIF, the proprotein SAP7 is cleaved in response to SA resulting in the release of PC13. The peptide PC13 also leads to transcriptional changes and genes associated with PCD and HR are upregulated (Fig. 2.18). Since the proprotein SAP7 from other species was previously shown to be involved in PCD and *U. maydis* expressing PC13 shows a reduced virulence, it might be possible that PC13 acts as a pro-death signal (Fig. 3.1).

In summary, this study identified two plant endogenous peptides that alert plant cells of danger and thus, can be classified as phytocytokines. These phytocytokines induce contrasting responses, which demonstrate that signaling cascades in response to SA are not always identical and require fine tuning. Future experiments will deepen our understanding of the regulation of the signaling cascades and how this is controlled.

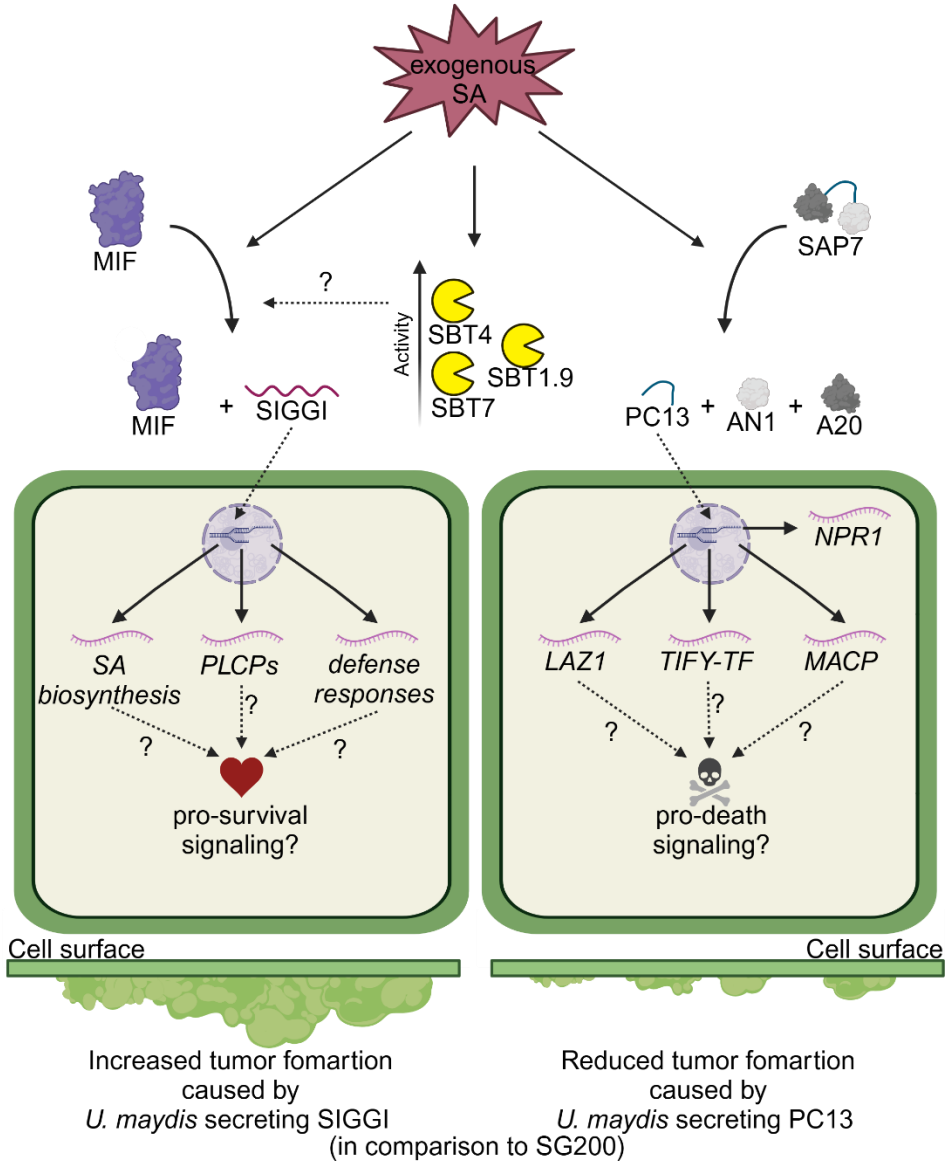

Figure 3.1: SBTs are activated and apoplastic peptides are released in response to SA. The infiltration of SA leads to the activation of the SBTs ZmSBT4, ZmSBT7 and ZmSBT1.9 and accumulation of the peptides SIGGI and PC13 in the apoplast at 3 hpi. The peptides might be released in a yet unknown cellular compartment through the action of activated SHs and lead to transcriptional changes. In response to SIGGI, SA biosynthesis and genes encoding for PLCPs as well as genes related to defense responses were upregulated. Enhanced tumor formation was observed for an U. maydis strain expressing SIGGI compared to SG200. This indicates that SIGGI might act as pro-survival signal. PC13 leads to an induction of NPR1, LAZ1, TIFY-TF and MACP genes which are involved in PCD and HR. U. maydis expressing PC13 showed a reduced tumor formation in comparison to SG200. Thus, PC13 might lead to pro-death signaling.

4. Material and Methods

4.1 Used Chemicals

All used chemicals were ordered from these following companies unless stated otherwise:
• Biozym (Hessisch Oldendorf, Germany)
• Difco (Augsburg, Germnay)
• Duchefa (Haarlem, Netherlands)
• GE Healthcare (Chicago, USA)
• Invitrogen (Carlsbad, USA)
• Merck (Darmstadt, Germany)
• Roche (Basel, Switzerland)
• Roth (Karlsruhe, Germany)
• Sigma-Aldrich (St. Louis, USA)

4.2 Buffer, Media and solutions

Unless not otherwise indicated, buffers, solutions, and media were prepared with distilled water (MilliQ) and sterilized by autoclaving for a minimum of 20 minutes at 121°C. Solutions susceptible to thermal degradation, including those containing vitamins, were filter-sterilized (0.2 µM pore size, GE Health Care Life Science, Freiburg, Germany). The recipes for buffers, solutions, and media are provided in the corresponding protocols.

Table 4.1: Composition of media used in the study

Name	Ingredients
Potato-Dextrose-Agar (PD)	3.9% (w/v) Potato-Dextrose Agar
PDA- Charcoal	Addition of 1 % (w/v) Charcoal to PD-Agar media
YEPSlight (modified from Tsukada et al., 1988)	1 % (w/v) Yeast extract 0.4% (w/v) Peptone 0.4% (w/v) Saccharose
Regeneration Agar (Schulz et al., 1990)	1.5 % (w/v) Bacto Agar 1M Sorbitol 1 % (w/v) Yeast extract 0.4% (w/v) Peptone 0.4% (w/v) Saccharose
YT-Agar	0.8 % (w/v) Tryptone 0.5 % (w/v) Yeast extract 0.5 % (w/v) NaCl 1.3 % (w/v) Agar

4.3 ABPP Probes, Inhibitors and Beads

Table 4.2: Used Probes for ABPP, inhibitors and Beads for Pull-down

Probe	**Catalog#**	**Manufacturer**	**Additional information**
ActivX™FP-TAMRA	88318	Thermo Fisher	Labels serine hydrolases, fluorescent probe
FP-Biotin	sc-215056A	Santa Cruz Biotechnology	Labels serine hydrolases
DCG04-Cy5		Van der Hoorn Lab, University of Oxford	Labels PLCP, fluorescent probe
Inhibitor	**Catalog#**	**Manufacturer**	**Additional information**
PMSF	36978	Thermo Fisher	Serine protease inhibitor
DCI	D7910	Sigma-Aldrich	Serine protease inhibitor
e-64	E3132	Sigma-Aldrich	PLCP inhibitor
Beads	**Catalog#**	**Manufacturer**	**Additional information**
Pierce™ NeutrAvidin™ Agarose	29200	Thermo Fisher	Pull-down with Biotin

4.4 Commercial kits

Table 4.3: Used commercial kits

Use	**Manufacturer**	**Additional information**
Plasmid extraction – Mini prep	Macherey-Nagel (Düren, Germany)	NucleoSpin Plasmid 740588.250
PCR and Gel clean-up	Macherey-Nagel (Düren, Germany)	NucleoSpin 740609.350
DNAse digestion	Thermo Fisher Scientific (Waltham, USA)	TURBO DNA-free Kit AM1907
cDNA	Thermo Fisher Scientific (Waltham, USA)	RevertAid H minus First strand cDNA synthesis Kit K1632

4.5 Enzymes

Table 4.4: Used Enzymes

Enzymes	Manufacturer	Additional information
Restriction enzymes	NEB (Ipswich, USA)	
Phusion High Fidelity DNA Polymerase	NEB (Ipswich, USA)	Amplification of PCR products
KOD Hot Start Polymerase T4	Sigma-Aldrich (St. Louis, USA), Merk (Darmstadt, Germany)	Amplification of PCR products
GoTaq Green MasterMix M712C	Promega (Madison, USA)	Amplification of PCR products
DNA Polymerase	NEB (Ipswich, USA)	Cloning
NEBuilder HF DNA Assembly Master Mix	NEB (Ipswich, USA)	Gibson assembly, Cloning
qPCR Master Mix	Promega (Madison, USA)	GoTaq qPCR Master Mix A6001
RNAse	Labmade by our TA	RNase treatment
Trypsin	Labmade by our TA	Trypsin treatment

4.6 Antibodies

Table 4.5: Used antibodies

Antibody	Donor organism	Working dilution/concentration	Supplier
HA	Mouse	1:30000	Sigma (St. Lous, USA)
His	Mouse	1:10000	Sigma (St. Lous, USA)
Strep-HRP	-	1:1000	Sigma (St. Lous, USA)
GFP	Mouse	1:1000	Roche (Basel, Switzerland)

4.7 Antibiotics and fungicides

Table 4.6: Used antibiotics and fungicides

Substances	Final concentration[µg/ml]
Carbenicillin (Carb)	100
Gentamycin (Gent)	50
Rifampicin (Rif)	40
Spectinomycin (Spec)	100
Kanamycin (Kana)	100
Carboxin (Cbx)	2-4

4.8 Ladder/Marker

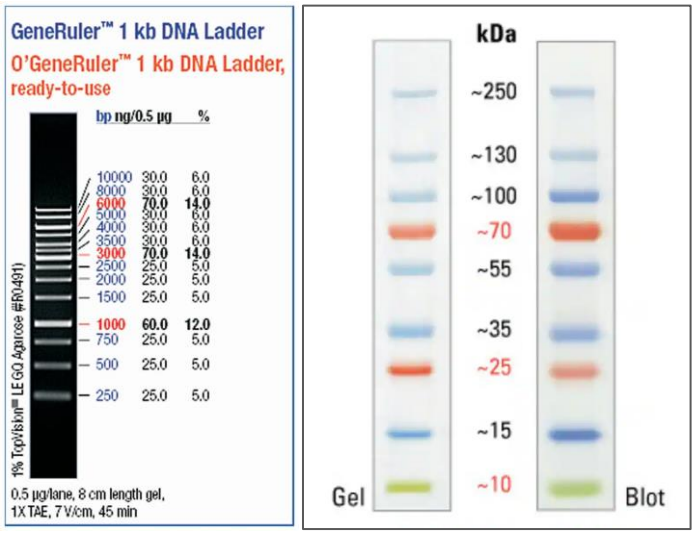

Figure 4.1: Used DNA and protein ladder. DNA ladder: GeneRuler 1 kb (Thermo Fisher Scientific, Waltham USA) and protein marker PageRuler Prestained protein ladder (Thermo Fisher Scientific, Waltham USA).

4.9 Plant growth conditions

Maize grains (*Zea mays*, cv. Golden Bantam, KY21 or B73) were placed in organic growth soil and cultivated a walk-in phytochamber for a period of seven to eight days in a plant growth chamber (15 h photoperiod at 28°C (humidity: 40%), 1h twilight morning and evening and 7 h darkness at 22°C (humidity: 60%)).

4.10 Plant treatments

SA treatment: Salicylic acid was solved in DMSO and filled up with ddH_2O for a solution of 2 mM SA in 1% DMSO. As Control 1% DMSO was used. The second leaf of eight to nine days old plants was used for each experiment and placed fixed in the solution in a beaker. The solution was infiltrated applying in 5 repetitions 240 mbar for 10 min, followed by ATM for 2 min. After the fifth repetition the leaves stayed 5 min in the solution at ATM. The leaves were kept in closed Petri dishes on wet paper towels to avoid leaf desiccation at RT on the bench. At the corresponding time leaves can be frozen in liquid nitrogen and stored at -80°C or continued with AF extraction for direct use.

4.11 AF extraction

For extraction of the apoplastic fluid (AF), the leaves were placed into either a Falcon tube or a beaker containing deionized water and fixed with a mesh under the surface of the water. The water was infiltrated applying in four repetitions 60 mbar for 15 min, followed by ATM for 2 min. Subsequently, the leaves were maintained in the water at ATM for another five minutes. Afterwards, the leaves were dried with tissue paper and up to 30 leaves placed bottom down into a 10 ml syringe. The syringe was placed into a 50 ml falcon tube, and everything was centrifuged for 10 min with 2000 xg at 4°C. The apoplastic fluid was collected in the falcon and transferred into 2 ml tubes. To remove potential leave fragments, the tubes were centrifuged another 5 min with 10,000 xg at 4°C. The supernatant can be used for further experiments.

4.12 Total leave extract (TE) – Protein extraction

Leave samples were frozen in liquid nitrogen and stored at -80°C. For protein extraction the leaves were ground with liquid nitrogen. Equal amounts of powder were dissolved in 50 mM NaOAc buffer (pH=6) using a VIBRAX shaker system (IKA) three times for one minute. Samples were centrifuged with 17,000 g for 20 minutes at 4°C and the supernatant was transferred to new tubes and kept on ice.

4.13 Activity Based Protease Profiling (ABPP)

For different usage different probes were used with corresponding inhibitors and appropriate inhibitors (see Tab. 4.7). In general, AF or total leave extract (TE) can be used for ABPPs. The AF was buffered with 1 M Na-Acetate Buffer pH 6 with a final concentration of 20 mM. For 50 µl labeling reactions 48 µl buffered AF or TE was used and added with 1 µl corresponding inhibitor. After the incubation time 1 µl of the probe was added and in case of Cy5 also 0.5 µl DTT. For fluorescent probes (TAMRA and Cy5) the following incubation was obtained in the dark at RT. The reaction with the fluorescent probes was stopped by adding 10 µl of Laemmli buffer and boiling 5 min. Samples with FP-Biotin were directly frozen for a later continued pull-down.

Table 4.7: Used antibiotics and fungicides

Probe	Inhibitors	Incubationtime	Final conc.	Target
FP-TAMARA	PMSF, DCI	30 min (15 min Inhibitors)	1 µM	Serine Hydrolases
FP-Biotin	PMSF, DCI	3 h (30 min Inhibitors)	1 µM	Serine Hydrolases
DCG04-Cy5	E64	3 h (30 min Inhibitors)	1 µM	PLCP

For detection of the fluorescent signal 15 µl of the sample was loaded on 12% PAA gels and ran for 70 minutes (Cy5) or 100 minutes (FP-TAMRA) at 200V in dark. The ABPP signals were analyzed using a ChemiDoc (BIORAD) system with the corresponding setting (Cy5-suitable setting or Rhodamine for TAMRA). For total protein staining, the gels were incubated in SyproRuby fixation solution (50% MeOH, 7% acetic acid) for 30 min and incubated overnight in SyproRuby staining solution (Thermo Fisher Scientific - S12000). The next day the gels were washed with washing solution (10% MeOH, 7% acetic acid) for 30 minutes. The signals were detected afterward using the SyproRuby setting from the ChemiDoc. ABPP and SyproRuby signals were quantified using the ImageLAB software. The calculation was performed as in Passarge et al., 2022.

4.14 Western Blot analysis

For the western blot the samples were run on an SDS-PAGE. For this, the samples were loaded on a 12% gel and run with 200 volt for 80 minutes. Afterwards, the SDS-PAGE gel was placed into 1x Transfer Buffer containing 20% methanol for 3 to 5 minutes. While the gel was preparing, the PVDF membrane and Whatman filter paper were cut into rectangular pieces measuring 6.5 cm by 8.5 cm. Next, the PVDF membrane was activated by immersing it in pure methanol for 3 to 5 minutes. In parallel, two pieces of Whatman filter paper were immersed in 1x transfer buffer for several minutes. Once these preparations were completed, a stack was assembled for the semi-dry blotting apparatus in the following order: one piece of Whatman paper, wetted with 1x transfer buffer, served as the base layer. On top of this, the activated PVDF membrane, rinsed with 1x transfer buffer, was placed, followed by the SDS-PAGE gel, which was also rinsed. Finally, another piece of Whatman paper, wetted with 1X Transfer Buffer, covered the gel. After assembling the stack, excess buffer was removed by gently rolling a small roller over it, and then the lid of the blotting machine was closed. The electrode module was inserted

into the semi-dry blotting machine, and the transfer was conducted until the marker lane was fully transferred to the membrane. Once the transfer was complete, the stack was disassembled, and the PVDF membrane was marked with a pencil. Next, the membrane was blocked by incubating in 10 ml of 3% milk powder dissolved in TBS-T for 1 to 2 hours at room temperature, or overnight at 4°C. Following the blocking step, 10 mL of TBS-T containing 3% milk powder and the primary antibody at the appropriate concentration was added. The membrane was incubated for 1 to 2 hours at room temperature with gentle agitation, or overnight at 4°C. After incubation with the primary antibody, the membrane was washed three times with TBS-T, for 10 minutes per wash. Then, 10 mL of TBS-T containing 3% milk powder and the secondary antibody at the appropriate concentration was added. The membrane was incubated again for 1 to 2 hours at room temperature with gentle agitation. Following the incubation with the secondary antibody, the membrane was washed three additional times with TBS-T, with each wash lasting 15 minutes. Finally, to detect the proteins, the Pierce Supersignal West Pico Chemiluminescent Signal Kit was utilized, following the manufacturer's instructions. This involved combining the two components of the kit in a 1:1 ratio, applying 500 µL of the mixture to the blot and exposing it using a film developer machine.

4.15 Pull down

During the pull-down assay, a series of control samples were collected for subsequent analysis via western blot, with the objective of detecting the presence of the sample in the final step. When the samples are taken is labeled in the protocol with letters (a) till (g). 6x SDS loading dye was added to each sample and stored at -20°C for western blot.
Leave apoplastic fluid was incubated for 3 h under agitation at room temperature in 50 mM sodium acetate pH 6 and 0.5 µM FP-Biotin (Tab. 4.7) in a total volume of 2 ml (a). As a no probe control (NPC), one set of samples was incubated with pure DMSO instead of FP-Biotin. While labelling, 100 µl of Pierce™ NeutrAvidin™ Agarose Beads per sample were washed and prepared. Beads were washed with 500 µl 50 mM Tris HCl, pH 8 and added to a Pierce™ centrifuge column (Thermo Fisher, Ref 89868) and centrifuged shortly to remove the supernatant. This was repeated twice. Beads were diluted in 500 µl buffer Tris-HCl with protease inhibitor cocktail (PIC) (for 500 µL 20 µL 25 x PIC

and 480 µL Tris) and transferred to a new tube. After labelling, 250 µl of washed beads were added to the samples and incubated rotating for another 1 hour at RT (b). Afterwards, samples including beads were transferred to Pierce™ centrifuge columns, shortly centrifuged and flow through removed. Repeating this until everything from the labelled supernatant with beads has been on the columns (c). The beads were then washed three times with 500 µl 1% SDS, centrifuged shortly and flow through removed (d). After that, Beads were washed with 6M UREA, again three times with 500 µl, centrifuged shortly and flow through removed (e). Finally washed two times with 500 µl 50 mM Tris-HCL (pH = 8) + 0,1% Tween-20, centrifuged shortly and flow through removed. To remove buffer remains, beads were washed twice with 500 µl MQH_2O centrifuged shortly and flow through removed. Beads were taken up in 200 µl MQH_2O and transferred to a new tube. Beads were stored in water at -20°C and shipped on dry ice to Dr. Farnusch Kaschani at the Center of Medical Biotechnology (ZMB) at the University of Duisburg-Essen for On-Bead digest and following MS analysis.

Samples for WB:
a: 25 µL after labelling
b: 25 µL after incubation for 1 h with beads
c: 25 µL flow through of supernatant on columns
d: 10 µL after washing with SDS
e: 10 µL after washing with UREA
f: 10 µL after washing with H2O
g: 10 µL of beads diluted in 500 µL

4.16 AF filtration

For generating the apoplastic peptide fraction smaller 10 kDa, the AF was directly after extraction loaded on Vivaspin® 10 kDa MWCO Polyethersulfone Columns from Sartorius and centrifuged about one hour with 3,000 g until only the dead volume was left. The flow through was kept on ice and used as APF.

Frozen APF was sent to CECAD/ZMMK Proteomics Facility of the University of Cologne and loaded there on StageTips as preparation for MS Peptidomics.

4.17 Syringe infiltration

For syringe infiltration of the APF or synthesized peptides needless syringes with 1 ml volume were used. The syringe was placed on the bottom side of the leave and the solution was infiltration by pressure. Infiltration was conducted using four points, comprising two upper and two lower points. The section between the two points was utilized for the analysis of gene expression and frozen in liquid nitrogen.

4.18 RNA extraction

RNA was extracted by adding 1 ml TRIzol™ reagent (Invitrogen Ref. 15596026) to the frozen leaf powder. Afterwards, samples were homogenized on a shaker for 5 min at room temperature. 200 µl of chloroform were added and samples were placed on a shaker for another 5 min. Subsequently, tubes were centrifuged for 15 min at 12,000 g at 4°C. The aqueous upper phase was transferred to a new tube and 400 µl of isopropanol were added. Samples were incubated for 10 min on ice and afterwards centrifuged for 10 min at 12,000 g at 4°C. Supernatant was removed and the pellet was washed two times by adding 700 µl of 75% ethanol. After washing the pellets were centrifuged for another 10 min at 12,000 g at 4°C. Supernatant was removed and pellets were dried until ethanol residues were evaporated. Pellets were dissolved in 50 µl in nuclease-free water at 65°C for 5 min. The quality of RNA was checked by gel electrophoresis with a 2% agarose gel.

4.19 DNase digestion and cDNA synthesis

For DNA digestion 10 µl of RNA were used and incubated with TURBO DNA-free™ Kit (Thermo Fisher Scientific) and following the manufacturers protocol. RNA was transcribed to cDNA using “RevertAid H minus First strand cDNA synthesis Kit” (Thermo Scientific #K1632). The obtained cDNA was diluted to 1:100 using Nuclease-free water.

4.20 Gene expression analysis

The diluted cDNA was used for qRT-PCR analyses with gene specific primers (Suppl). IQSYBRGreen (PROMEGA) reagent was used for measurements. *ZmGAPDH* was used as a housekeeping gene. *ZmPR3*, *ZmPR4*, *ZmPR5*, *ZmPRm6b* and *ZmPR10* were used

as SA and defense marker genes. *ZmCC9* was included as JA marker gene and indication potential wounding during the treatment.

4.21 Trypsin, DNase and RNase treatment of APF

APF of SA and mock treated leaves were harvested and prepared as described. 1 ml of APF was incubated with 10 µl Trypsin, 5 µl RNase and 5 µl DNase and incubated for 1 hour at 37°C. Afterwards APF was filtered again through a Vivaspin® 10 kDa MWCO Polyethersulfone Columns from Sartorius and centrifuged about one hour with 3,000 g until only the dead volume was left. Flow through was used and infiltrated with a syringe in second leaves of 8-days old maize seedlings. *PR*-gene expression was measured at 24 hpi via qRT-PCR as described.

4.22 Cultivation of *E. coli*

E. coli strains were cultured at 37 °C on YT liquid with shaking at 200 rpm or on YT solid media with agar. Glycerol stocks were prepared by adding 50% (v/v) glycerol to an overnight culture in a total volume of 1.5 ml and stored in a screw cap vial at -80 °C. For selection, media were supplied with antibiotics according to Table 4.1.

4.23 Transformation of *E. coli*

5 ng of plasmid DNA was added to 50 µl of the competent cells (DH5α) and incubated on ice for 30 min. Following, the reaction tubes were placed in a thermo block at 42 °C for 45 s to heat shock the cells, and incubated on ice for another 2 min. Subsequently, 700 µl dYT was added and the cells were incubated for 30 min at 37°C with 200 rpm shaking. Finally, the cells were plated on YT plates containing the respective antibiotics for selection and incubated overnight at 37°C.

4.24 Cultivation of *A. tumefaciens*

A. tumefaciens strains were cultured at 28 °C either on YT liquid with shaking at 200 rpm or on YT solid media with agar. Glycerol stocks were prepared by adding 50% (v/v) glycerol to an overnight culture in a total volume of 1.5 ml and stored in a screw cap vial at -80 °C. For selection, media were supplied with antibiotics according to Table 4.1.

4.25 Deglycosylation

For deglycosylation of ZmSBT7 the PNGase F Kit (NEB) was used according to manufacturer's instructions.

4.26 Generation of *Ustilago*-phytocytokine overexpression lines

Corresponding sequences of the phytocytokine candidates PC10 to 14 were cloned into the p123 vector system using the Gibson assembly method (Gibson et al., 2009). The vector includes a constitutive promoter (pro^{pit2}) for overexpression, a terminator (Tnos), and a resistance marker cassette (carboxin (cbx)). The assembled vectors were transformed into TOP10 *E. coli* cells by heat shock for plasmid multiplication. Purified plasmids were digested by *SspI* restriction enzyme for linearization to allow the homologous recombination into the *ip* locus. 50 µl protoplasts of *Ustilago maydis* (SG200; solo pathogenic mutant) were transfected by adding 5 µg of linearized plasmid, 1 µl Heparin and 0.5 ml STC / 40%PEG (sterile) incubating for 15 minutes on ice. The samples were plated on Regeneration agar (Reg-agar) - poured as a two-layer system (without (top) and with cbx (bottom). Plates were incubated at 28°C for 4-5 days. Colonies were picked and singled out onto Potato-Dextrose-agar (PDA) plates for two days at 28°C. 2 ml overnight cultures of singled-out colonies were used for DNA extraction (Hoffman & Winston, 1987). The extracted DNA was digested by *HindIII*, separated on 0.9% agarose gel (100 V, 2 h), and blotted on a nylon membrane for Southern Blot analysis. The detection of cbx-containing DNA fragments was performed using a digoxigenin (DIG) antibody targeting the *ip* locus via a cbx probe. Successfully confirmed strains were used for infections.

4.27 *Ustilago* cultivation and infection assays

SG200, SG200_ZmPC1, SG200_ZmPC10, SG200_ZmPC11, SG200_ZmPC13 and SG200_ZmPC14 were grown to an OD_{600} of 0.8 in 55 ml YEPSlight. The cultures were pelleted at 2850 g for seven minutes and the supernatant was discarded. The pellets were washed with 20 ml ddH_2O. Finally, the pellets were resuspended in the calculated volume of water to reach an OD600 of 1.0. To check for filamentation (pathogenicity) 10 µl droplets of each culture were placed on charcoal plates. Seven-day old maize

seedlings were infected using a 1 ml syringe with a needle. *Ustilago* suspensions were injected into the stem of the seedlings. The plant's phenotype was investigated 12 dpi using a disease rating chart for *Ustilago maydis* comprising healthy plants, chlorosis, small tumours (<2 mm), normal tumours (2 to 10 mm diameter), heavy tumours (>10 mm or stunted growth) and dead plants. Infected plants were categorized based on phenotypical symptoms and compared to SG200 for the analyses.

4.28 RNA sequencing

Total RNA of 2, 6, 12 and 24 hours of *B73* leaves after MAP1, Zip1, PC13 and SIGGI treatment was prepared as described and shipped to Novogene. RNA libraries were prepared by Novogene using an Illumina TruSeq Stranded mRNA kit (Illumina, SanDiego, CA, USA), and paired-end sequencing was performed on a HiSeq4000 platform. Reads of three biological replicates were filtered using the Trinity software and standard settings. For mapping to a reference genome *Z. mays B73* v5 (maize-gdb) was used. Reads were counted using HISAT2. The DESeq2 package of R was used for statistical analysis of differential gene expression (counts per million, CPM). Excel was used to determine the transcripts per million (TPM). Furthermore, a standard bioinformatics analysis of the RNAseq data was conducted by Novogene (overview below).

Table 4.8: bioinformatics analysis methods used by Novogene

Standard Analysis (de novo transcriptome)	Software
Data quality control: filtering reads containing adapter or with low quality	
Statistics Analysis of Data Production and Quality	
De novo Transcriptome Assembly	Trinity
Gene Functional Annotation Using Seven Databases (NR, NT, KOG, KO, Swiss-Prot, GO, PFAM)	blast+, Diamond, hmmscan, KAAS, blast2go
GO, COG, KEGG Classification	
CDS Prediction	BLAST, ESTScan
SNP/INDELs calling	Samtools
Gene Expression Analysis	RSEM
Correlation Analysis (For biological replicates)	
Differential Expression Analysis (two or more groups of samples)	DESeq2 (with biological replicates), edgeR/ (without biological replicates)
Enrichment analysis of differentially expressed coding genes (GO Enrichment, KEGG Pathway Enrichment)	GOSeq, topGO, hmmscan, KOBAS
Protein Protein Interaction Analysis of differentially expressed coding genes	BLAST

4.29 Primer

All the oligonucleotides used in this study were purchased from Sigma-Aldrich (Darmstadt, Germany) or Eurofins (Luxemburg). The names, sequences, and usage of the different oligonucleotides are listed below.

Table 4.9: Primer used in this study.

Name	Sequenz	Descriotion
PR3_Zm1085_fw	GAACAACTACAGCAGCCAGGTG	qRT-PCR
PR3_Zm1085_rv	GAGACAATAGCTGACATGCGTC	qRT-PCR
PR4_Zm2227_fw	GCGTTCAAGCCCATCGACA	qRT-PCR
PR4_Zm2227_rv	CGTGTGGGATCACATCCATATAAC	qRT-PCR
PR5-fw	TATCGGCCGGAATAGGCTCTG	qRT-PCR
PR5-rv	CGCGTACATACAAATGCGTGC	qRT-PCR
PRm6b_fw	CATCTTCGCCATGTTCAACG	qRT-PCR
PRm6b_rev	ATTTGTCCGGGTTGAAGAGG	qRT-PCR
ZmPR10.1 fw	CAAGCTCATCGCAGACCAC	qRT-PCR
ZmPR10.1 rv	CGATCTCAACAGTCCAGCTGTT	qRT-PCR
Zm_GAPDH-RT-Fw	CTTCGGCATTGTTGAGGGTTTG	qRT-PCR
Zm_GAPDH-RT-Rv	TCCTTGGCTGAGGGTCCGTC	qRT-PCR
CC9-qRT_Fw	TATGGGTCCTTGACGTTCTC	qRT-PCR
CC9-qRT_Rv	GGATCATCCGTAGCCATCTG	qRT-PCR
Ky21_PRm6b_rev	GATTTGTCCGGGTTGAAGAG	pRT-PCR for PRm6b in Ky21 (fw Primer No.837)
PK_Zm050140_Fw	GAAGACAAAATGATGCGTAACATCGGCATGCT	ZmSBT7 cDNA template

PK_Zm050140_Rev	GAAGACAACGAACCGGTCCACGTGAACGCTATCG	ZmSBT7 cDNA template
PK_SBT_L0_Fw	ACGTCGTCGTCGGCGT	Sequencing
PK_SBT_L0_Rev	GTCCACGACGCCAGGATGTT	Sequencing
PK_Propep1_qRT_fw	GCTCAGGTTCTGTTCGTGG	qRT-PCR
PK_Propep1_qRT_rev	CTCTGATTCCGCCTCCCTTC	qRT-PCR
PK_Propep10_qRT_fw	AATCGGAGCCACAGCTTCTG	qRT-PCR
PK_Propep10_qRT_rev	GCTGCAACATCTTGTTGGTCA	qRT-PCR
PK_Propep11_qRT_fw	AGAGAAACAGCCTCCGAACC	qRT-PCR
PK_Propep11_qRT_rev	GTTGAGGTTGAGGCCTTCCC	qRT-PCR
PK_Propep12_qRT_fw	GACATCATCGAGTGCGGCTA	qRT-PCR
PK_Propep12_qRT_rev	AAGTAGTGGTCCACCTTGCG	qRT-PCR
PK_Propep13_qRT_fw	GGCGGGAAAGGACCTGTAAT	qRT-PCR
PK_Propep13_qRT_rev	CCTCGCTGGTTTCAGCTACA	qRT-PCR
PK_Pep1_Trojan_fw	CAACATGTTCAAGCTATTCCGCCCGGGTTCGATGGGGAGAAGCCGGAGCC	Trojan horse approach
PK_Pep1_Trojan_re	ATCTGCAGCCGGGCGGCTCTAGACGCCGGCTCCGGCTTCTCCCCATCGAA	Trojan horse approach
PK_Pep10_Trojan_fw	TGCAACATGTTCAAGCTATTCCGCCCGGGCAGCTTGGGAAGGATGCATCTGCAGCAGGAGCTGCA	Trojan horse approach
PK_Pep10_Trojan_re	GTTTGAACGATCTGCAGCCGGGCGGCTCTAGATCATGCAGCTCCTGCTGCAGATG	Trojan horse approach
PK_Pep11_Trojan_fw	GCAACATGTTCAAGCTATTCCGCCCGGGAGTACGAAATCCAAGGAGCTCAGTGGTCACGACATCTTTGCCGATCACGAAGATCC	Trojan horse approach
PK_Pep11_Trojan_re	AACGATCTGCAGCCGGGCGGCTCTAGATCAGTTGGGCTTGGGATCTTCGTGATCGGCAAAGATGTCGTGACCACTGAGCT	Trojan horse approach
PK_Pep12_Trojan_fw	TGCAACATGTTCAAGCTATTCCGCCCGGGGACGCCCCCGCTGCCGCTCCAGCCCCTGAGGAAGCAGAGAGCAAGGCCGAGGAGAA	Trojan horse approach
PK_Pep12_Trojan_re	GAACGATCTGCAGCCGGGCGGCTCTAGATCAGCTCACCTCCTTGTCGGCCTTCTCCTCGGCCTTGCTCTCTGCTTCCTCA	Trojan horse approach
PK_Pep13_Trojan_fw	GGTGCAACATGTTCAAGCTATTCCGCCCGGGATCGATAGCATTGTCAATGGCGGTGACGGCGGGAA	Trojan horse approach
PK_Pep13_Trojan_re	CGATCTGCAGCCGGGCGGCTCTAGATCAAGCAATTACAGGTCCTTTCCCGCCGTCACCGCCATTGAC	Trojan horse approach
PK_ProSIGGI_qRT_fw	CGACATCCTCAGGGACTGC	MIF qRT-PCR
PK_ProSIGGI_qRT_re	GACCGACACCATGACATAGGA	MIF qRT-PCR
PK_SBT_seq_rev	TGAACCTCACCGTGTAGCTCTTCTTCTCCC	Sequencing
PK-Seq-SBT_fw	ACGTCGTGCTCGGCGACGGGAAG	Sequencing
PK-Seq-eGFP_rv	TCGAACTTCACCTCGGCGCGGGTCT	Sequencing
PK-Seq-SBT_fw	GCTCTCGCTCTCGCTGGGCGG	Sequencing
Propep1 MoClo L0 Fw	GAAGACAAAATGATGGCATATCTAGCTCCCGC	MoClo Level 0 Proproteins
Propep1 MoClo L0 Rev	GAAGACAACGAACCTCAAACCTTCGCCGGCTCCG	MoClo Level 0 Proproteins
Propep10 MoClo L0 Fw	GAAGACAAAATGATGGAGTCGACCTCCGGCGA	MoClo Level 0 Proproteins

Propep10 MoClo L0 Rev	GAAGACAACGAACCTTAGGCTGCTGAGGGAGCTT	MoClo Level 0 Proproteins
Propep11 MoClo L0 Fw	GAAGACAAAATGATGGAGAGAGCGGCCCCCGT	MoClo Level 0 Proproteins
Propep11 MoClo L0 Rev	GAAGACAACGAACCCTAGCCCAGCAAAATGCTGC	MoClo Level 0 Proproteins
Propep12 MoClo L0 Fw	GAAGACAAAATGATGACGCTGACGATCCCGGA	MoClo Level 0 Proproteins
Propep12 MoClo L0 Rev	GAAGACAACGAACCTCACCTCCTTGTCGGCCTTC	MoClo Level 0 Proproteins
Propep13 MoClo L0 Fw	GAAGACAAAATGATGGAACACAAGGAGGCGGG	MoClo Level 0 Proproteins
Propep13 MoClo L0 Rev	GAAGACAACGAACCTCAGATCTTGTCGAGCTTCT	MoClo Level 0 Proproteins
MIF MoClo L0 Fw	GAAGACAAAATGATGCCGACACTAAACCTGAG	MoClo Level 0 Proproteins
MIF MoClo L0 Rev	GAAGACAACGAACCTTAGAATGTGGATCCGTTGA	MoClo Level 0 Proproteins
Propep1 MoClo L1 Fw	GGTCTCTAATGATGGCATATCTAGCTCCCGC	MoClo Level 1 Proproteins
Propep1 MoClo L1 Rev	GGTCTCTCGAATTAACCTTCGCCGGCTCCG	MoClo Level 1 Proproteins
Propep10 MoClo L1 Fw1	GGTCTCTAATGATGGAGTCGACCTCCGGCGA	MoClo Level 1 Proproteins
Propep10 MoClo L1 Rev2	GGTCTCAGTCCCGCCGACCGGATCCCC	Domestication
Propep10 MoClo L1 Fw3	GGTCTCAGGACTCGCGGCGCTCGTCGA	Domestication
Propep10 MoClo L1 Rev4	GGTCTCTCGAATTGGCTGCTGAGGGAGCTT	MoClo Level 1 Proproteins
Propep11 MoClo L1 Fw	GGTCTCTAATGATGGAGAGAGCGGCCCCCGT	MoClo Level 1 Proproteins
Propep11 MoClo L1 Rev	GGTCTCTCGAATTGCCCAGCAAAATGCTGC	MoClo Level 1 Proproteins
Propep12 MoClo L1 Fw	GGTCTCTAATGATGACGCTGACGATCCCGGA	MoClo Level 1 Proproteins
Propep12 MoClo L1 Rev	GGTCTCTCGAATTGTTCTTGGCGGCCAGCGCCT	MoClo Level 1 Proproteins
Propep13 MoClo L1 Fw	GGTCTCTAATGATGGAACACAAGGAGGCGGG	MoClo Level 1 Proproteins
Propep13 MoClo L1 Rev	GGTCTCTCGAATTGATCTTGTCGAGCTTCT	MoClo Level 1 Proproteins
MIF MoClo L1 Fw	GGTCTCTAATGATGCCGACACTAAACCTGAG	MoClo Level 1 Proproteins
MIF MoClo L1 Rev	GGTCTCTCGAATTGAATGTGGATCCGTTGA	MoClo Level 1 Proproteins

4.30 Availability of data

All generated data in this study are available on the internal server of the working group of Prof. Dr. Gunther Döhlemann.

5. Bibliography

Aerts, N., Pereira Mendes, M., & Van Wees, S. C. M. (2021). Multiple levels of crosstalk in hormone networks regulating plant defense. *Plant Journal*, *105*(2), 489–504. https://doi.org/10.1111/tpj.15124

Amano, Y., Tsubouchi, H., Shinohara, H., Ogawa, M., & Matsubayashi, Y. (2007). Tyrosine-sulfated glycopeptide involved in cellular proliferation and expansion in Arabidopsis. *Proceedings of the National Academy of Sciences*, *104*(46), 18333–18338. https://doi.org/10.1073/pnas.0706403104

Antão, C. M., & Malcata, F. X. (2005). Plant serine proteases: Biochemical, physiological and molecular features. *Plant Physiology and Biochemistry*, *43*(7), 637–650. https://doi.org/10.1016/j.plaphy.2005.05.001

Arif, Y., Sami, F., Siddiqui, H., Bajguz, A., & Hayat, S. (2020). Salicylic acid in relation to other phytohormones in plant: A study towards physiology and signal transduction under challenging environment. *Environmental and Experimental Botany*, *175*(November 2019), 104040. https://doi.org/10.1016/j.envexpbot.2020.104040

Balakireva, A. V., & Zamyatnin, A. A. (2018). Indispensable role of proteases in plant innate immunity. *International Journal of Molecular Sciences*, *19*(2). https://doi.org/10.3390/ijms19020629

Bao, Y., Wang, C., Jiang, C., Pan, J., Zhang, G., Liu, H., & Zhang, H. (2014). The tumor necrosis factor receptor-associated factor (TRAF)-like family protein SEVEN IN ABSENTIA 2 (SINA2) promotes drought tolerance in an ABA-dependent manner in Arabidopsis. *New Phytologist*, *202*(1), 174–187. https://doi.org/https://doi.org/10.1111/nph.12644

Barghahn, S., Saridis, G., Mantz, M., Meyer, U., Mellüh, J. C., Misas Villamil, J. C., Huesgen, P. F., & Doehlemann, G. (2023). Combination of transcriptomic, proteomic, and degradomic profiling reveals common and distinct patterns of pathogen-induced cell death in maize. *Plant Journal*, *116*(2), 574–596. https://doi.org/10.1111/tpj.16356

Barna, B., Fodor, J., Harrach, B. D., Pogány, M., & Király, Z. (2012). The Janus face of reactive oxygen species in resistance and susceptibility of plants to necrotrophic and biotrophic pathogens. *Plant Physiology and Biochemistry*, *59*, 37–43. https://doi.org/https://doi.org/10.1016/j.plaphy.2012.01.014

Ben Saad, R., Ben Romdhane, W., Čmiková, N., Baazaoui, N., Bouteraa, M. T., Ben Akacha, B., Chouaibi, Y., Maisto, M., Ben Hsouna, A., Garzoli, S., Wiszniewska, A., & Kačániová, M. (2024). Research progress on plant stress-associated protein (SAP) family: Master regulators to deal with environmental stresses. *BioEssays*, *46*(11), 2400097. https://doi.org/https://doi.org/10.1002/bies.202400097

Bittel, P., & Robatzek, S. (2007). Microbe-associated molecular patterns (MAMPs) probe plant immunity. *Current Opinion in Plant Biology*, *10*(4), 335–341. https://doi.org/https://doi.org/10.1016/j.pbi.2007.04.021

Bloom, B. R., & Bennett, B. (1966). Mechanism of a Reaction in Vitro Associated with Delayed-Type Hypersensitivity. *Science*, *153*(3731), 80–82. https://doi.org/10.1126/science.153.3731.80

Brefort, T., Doehlemann, G., Mendoza-Mendoza, A., Reissmann, S., Djamei, A., & Kahmann, R. (2009). Ustilago maydis as a Pathogen . *Annual Review of Phytopathology*, *47*(1), 423–445. https://doi.org/10.1146/annurev-phyto-080508-081923

Buscaill, P., Sanguankiattichai, N., Kaschani, F., Huang, J., Li, Y., Lyu, J., Sueldo, D. J., Kaiser, M., & Hoorn, R. A. L. van der. (2024). Subtilase SBT5.2 counterbalances flagellin immunogenicity in the plant apoplast. *BioRxiv*, *2*, 595557. https://www.biorxiv.org/content/10.1101/2024.05.23.595557v1

Butenko, M. A., Patterson, S. E., Grini, P. E., Stenvik, G.-E., Amundsen, S. S., Mandal, A., & Aalen, R. B. (2003). INFLORESCENCE DEFICIENT IN ABSCISSION Controls Floral Organ Abscission in Arabidopsis and Identifies a Novel Family of Putative Ligands in Plants . *The Plant Cell*, *15*(10), 2296–2307. https://doi.org/10.1105/tpc.014365

Cao, H., Bowling, S. A., Gordon, A. S., & Dong, X. (1994). Characterization of an Arabidopsis Mutant That Is Nonresponsive to Inducers of Systemic Acquired Resistance. *The Plant Cell*, *6*(11), 1583–1592. https://doi.org/10.1105/tpc.6.11.1583

Castro-Camba, R., Sánchez, C., Vidal, N., & Vielba, J. M. (2022). Interactions of Gibberellins with Phytohormones and Their Role in Stress Responses. In *Horticulturae* (Vol. 8, Issue 3). https://doi.org/10.3390/horticulturae8030241

Cedzich, A., Huttenlocher, F., Kuhn, B. M., Pfannstiel, J., Gabler, L., Stintzi, A., & Schaller, A. (2009). The Protease-associated Domain and C-terminal Extension Are Required for Zymogen Processing, Sorting within the Secretory Pathway, and Activity of Tomato Subtilase 3 (SlSBT3) * . *Journal of Biological Chemistry*, *284*(21), 14068–14078. https://doi.org/10.1074/jbc.M900370200

Chang, E.-J., Ha, J., Kang, S.-S., Lee, Z. H., & Kim, H.-H. (2011). AWP1 binds to tumor necrosis factor receptor-associated factor 2 (TRAF2) and is involved in TRAF2-mediated nuclear factor-kappaB signaling. *The International Journal of Biochemistry & Cell Biology*, *43*(11), 1612–1620. https://doi.org/https://doi.org/10.1016/j.biocel.2011.07.010

Chang, L., Chang, H.-H., Chang, J.-C., Lu, H.-C., Wang, T.-T., Hsu, D.-W., Tzean, Y., Cheng, A.-P., Chiu, Y.-S., & Yeh, H.-H. (2018). Plant A20/AN1 protein serves as the important hub to mediate antiviral immunity. *PLOS Pathogens*, *14*(9), e1007288. https://doi.org/10.1371/journal.ppat.1007288

Charrier, A., Lelièvre, E., Limami, A. M., & Planchet, E. (2013). Medicago truncatula stress associated protein 1 gene (MtSAP1) overexpression confers tolerance to abiotic stress and impacts proline accumulation in transgenic tobacco. *Journal of Plant Physiology*, *170*(9), 874–877. https://doi.org/https://doi.org/10.1016/j.jplph.2013.01.008

Checker, V. G., Kushwaha, H. R., Kumari, P., & Yadav, S. (2018). *Role of Phytohormones in Plant Defense: Signaling and Cross Talk BT - Molecular Aspects of Plant-Pathogen Interaction* (Archana Singh & I. K. Singh (eds.); pp. 159–184). Springer Singapore. https://doi.org/10.1007/978-981-10-7371-7_7

Chen, C., Buscaill, P., Sanguankiattichai, N., Huang, J., Kaschani, F., Kaiser, M., & Van Der Hoorn, R. A. L. (2024). Extracellular plant subtilases dampen cold shock peptide elicitor levels. *Nature Plants*, *10*(November). https://doi.org/10.1038/s41477-024-01815-8

Chen, Y.-C., Siems, W. F., Pearce, G., & Ryan, C. A. (2008). Six Peptide Wound Signals Derived from a Single Precursor Protein in Ipomoea batatas Leaves Activate the Expression of the Defense Gene Sporamin *. *Journal of Biological Chemistry*, *283*(17), 11469–11476. https://doi.org/10.1074/jbc.M709002200

Chen, Yang, Fokar, M., Kang, M., Chen, N., Allen, R. D., & Chen, Y. (2018). Phosphorylation of Arabidopsis SINA2 by CDKG1 affects its ubiquitin ligase activity. *BMC Plant Biology*, *18*(1), 147. https://doi.org/10.1186/s12870-018-1364-8

Chen, Yue, Han, Y., Huang, W., Zhang, Y., Chen, X., Li, D., Hong, Y., Gao, H., Zhang, K., Zhang, Y., & Sun, T. (2024). LAZARUS 1 functions as a positive regulator of plant immunity and systemic acquired resistance. *Frontiers in Plant Science*, *15*. https://doi.org/10.3389/fpls.2024.1490466

Chichkova, N. V, Kim, S. H., Titova, E. S., Kalkum, M., Morozov, V. S., Rubtsov, Y. P., Kalinina, N. O., Taliansky, M. E., & Vartapetian, A. B. (2004). A Plant Caspase-Like Protease Activated during the Hypersensitive Response . *The Plant Cell*, *16*(1), 157–171. https://doi.org/10.1105/tpc.017889

Chichkova, N. V, Shaw, J., Galiullina, R. A., Drury, G. E., Tuzhikov, A. I., Kim, S. H., Kalkum, M., Hong, T. B., Gorshkova, E. N., Torrance, L., Vartapetian, A. B., & Taliansky, M. (2010). Phytaspase, a relocalisable cell death promoting plant protease with caspase specificity. *The EMBO Journal*, *29*(6), 1149–1161. https://doi.org/https://doi.org/10.1038/emboj.2010.1

Choi, H. W., & Klessig, D. F. (2016). DAMPs, MAMPs, and NAMPs in plant innate immunity. *BMC Plant Biology*, *16*(1), 232. https://doi.org/10.1186/s12870-016-0921-2

Choi, J., Tanaka, K., Cao, Y., Qi, Y., Qiu, J., Liang, Y., Lee, S. Y., & Stacey, G. (2014). Identification of a Plant Receptor for Extracellular ATP. *Science*, *343*(6168), 290–294. https://doi.org/10.1126/science.343.6168.290

Cock, P. J. A., Antao, T., Chang, J. T., Chapman, B. A., Cox, C. J., Dalke, A., Friedberg, I., Hamelryck, T., Kauff, F., Wilczynski, B., & de Hoon, M. J. L. (2009). Biopython: freely available Python tools for computational molecular biology and bioinformatics. *Bioinformatics*, *25*(11), 1422–1423. https://doi.org/10.1093/bioinformatics/btp163

Craig, A., Ewan, R., Mesmar, J., Gudipati, V., & Sadanandom, A. (2009). E3 ubiquitin ligases and plant innate immunity. *Journal of Experimental Botany*, *60*(4), 1123–1132. https://doi.org/10.1093/jxb/erp059

Cui, H., Zhou, G., Ruan, H., Zhao, J., Hasi, A., & Zong, N. (2023). Genome-Wide Identification and Analysis of the Maize Serine Peptidase S8 Family Genes in Response to Drought at Seedling Stage. In *Plants* (Vol. 12, Issue 2). https://doi.org/10.3390/plants12020369

Del Corpo, D., Coculo, D., Greco, M., De Lorenzo, G., & Lionetti, V. (2024). Pull the fuzes: Processing protein precursors to generate apoplastic danger signals for triggering plant immunity. *Plant Communications*, *5*(8). https://doi.org/10.1016/j.xplc.2024.100931

Depotter, J. R. L., Misas Villamil, J. C., & Doehlemann, G. (2022a). Maize immune signalling peptide ZIP1 evolved de novo from a retrotransposon. *BioRxiv*, 2022.05.18.492421. https://doi.org/10.1101/2022.05.18.492421

Depotter, J. R. L., Misas Villamil, J. C., & Doehlemann, G. (2022b). Maize immune signalling peptide ZIP1 evolved de novo from a retrotransposon. *BioRxiv*, 2022.05.18.492421. https://doi.org/10.1101/2022.05.18.492421

Ding, Y., Wang, J., Wang, J., Stierhof, Y.-D., Robinson, D. G., & Jiang, L. (2012). Unconventional protein secretion. *Trends in Plant Science*, *17*(10), 606–615. https://doi.org/10.1016/j.tplants.2012.06.004

Djamei, A., Schipper, K., Rabe, F., Ghosh, A., Vincon, V., Kahnt, J., Osorio, S., Tohge, T., Fernie, A. R., Feussner, I., Feussner, K., Meinicke, P., Stierhof, Y.-D., Schwarz, H., Macek, B., Mann, M., & Kahmann, R. (2011). Metabolic priming by a secreted fungal effector. *Nature*, *478*(7369), 395–398. https://doi.org/10.1038/nature10454

Doehlemann, G., & Hemetsberger, C. (2013). Apoplastic immunity and its suppression by filamentous plant pathogens. *New Phytologist*, *198*(4), 1001–1016. https://doi.org/10.1111/nph.12277

Doehlemann, G., van der Linde, K., Aßmann, D., Schwammbach, D., Hof, A., Mohanty, A., Jackson, D., & Kahmann, R. (2009). Pep1, a Secreted Effector Protein of Ustilago maydis, Is Required for Successful Invasion of Plant Cells. *PLOS Pathogens*, *5*(2), e1000290. https://doi.org/10.1371/journal.ppat.1000290

Doehlemann, G., Wahl, R., Horst, R. J., Voll, L. M., Usadel, B., Poree, F., Stitt, M., Pons-Kühnemann, J., Sonnewald, U., Kahmann, R., & Kämper, J. (2008). Reprogramming a maize plant: transcriptional and metabolic changes induced by the fungal biotroph Ustilago maydis. *The Plant Journal*, *56*(2), 181–195. https://doi.org/https://doi.org/10.1111/j.1365-313X.2008.03590.x

Duceppe, M.-O., Cloutier, C., & Michaud, D. (2012). Wounding, insect chewing and phloem sap feeding differentially alter the leaf proteome of potato, Solanum tuberosum L. *Proteome Science*, *10*(1), 73. https://doi.org/10.1186/1477-5956-10-73

Fan, W., & Dong, X. (2002). In Vivo Interaction between NPR1 and Transcription Factor TGA2 Leads to Salicylic Acid–Mediated Gene Activation in Arabidopsis . *The Plant Cell*, *14*(6), 1377–1389. https://doi.org/10.1105/tpc.001628

Figueiredo, A., Monteiro, F., & Sebastiana, M. (2014). Subtilisin-like proteases in plant–pathogen recognition and immune priming: a perspective. *Frontiers in Plant Science*, *5*. https://doi.org/10.3389/fpls.2014.00739

Filippova, A., Lyapina, I., Kirov, I., Zgoda, V., Belogurov, A., Kudriaeva, A., Ivanov, V., & Fesenko, I. (2019). Salicylic acid influences the protease activity and posttranslation modifications of the secreted peptides in the moss. *Journal of Peptide Science*, *25*(2), e3138. https://doi.org/https://doi.org/10.1002/psc.3138

Fu, Q., Duan, H., Cao, Y., Li, Y., Lin, X., Pang, H., Yang, Q., Li, W., Fu, F., Zhang, Y., & Yu, H. (2022). Comprehensive Identification and Functional Analysis of Stress-Associated Protein (SAP) Genes in Osmotic Stress in Maize. In *International Journal of Molecular Sciences* (Vol. 23, Issue 22). https://doi.org/10.3390/ijms232214010

Gao, C., Tang, D., & Wang, W. (2022). The Role of Ubiquitination in Plant Immunity: Fine-Tuning Immune Signaling and Beyond. *Plant and Cell Physiology*, *63*(10), 1405–1413. https://doi.org/10.1093/pcp/pcac105

Ge, S. X., Jung, D., & Yao, R. (2020). ShinyGO: a graphical gene-set enrichment tool for animals and plants. *Bioinformatics*, *36*(8), 2628–2629. https://doi.org/10.1093/bioinformatics/btz931

Ghorbel, M., Brini, F., Sharma, A., & Landi, M. (2021a). Role of jasmonic acid in plants: the molecular point of view. *Plant Cell Reports*, *40*(8), 1471–1494. https://doi.org/10.1007/s00299-021-02687-4

Ghorbel, M., Brini, F., Sharma, A., & Landi, M. (2021b). Role of jasmonic acid in plants: the molecular point of view. *Plant Cell Reports*, *40*(8), 1471–1494. https://doi.org/10.1007/s00299-021-02687-4

Gil, M. J., Coego, A., Mauch-Mani, B., Jordá, L., & Vera, P. (2005). The Arabidopsis csb3

mutant reveals a regulatory link between salicylic acid-mediated disease resistance and the methyl-erythritol 4-phosphate pathway. *The Plant Journal*, *44*(1), 155–166. https://doi.org/https://doi.org/10.1111/j.1365-313X.2005.02517.x

Gindro, K., Berger, V., Godard, S., Voinesco, F., Schnee, S., Viret, O., & Alonso-Villaverde, V. (2012). Protease inhibitors decrease the resistance of Vitaceae to Plasmopara viticola. *Plant Physiology and Biochemistry*, *60*, 74–80. https://doi.org/https://doi.org/10.1016/j.plaphy.2012.07.028

Giri, J., Dansana, P. K., Kothari, K. S., Sharma, G., Vij, S., & Tyagi, A. K. (2013). SAPs as novel regulators of abiotic stress response in plants. *BioEssays*, *35*(7), 639–648. https://doi.org/https://doi.org/10.1002/bies.201200181

Godson, A., & Van Der Hoorn, R. A. L. (2021). The front line of defence: A meta-analysis of apoplastic proteases in plant immunity. *Journal of Experimental Botany*, *72*(9), 3381–3394. https://doi.org/10.1093/jxb/eraa602

Gómez-Gómez, L., & Boller, T. (2000). FLS2: An LRR Receptor–like Kinase Involved in the Perception of the Bacterial Elicitor Flagellin in Arabidopsis. *Molecular Cell*, *5*(6), 1003–1011. https://doi.org/10.1016/S1097-2765(00)80265-8

González-Rábade, N., Badillo-Corona, J. A., Aranda-Barradas, J. S., & Oliver-Salvador, M. del C. (2011). Production of plant proteases in vivo and in vitro — A review. *Biotechnology Advances*, *29*(6), 983–996. https://doi.org/https://doi.org/10.1016/j.biotechadv.2011.08.017

Goodluck, B., Pandharikar, G., & Frendo, P. (2022). Salicylic Acid in Plant Symbioses: Beyond Plant Pathogen Interactions. *Biology*, *11*(6). https://doi.org/10.3390/biology11060861

Grosse-Holz, F., Kelly, S., Blaskowski, S., Kaschani, F., Kaiser, M., & van der Hoorn, R. A. L. (2018). The transcriptome, extracellular proteome and active secretome of agroinfiltrated Nicotiana benthamiana uncover a large, diverse protease repertoire. *Plant Biotechnology Journal*, *16*(5), 1068–1084. https://doi.org/10.1111/pbi.12852

Gruner, K., Leissing, F., Sinitski, D., Thieron, H., Axstmann, C., Baumgarten, K., Reinstädler, A., Winkler, P., Altmann, M., Flatley, A., Jaouannet, M., Zienkiewicz, K., Feussner, I., Keller, H., Coustau, C., Falter-Braun, P., Feederle, R., Bernhagen, J., & Panstruga, R. (2021). Chemokine-like MDL proteins modulate flowering time and innate immunity in plants. *Journal of Biological Chemistry*, *296*. https://doi.org/10.1016/j.jbc.2021.100611

Gully, K., Pelletier, S., Guillou, M.-C., Ferrand, M., Aligon, S., Pokotylo, I., Perrin, A., Vergne, E., Fagard, M., Ruelland, E., Grappin, P., Bucher, E., Renou, J.-P., & Aubourg, S. (2019). The SCOOP12 peptide regulates defense response and root elongation in Arabidopsis thaliana. *Journal of Experimental Botany*, *70*(4), 1349–1365. https://doi.org/10.1093/jxb/ery454

Guo, H., Nolan, T. M., Song, G., Liu, S., Xie, Z., Chen, J., Schnable, P. S., Walley, J. W., & Yin, Y. (2018). FERONIA Receptor Kinase Contributes to Plant Immunity by Suppressing Jasmonic Acid Signaling in Arabidopsis thaliana. *Current Biology*, *28*(20), 3316-3324.e6. https://doi.org/10.1016/j.cub.2018.07.078

Gust, A. A., Pruitt, R., & Nürnberger, T. (2017). Sensing Danger: Key to Activating Plant Immunity. *Trends in Plant Science*, *22*(9), 779–791. https://doi.org/10.1016/j.tplants.2017.07.005

Hander, T., Fernández-Fernández, Á. D., Kumpf, R. P., Willems, P., Schatowitz, H., Rombaut, D., Staes, A., Nolf, J., Pottie, R., Yao, P., Gonçalves, A., Pavie, B., Boller, T., Gevaert, K., Van Breusegem, F., Bartels, S., & Stael, S. (2019). Damage on plants activates Ca2+-dependent metacaspases for release of immunomodulatory peptides. *Science*, *363*(6433), eaar7486. https://doi.org/10.1126/science.aar7486

Hemetsberger, C., Herrberger, C., Zechmann, B., Hillmer, M., & Doehlemann, G. (2012). The Ustilago maydis Effector Pep1 Suppresses Plant Immunity by Inhibition of Host Peroxidase Activity. *PLOS Pathogens*, *8*(5), e1002684. https://doi.org/10.1371/journal.ppat.1002684

Hohl, M., Stintzi, A., & Schaller, A. (2017). A novel subtilase inhibitor in plants shows structural and functional similarities to protease propeptides. *Journal of Biological Chemistry*, *292*(15), 6389–6401. https://doi.org/10.1074/jbc.M117.775445

Hou, Q., Wang, L., Qi, Y., Yan, T., Zhang, F., Zhao, W., & Wan, X. (2023). A systematic analysis of the subtilase gene family and expression and subcellular localization investigation of anther-specific members in maize. *Plant Physiology and Biochemistry*, *203*(September), 108041. https://doi.org/10.1016/j.plaphy.2023.108041

Hou, S., Liu, D., & He, P. (2021). Phytocytokines function as immunological modulators of plant immunity. *Stress Biology*, *1*(1), 8. https://doi.org/10.1007/s44154-021-00009-y

Hou, S., Liu, D., Huang, S., Luo, D., Liu, Z., Xiang, Q., Wang, P., Mu, R., Han, Z., Chen, S., Chai, J., Shan, L., & He, P. (2021). The Arabidopsis MIK2 receptor elicits immunity by sensing a conserved signature from phytocytokines and microbes. *Nature Communications*, *12*(1), 5494. https://doi.org/10.1038/s41467-021-25580-w

Hou, S., Shen, H., & Shao, H. (2019). PAMP-induced peptide 1 cooperates with salicylic acid to regulate stomatal immunity in Arabidopsis thaliana. *Plant Signaling & Behavior*, *14*(11), 1666657. https://doi.org/10.1080/15592324.2019.1666657

Hou, S., Wang, X., Chen, D., Yang, X., Wang, M., Turrà, D., Di Pietro, A., & Zhang, W. (2014). The Secreted Peptide PIP1 Amplifies Immunity through Receptor-Like Kinase 7. *PLOS Pathogens*, *10*(9), e1004331. https://doi.org/10.1371/journal.ppat.1004331

Hou, S., Zhang, J., & He, P. (2021). Stress-induced activation of receptor signaling by protease-mediated cleavage. *Biochemical Journal*, *478*(10), 1847–1852. https://doi.org/10.1042/BCJ20200941

Hozain, M., Abdelmageed, H., Lee, J., Kang, M., Fokar, M., Allen, R. D., & Holaday, A. S. (2012). Expression of AtSAP5 in cotton up-regulates putative stress-responsive genes and improves the tolerance to rapidly developing water deficit and moderate heat stress. *Journal of Plant Physiology*, *169*(13), 1261–1270. https://doi.org/https://doi.org/10.1016/j.jplph.2012.04.007

Huang, Ji, Wang, M.-M., Jiang, Y., Bao, Y.-M., Huang, X., Sun, H., Xu, D.-Q., Lan, H.-X., & Zhang, H.-S. (2008). Expression analysis of rice A20/AN1-type zinc finger genes and characterization of ZFP177 that contributes to temperature stress tolerance. *Gene*, *420*(2), 135–144. https://doi.org/https://doi.org/10.1016/j.gene.2008.05.019

Huang, Jun, Teng, L., Li, L., Liu, T., Li, L., Chen, D., Xu, L. G., Zhai, Z., & Shu, H. B. (2004). ZNF216 Is an A20-like and IκB Kinase γ-Interacting Inhibitor of NFκB Activation. *Journal of Biological Chemistry*, *279*(16), 16847–16853.

https://doi.org/10.1074/jbc.M309491200
Huffaker, A., Dafoe, N. J., & Schmelz, E. A. (2011). ZmPep1, an ortholog of arabidopsis elicitor peptide 1, regulates maize innate immunity and enhances disease resistance. *Plant Physiology*, *155*(3), 1325–1338. https://doi.org/10.1104/pp.110.166710
Huffaker, A., Pearce, G., & Ryan, C. A. (2006). An endogenous peptide signal in Arabidopsis activates components of the innate immune response. *Proceedings of the National Academy of Sciences*, *103*(26), 10098–10103. https://doi.org/10.1073/pnas.0603727103
Iwasaki, W., & Miki, K. (2007). Crystal Structure of the Stationary Phase Survival Protein SurE with Metal Ion and AMP. *Journal of Molecular Biology*, *371*(1), 123–136. https://doi.org/https://doi.org/10.1016/j.jmb.2007.05.007
Jan, M., Muhammad, S., Jin, W., Zhong, W., Zhang, S., Lin, Y., Zhou, Y., Liu, J., Liu, H., Munir, R., Yue, Q., Afzal, M., & Wang, G. (2024). Modulating root system architecture: cross-talk between auxin and phytohormones. *Frontiers in Plant Science*, *15*. https://doi.org/10.3389/fpls.2024.1343928
Jin, X., Liu, Y., Hou, Z., Zhang, Y., Fang, Y., Huang, Y., Cai, H., Qin, Y., & Cheng, Y. (2021). Genome-Wide Investigation of SBT Family Genes in Pineapple and Functional Analysis of AcoSBT1.12 in Floral Transition. *Frontiers in Genetics*, *12*. https://doi.org/10.3389/fgene.2021.730821
Jordá, L., Coego, A., Conejero, V., & Vera, P. (1999). A Genomic Cluster Containing Four Differentially Regulated Subtilisin-like Processing Protease Genes Is in Tomato Plants *. *Journal of Biological Chemistry*, *274*(4), 2360–2365. https://doi.org/10.1074/jbc.274.4.2360
Jordá, L., Conejero, V., & Vera, P. (2000a). Characterization of P69E and P69F, Two Differentially Regulated Genes Encoding New Members of the Subtilisin-Like Proteinase Family from Tomato Plants. *Plant Physiology*, *122*(1), 67–74. https://doi.org/10.1104/pp.122.1.67
Jordá, L., Conejero, V., & Vera, P. (2000b). Characterization of P69E and P69F, Two Differentially Regulated Genes Encoding New Members of the Subtilisin-Like Proteinase Family from Tomato Plants. *Plant Physiology*, *122*(1), 67–74. https://doi.org/10.1104/pp.122.1.67
Jordá, L., & Vera, P. (2000a). Local and Systemic Induction of Two Defense-Related Subtilisin-Like Protease Promoters in Transgenic Arabidopsis Plants. Luciferin Induction of PR Gene Expression1. *Plant Physiology*, *124*(3), 1049–1058. https://doi.org/10.1104/pp.124.3.1049
Jordá, L., & Vera, P. (2000b). Local and Systemic Induction of Two Defense-Related Subtilisin-Like Protease Promoters in Transgenic Arabidopsis Plants. Luciferin Induction of PR Gene Expression1. *Plant Physiology*, *124*(3), 1049–1058. https://doi.org/10.1104/pp.124.3.1049
Kahmann, R., & Kämper, J. (2004). Ustilago maydis: how its biology relates to pathogenic development. *New Phytologist*, *164*(1), 31–42. https://doi.org/https://doi.org/10.1111/j.1469-8137.2004.01156.x
Kamle, M., Borah, R., Bora, H., Jaiswal, A. K., Singh, R. K., & Kumar, P. (2020). *Systemic Acquired Resistance (SAR) and Induced Systemic Resistance (ISR): Role and Mechanism of Action Against Phytopathogens BT - Fungal Biotechnology and Bioengineering* (A. E.-L. Hesham, R. S. Upadhyay, G. D. Sharma, C.

Manoharachary, & V. K. Gupta (eds.); pp. 457–470). Springer International Publishing. https://doi.org/10.1007/978-3-030-41870-0_20

Kang, M., Fokar, M., Abdelmageed, H., & Allen, R. D. (2011). Arabidopsis SAP5 functions as a positive regulator of stress responses and exhibits E3 ubiquitin ligase activity. *Plant Molecular Biology*, *75*(4), 451–466. https://doi.org/10.1007/s11103-011-9748-2

Kang, M., Lee, S., Abdelmageed, H., Reichert, A., Lee, H.-K., Fokar, M., Mysore, K. S., & Allen, R. D. (2017). Arabidopsis stress associated protein 9 mediates biotic and abiotic stress responsive ABA signaling via the proteasome pathway. *Plant, Cell & Environment*, *40*(5), 702–716. https://doi.org/https://doi.org/10.1111/pce.12892

Kanneganti, V., & Gupta, A. K. (2008). Overexpression of OsiSAP8, a member of stress associated protein (SAP) gene family of rice confers tolerance to salt, drought and cold stress in transgenic tobacco and rice. *Plant Molecular Biology*, *66*(5), 445–462. https://doi.org/10.1007/s11103-007-9284-2

Kaschani, F., Gu, C., Niessen, S., Hoover, H., Cravatt, B. F., & van der Hoorn, R. A. L. (2009). Diversity of serine hydrolase activities of unchallenged and botrytis-infected Arabidopsis thaliana. *Molecular & Cellular Proteomics : MCP*, *8*(5), 1082–1093. https://doi.org/10.1074/mcp.M800494-MCP200

Koenig, M., Moser, D., Leusner, J., Depotter, J. R. L., Doehlemann, G., & Villamil, J. M. (2023). Maize Phytocytokines Modulate Pro-Survival Host Responses and Pathogen Resistance. *Molecular Plant-Microbe Interactions*, *36*(9), 592–604. https://doi.org/10.1094/MPMI-01-23-0005-R

Koenig, M., Sorger, Z., Keh, S. P. Y., Doehlemann, G., & Misas Villamil, J. C. (2024). Quantitative detection of the maize phytocytokine Zip1 utilizing ELISA. *Journal of Experimental Botany*, erae423. https://doi.org/10.1093/jxb/erae423

Kong, Y.-Z., Chen, Q., & Lan, H.-Y. (2022). Macrophage Migration Inhibitory Factor (MIF) as a Stress Molecule in Renal Inflammation. In *International Journal of Molecular Sciences* (Vol. 23, Issue 9). https://doi.org/10.3390/ijms23094908

Kumar, S., Stecher, G., Li, M., Knyaz, C., & Tamura, K. (2018). MEGA X: Molecular evolutionary genetics analysis across computing platforms. *Molecular Biology and Evolution*, *35*(6), 1547–1549. https://doi.org/10.1093/molbev/msy096

Landström, M. (2010). The TAK1–TRAF6 signalling pathway. *The International Journal of Biochemistry & Cell Biology*, *42*(5), 585–589. https://doi.org/https://doi.org/10.1016/j.biocel.2009.12.023

Lapin, D., Kovacova, V., Sun, X., Dongus, J. A., Bhandari, D., von Born, P., Bautor, J., Guarneri, N., Rzemieniewski, J., Stuttmann, J., Beyer, A., & Parker, J. E. (2019). A Coevolved EDS1-SAG101-NRG1 Module Mediates Cell Death Signaling by TIR-Domain Immune Receptors. *The Plant Cell*, *31*(10), 2430–2455. https://doi.org/10.1105/tpc.19.00118

Lee, Donghoon, Zhu, Y., Colson, L., Wang, X., Chen, S., Tkacik, E., Huang, L., Ouyang, Q., Goldberg, A. L., & Lu, Y. (2023). Molecular mechanism for activation of the 26S proteasome by ZFAND5. *Molecular Cell*, *83*(16), 2959-2975.e7. https://doi.org/10.1016/j.molcel.2023.07.023

Lee, DongHyuk, Lal, N. K., Lin, Z.-J. D., Ma, S., Liu, J., Castro, B., Toruño, T., Dinesh-Kumar, S. P., & Coaker, G. (2020). Regulation of reactive oxygen species during plant immunity through phosphorylation and ubiquitination of RBOHD. *Nature*

Communications, *11*(1), 1838. https://doi.org/10.1038/s41467-020-15601-5

Lee, E. G., Boone, D. L., Chai, S., Libby, S. L., Chien, M., Lodolce, J. P., & Ma, A. (2000). Failure to Regulate TNF-Induced NF-κB and Cell Death Responses in A20-Deficient Mice. *Science*, *289*(5488), 2350–2354. https://doi.org/10.1126/science.289.5488.2350

Leng, L., Wang, W., Roger, T., Merk, M., Wuttke, M., Calandra, T., & Bucala, R. (2009). Glucocorticoid-induced MIF expression by human CEM T cells. *Cytokine*, *48*(3), 177–185. https://doi.org/https://doi.org/10.1016/j.cyto.2009.07.002

Letunic, I., & Bork, P. (2024). Interactive Tree of Life (iTOL) v6: recent updates to the phylogenetic tree display and annotation tool. *Nucleic Acids Research*, *52*(W1), W78–W82. https://doi.org/10.1093/nar/gkae268

Li, C., Gong, B.-Q., Luo, S., Wang, T., Long, R., Jiang, X., Deng, Y. Z., & Li, J.-F. (2024). Engineering a conserved immune coreceptor into a primed state enhances fungal resistance in crops without growth penalty. *Plant Physiology*, *196*(4), 2956–2972. https://doi.org/10.1093/plphys/kiae499

Linnen, J. M., Bailey, C. P., & Weeks, D. L. (1993). Two related localized mRNAs from Xenopus laevis encode ubiquitin-like fusion proteins. *Gene*, *128*(2), 181–188. https://doi.org/https://doi.org/10.1016/0378-1119(93)90561-G

Liu, Yanan, Jackson, E., Liu, X., Huang, X., Van Der Hoorn, R. A. L., Zhang, Y., & Li, X. (2024a). Proteolysis in plant immunity. *Plant Cell*, *36*(9), 3099–3115. https://doi.org/10.1093/plcell/koae142

Liu, Yanan, Jackson, E., Liu, X., Huang, X., Van Der Hoorn, R. A. L., Zhang, Y., & Li, X. (2024b). Proteolysis in plant immunity. *Plant Cell*, *36*(9), 3099–3115. https://doi.org/10.1093/plcell/koae142

Liu, Yang, Gong, T., Kong, X., Sun, J., & Liu, L. (2024). XYLEM CYSTEINE PEPTIDASE 1 and its inhibitor CYSTATIN 6 regulate pattern-triggered immunity by modulating the stability of the NADPH oxidase RESPIRATORY BURST OXIDASE HOMOLOG D. *The Plant Cell*, *36*(2), 471–488. https://doi.org/10.1093/plcell/koad262

Liu, Z., Wu, Y., Yang, F., Zhang, Y., Chen, S., Xie, Q., Tian, X., & Zhou, J.-M. (2013). BIK1 interacts with PEPRs to mediate ethylene-induced immunity. *Proceedings of the National Academy of Sciences*, *110*(15), 6205–6210. https://doi.org/10.1073/pnas.1215543110

Lloret, A., Conejero, A., Leida, C., Petri, C., Gil-Muñoz, F., Burgos, L., Badenes, M. L., & Ríos, G. (2017). Dual regulation of water retention and cell growth by a stress-associated protein (SAP) gene in Prunus. *Scientific Reports*, *7*(1), 332. https://doi.org/10.1038/s41598-017-00471-7

Lu, D., Lin, W., Gao, X., Wu, S., Cheng, C., Avila, J., Heese, A., Devarenne, T. P., He, P., & Shan, L. (2011). Direct Ubiquitination of Pattern Recognition Receptor FLS2 Attenuates Plant Innate Immunity. *Science*, *332*(6036), 1439–1442. https://doi.org/10.1126/science.1204903

Lue, H., Kleemann, R., Calandra, T., Roger, T., & Bernhagen, J. (2002). Macrophage migration inhibitory factor (MIF): mechanisms of action and role in disease. *Microbes and Infection*, *4*(4), 449–460. https://doi.org/https://doi.org/10.1016/S1286-4579(02)01560-5

Luo, X., & Hofmann, K. (2001). The protease-associated domain: a homology domain associated with multiple classes of proteases. *Trends in Biochemical Sciences*,

26(3), 147–148. https://doi.org/https://doi.org/10.1016/S0968-0004(00)01768-0

Malinovsky, F. G., Brodersen, P., Fiil, B. K., McKinney, L. V., Thorgrimsen, S., Beck, M., Nielsen, H. B., Pietra, S., Zipfel, C., Robatzek, S., Petersen, M., Hofius, D., & Mundy, J. (2010). Lazarus1, a DUF300 Protein, Contributes to Programmed Cell Death Associated with Arabidopsis acd11 and the Hypersensitive Response. *PLOS ONE*, *5*(9), e12586. https://doi.org/10.1371/journal.pone.0012586

Mao, X., Yu, C., Li, L., Wang, M., Yang, L., Zhang, Y., Zhang, Y., Wang, J., Li, C., Reynolds, M. P., & Jing, R. (2022). How Many Faces Does the Plant U-Box E3 Ligase Have? In *International Journal of Molecular Sciences* (Vol. 23, Issue 4). https://doi.org/10.3390/ijms23042285

Matsui, S., Noda, S., Kuwata, K., Nomoto, M., Tada, Y., Shinohara, H., & Matsubayashi, Y. (2024). Arabidopsis SBT5.2 and SBT1.7 subtilases mediate C-terminal cleavage of flg22 epitope from bacterial flagellin. *Nature Communications*, *15*(1), 3762. https://doi.org/10.1038/s41467-024-48108-4

McGurl, B., Pearce, G., Orozco-Cardenas, M., & Ryan, C. A. (1992). Structure, Expression, and Antisense Inhibition of the Systemin Precursor Gene. *Science*, *255*(5051), 1570–1573. https://doi.org/10.1126/science.1549783

McLellan, H., Chen, K., He, Q., Wu, X., Boevink, P. C., Tian, Z., & Birch, P. R. J. (2020). The Ubiquitin E3 Ligase PUB17 Positively Regulates Immunity by Targeting a Negative Regulator, KH17, for Degradation. *Plant Communications*, *1*(4). https://doi.org/10.1016/j.xplc.2020.100020

Miao, M., Niu, X., Kud, J., Du, X., Avila, J., Devarenne, T. P., Kuhl, J. C., Liu, Y., & Xiao, F. (2016). The ubiquitin ligase SEVEN IN ABSENTIA (SINA) ubiquitinates a defense-related NAC transcription factor and is involved in defense signaling. *New Phytologist*, *211*(1), 138–148. https://doi.org/https://doi.org/10.1111/nph.13890

Misas-Villamil, J. C., van der Hoorn, R. A. L., & Doehlemann, G. (2016). Papain-like cysteine proteases as hubs in plant immunity. *New Phytologist*, *212*(4), 902–907. https://doi.org/10.1111/nph.14117

Misas Villamil, J. C., Mueller, A. N., Demir, F., Meyer, U., Ökmen, B., Schulze Hüynck, J., Breuer, M., Dauben, H., Win, J., Huesgen, P. F., & Doehlemann, G. (2019). A fungal substrate mimicking molecule suppresses plant immunity via an inter-kingdom conserved motif. *Nature Communications*, *10*(1). https://doi.org/10.1038/s41467-019-09472-8

Miya, A., Albert, P., Shinya, T., Desaki, Y., Ichimura, K., Shirasu, K., Narusaka, Y., Kawakami, N., Kaku, H., & Shibuya, N. (2007). CERK1, a LysM receptor kinase, is essential for chitin elicitor signaling in Arabidopsis. *Proceedings of the National Academy of Sciences*, *104*(49), 19613–19618. https://doi.org/10.1073/pnas.0705147104

Morales-Navarro, S., Pérez-Díaz, R., Ortega, A., de Marcos, A., Mena, M., Fenoll, C., González-Villanueva, E., & Ruiz-Lara, S. (2018). Overexpression of a SDD1-Like Gene From Wild Tomato Decreases Stomatal Density and Enhances Dehydration Avoidance in Arabidopsis and Cultivated Tomato. *Frontiers in Plant Science*, *9*. https://doi.org/10.3389/fpls.2018.00940

Morgan, B. P. (2016). The membrane attack complex as an inflammatory trigger. *Immunobiology*, *221*(6), 747–751. https://doi.org/https://doi.org/10.1016/j.imbio.2015.04.006

Mosher, S., Seybold, H., Rodriguez, P., Stahl, M., Davies, K. A., Dayaratne, S., Morillo, S. A., Wierzba, M., Favery, B., Keller, H., Tax, F. E., & Kemmerling, B. (2013). The tyrosine-sulfated peptide receptors PSKR1 and PSY1R modify the immunity of Arabidopsis to biotrophic and necrotrophic pathogens in an antagonistic manner. *The Plant Journal*, *73*(3), 469–482. https://doi.org/https://doi.org/10.1111/tpj.12050

Mueller, A. N., Ziemann, S., Treitschke, S., Aßmann, D., & Doehlemann, G. (2013). Compatibility in the Ustilago maydis-Maize Interaction Requires Inhibition of Host Cysteine Proteases by the Fungal Effector Pit2. *PLoS Pathogens*, *9*(2). https://doi.org/10.1371/journal.ppat.1003177

Mukhopadhyay, A., Vij, S., & Tyagi, A. K. (2004). Overexpression of a zinc-finger protein gene from rice confers tolerance to cold, dehydration, and salt stress in transgenic tobacco. *Proceedings of the National Academy of Sciences*, *101*(16), 6309–6314. https://doi.org/10.1073/pnas.0401572101

Nakaminami, K., Okamoto, M., Higuchi-Takeuchi, M., Yoshizumi, T., Yamaguchi, Y., Fukao, Y., Shimizu, M., Ohashi, C., Tanaka, M., Matsui, M., Shinozaki, K., Seki, M., & Hanada, K. (2018). AtPep3 is a hormone-like peptide that plays a role in the salinity stress tolerance of plants. *Proceedings of the National Academy of Sciences*, *115*(22), 5810–5815. https://doi.org/10.1073/pnas.1719491115

Ngou, B. P. M., Ding, P., & Jones, J. D. G. (2022). Thirty years of resistance: Zig-zag through the plant immune system. *Plant Cell*, *34*(5), 1447–1478. https://doi.org/10.1093/plcell/koac041

Ngou, B. P. M., Wyler, M., Schmid, M. W., Kadota, Y., & Shirasu, K. (2024). Evolutionary trajectory of pattern recognition receptors in plants. *Nature Communications*, *15*(1), 308. https://doi.org/10.1038/s41467-023-44408-3

Ning, Y., Jantasuriyarat, C., Zhao, Q., Zhang, H., Chen, S., Liu, J., Liu, L., Tang, S., Park, C. H., Wang, X., Liu, X., Dai, L., Xie, Q., & Wang, G.-L. (2011). The SINA E3 Ligase OsDIS1 Negatively Regulates Drought Response in Rice . *Plant Physiology*, *157*(1), 242–255. https://doi.org/10.1104/pp.111.180893

Olsson, V., Joos, L., Zhu, S., Gevaert, K., Butenko, M. A., & De Smet, I. (2019). Look Closely, the Beautiful May Be Small: Precursor-Derived Peptides in Plants. *Annual Review of Plant Biology*, *70*(Volume 70, 2019), 153–186. https://doi.org/https://doi.org/10.1146/annurev-arplant-042817-040413

Opipari Jr, A. W., Boguski, M. S., & Dixit, V. M. (1990). The A20 cDNA induced by tumor necrosis factor alpha encodes a novel type of zinc finger protein. *Journal of Biological Chemistry*, *265*(25), 14705–14708. https://doi.org/10.1016/S0021-9258(18)77165-2

Passarge, A., Demir, F., Green, K., Depotter, J. R. L., Scott, B., Huesgen, P. F., Doehlemann, G., & Misas Villamil, J. C. (2021). Host apoplastic cysteine protease activity is suppressed during the mutualistic association of Lolium perenne and Epichloë festucae. *Journal of Experimental Botany*, *72*(9), 3410–3426. https://doi.org/10.1093/jxb/erab088

Passarge, A., Doehlemann, G., & Misas Villamil, J. C. (2022). Detection of Apoplastic Protease InhibitorsProteaseinhibitors Using Convolution Activity-Based Protein Profiling. In M. Klemenčič, S. Stael, & P. F. Huesgen (Eds.), *Plant Proteases and Plant Cell Death: Methods and Protocols* (pp. 95–104). Springer US. https://doi.org/10.1007/978-1-0716-2079-3_8

Paulus, J. K., Kourelis, J., Ramasubramanian, S., Homma, F., Godson, A., Hörger, A. C.,

Hong, T. N., Krahn, D., Carballo, L. O., Wang, S., Win, J., Smoker, M., Kamoun, S., Dong, S., & Van Der Hoorn, R. A. L. (2020). Extracellular proteolytic cascade in tomato activates immune protease Rcr3. *Proceedings of the National Academy of Sciences of the United States of America*, *117*(29), 17409–17417. https://doi.org/10.1073/pnas.1921101117

Pieterse, C. M. J., Leon-Reyes, A., Van der Ent, S., & Van Wees, S. C. M. (2009). Networking by small-molecule hormones in plant immunity. *Nature Chemical Biology*, *5*(5), 308–316. https://doi.org/10.1038/nchembio.164

Pieterse, C. M. J., Van Der Does, D., Zamioudis, C., Leon-Reyes, A., & Van Wees, S. C. M. (2012). Hormonal modulation of plant immunity. *Annual Review of Cell and Developmental Biology*, *28*, 489–521. https://doi.org/10.1146/annurev-cellbio-092910-154055

Plattner, S., Gruber, C., Altmann, F., & Bohlmann, H. (2014). Self-processing of a barley subtilase expressed in E. coli. *Protein Expression and Purification*, *101*, 76–83. https://doi.org/https://doi.org/10.1016/j.pep.2014.05.014

Purwar, S., Chugh, V., Singh, P., Srivastava, A. K., Singh, A. K., Mishra, A. C., Singh, A., & Singh, C. M. (2024a). Genome-wide identification and analysis of Subtilisin-like serine protease gene family in banana (Musa accuminta L.) and their expression under abiotic stresses. *Plant Biotechnology Reports*, *18*(1), 143–160. https://doi.org/10.1007/s11816-023-00855-4

Purwar, S., Chugh, V., Singh, P., Srivastava, A. K., Singh, A. K., Mishra, A. C., Singh, A., & Singh, C. M. (2024b). Genome-wide identification and analysis of Subtilisin-like serine protease gene family in banana (Musa accuminta L.) and their expression under abiotic stresses. *Plant Biotechnology Reports*, *18*(1), 143–160. https://doi.org/10.1007/s11816-023-00855-4

Ramírez, V., López, A., Mauch-Mani, B., Gil, M. J., & Vera, P. (2013). An Extracellular Subtilase Switch for Immune Priming in Arabidopsis. *PLOS Pathogens*, *9*(6), e1003445. https://doi.org/10.1371/journal.ppat.1003445

Ramírez, V., López, A., Mauch-Mani, B., Gil, M. J., & Vera, P. (2016). Correction: An Extracellular Subtilase Switch for Immune Priming in Arabidopsis. *PLOS Pathogens*, *12*(11), e1006003.

Rawlings, N. D., Barrett, A. J., Thomas, P. D., Huang, X., Bateman, A., & Finn, R. D. (2018). The MEROPS database of proteolytic enzymes, their substrates and inhibitors in 2017 and a comparison with peptidases in the PANTHER database. *Nucleic Acids Research*, *46*(D1), D624–D632. https://doi.org/10.1093/nar/gkx1134

Reichardt, S., Repper, D., Tuzhikov, A. I., Galiullina, R. A., Planas-Marquès, M., Chichkova, N. V, Vartapetian, A. B., Stintzi, A., & Schaller, A. (2018). The tomato subtilase family includes several cell death-related proteinases with caspase specificity. *Scientific Reports*, *8*(1), 10531. https://doi.org/10.1038/s41598-018-28769-0

Ribeiro, A., Akkermans, A. D., van Kammen, A., Bisseling, T., & Pawlowski, K. (1995). A nodule-specific gene encoding a subtilisin-like protease is expressed in early stages of actinorhizal nodule development. *The Plant Cell*, *7*(6), 785–794. https://doi.org/10.1105/tpc.7.6.785

Richau, K. H., Kaschani, F., Verdoes, M., Pansuriya, T. C., Niessen, S., Stüber, K., Colby, T., Overkleeft, H. S., Bogyo, M., & Van der Hoorn, R. A. L. (2012). Subclassification

and Biochemical Analysis of Plant Papain-Like Cysteine Proteases Displays Subfamily-Specific Characteristics . *Plant Physiology*, *158*(4), 1583–1599. https://doi.org/10.1104/pp.112.194001

Roger, T., Froidevaux, C., Martin, C., & Calandra, T. (2003). Macrophage migration inhibitory factor (MIF) regulates host responses to endotoxin through modulation of Toll-like receptor 4 (TLR4). *Journal of Endotoxin Research*, *9*(2), 119–123. https://doi.org/10.1177/09680519030090020801

Roger, T., Glauser, M. P., & Calandra, T. (2001). Macrophage migration inhibitory factor (MIF) modulates innate immune responses induced by endotoxin and Gram-negative bacteria. *Journal of Endotoxin Research*, *7*(6), 456–460. https://doi.org/10.1177/09680519010070061101

Rose, L., Atwell, S., Grant, M., & Holub, E. B. (2012). Parallel loss-of-function at the RPM1 bacterial resistance locus in Arabidopsis thaliana. *Frontiers in Plant Science*, *3*(DEC), 1–16. https://doi.org/10.3389/fpls.2012.00287

Royek, S., Bayer, M., Pfannstiel, J., Pleiss, J., Ingram, G., Stintzi, A., & Schaller, A. (2022). Processing of a plant peptide hormone precursor facilitated by posttranslational tyrosine sulfation. *Proceedings of the National Academy of Sciences*, *119*(16), e2201195119. https://doi.org/10.1073/pnas.2201195119

Rozewicki, J., Li, S., Amada, K. M., Standley, D. M., & Katoh, K. (2019). MAFFT-DASH: integrated protein sequence and structural alignment. *Nucleic Acids Research*, *47*(W1), W5–W10. https://doi.org/10.1093/nar/gkz342

Sánchez-Vallet, A., Mesters, J. R., & Thomma, B. P. H. J. (2015). The battle for chitin recognition in plant-microbe interactions. *FEMS Microbiology Reviews*, *39*(2), 171–183. https://doi.org/10.1093/femsre/fuu003

Schaller, A. (2004). A cut above the rest: the regulatory function of plant proteases. *Planta*, *220*(2), 183–197. https://doi.org/10.1007/s00425-004-1407-2

Schaller, A., Stintzi, A., Rivas, S., Serrano, I., Chichkova, N. V., Vartapetian, A. B., Martínez, D., Guiamét, J. J., Sueldo, D. J., van der Hoorn, R. A. L., Ramírez, V., & Vera, P. (2018). From structure to function – a family portrait of plant subtilases. *New Phytologist*, *218*(3), 901–915. https://doi.org/10.1111/nph.14582

Schulze Hüynck, J., Kaschani, F., van der Linde, K., Ziemann, S., Müller, A. N., Colby, T., Kaiser, M., Misas Villamil, J. C., & Doehlemann, G. (2019). Proteases underground: Analysis of the maize root apoplast identifies organ specific papain-like cysteine protease activity. *Frontiers in Plant Science*, *10*(April), 1–16. https://doi.org/10.3389/fpls.2019.00473

Selin, C., de Kievit, T. R., Belmonte, M. F., & Fernando, W. G. D. (2016). Elucidating the role of effectors in plant-fungal interactions: Progress and challenges. *Frontiers in Microbiology*, *7*(APR), 1–21. https://doi.org/10.3389/fmicb.2016.00600

Shen, W., Liu, J., & Li, J. F. (2019). Type-II Metacaspases Mediate the Processing of Plant Elicitor Peptides in Arabidopsis. *Molecular Plant*, *12*(11), 1524–1533. https://doi.org/10.1016/j.molp.2019.08.003

Shimizu, T., Nakano, T., Takamizawa, D., Desaki, Y., Ishii-Minami, N., Nishizawa, Y., Minami, E., Okada, K., Yamane, H., Kaku, H., & Shibuya, N. (2010). Two LysM receptor molecules, CEBiP and OsCERK1, cooperatively regulate chitin elicitor signaling in rice. *The Plant Journal*, *64*(2), 204–214. https://doi.org/https://doi.org/10.1111/j.1365-313X.2010.04324.x

Singh, Ankur, & Roychoudhury, A. (2023). Abscisic acid in plants under abiotic stress: crosstalk with major phytohormones. *Plant Cell Reports*, *42*(6), 961–974. https://doi.org/10.1007/s00299-023-03013-w

Singh, P., & Mukhopadhyay, K. (2021). Comprehensive molecular dissection of TIFY Transcription factors reveal their dynamic responses to biotic and abiotic stress in wheat (Triticum aestivum L.). *Scientific Reports*, *11*(1), 9739. https://doi.org/10.1038/s41598-021-87722-w

Siritapetawee, J., Attarataya, J., & Charoenwattanasatien, R. (2022). Sequence analysis and crystal structure of a glycosylated protease from Euphorbia resinifera latex for its proteolytic activity aspect. *Biotechnology and Applied Biochemistry*, *69*(6), 2580–2591. https://doi.org/https://doi.org/10.1002/bab.2307

Spiller, L., Manjula, R., Leissing, F., Basquin, J., Bourilhon, P., Sinitski, D., Brandhofer, M., Levecque, S., Sabelleck, B., Feederle, R., Flatley, A., Panstruga, R., Bernhagen, J., & Lolis, E. (2023). Structures of Arabidopsis thaliana MDL Proteins and Synergistic Effects with the Cytokine MIF on Human Receptors. *BioRxiv*, 2023.01.30.525655. https://doi.org/10.1101/2023.01.30.525655

Spoel, S. H., & Dong, X. (2024a). Salicylic acid in plant immunity and beyond. *The Plant Cell*, *36*(5), 1451–1464. https://doi.org/10.1093/plcell/koad329

Spoel, S. H., & Dong, X. (2024b). Salicylic acid in plant immunity and beyond. *The Plant Cell*, *36*(5), 1451–1464. https://doi.org/10.1093/plcell/koad329

Stamatakis, A. (2014). RAxML version 8: a tool for phylogenetic analysis and post-analysis of large phylogenies. *Bioinformatics*, *30*(9), 1312–1313. https://doi.org/10.1093/bioinformatics/btu033

Stegmann, M., Monaghan, J., Smakowska-Luzan, E., Rovenich, H., Lehner, A., Holton, N., Belkhadir, Y., & Zipfel, C. (2017). The receptor kinase FER is a RALF-regulated scaffold controlling plant immune signaling. *Science*, *355*(6322), 287–289. https://doi.org/10.1126/science.aal2541

Strawn, M. A., Marr, S. K., Inoue, K., Inada, N., Zubieta, C., & Wildermuth, M. C. (2007). Arabidopsis Isochorismate Synthase Functional in Pathogen-induced Salicylate Biosynthesis Exhibits Properties Consistent with a Role in Diverse Stress Responses * . *Journal of Biological Chemistry*, *282*(8), 5919–5933. https://doi.org/10.1074/jbc.M605193200

Ströher, E., Wang, X.-J., Roloff, N., Klein, P., Husemann, A., & Dietz, K.-J. (2009). Redox-Dependent Regulation of the Stress-Induced Zinc-Finger Protein SAP12 in Arabidopsis thaliana. *Molecular Plant*, *2*(2), 357–367. https://doi.org/10.1093/mp/ssn084

Stührwohldt, N., Ehinger, A., Thellmann, K., & Schaller, A. (2020). Processing and Formation of Bioactive CLE40 Peptide Are Controlled by Posttranslational Proline Hydroxylation. *Plant Physiology*, *184*(3), 1573–1584. https://doi.org/10.1104/pp.20.00528

Su, A., Qin, Q., Liu, C., Zhang, J., Yu, B., Cheng, Y., Wang, S., Tang, J., & Si, W. (2022). Identification and Analysis of Stress-Associated Proteins (SAPs) Protein Family and Drought Tolerance of ZmSAP8 in Transgenic Arabidopsis. In *International Journal of Molecular Sciences* (Vol. 23, Issue 22). https://doi.org/10.3390/ijms232214109

Subramanian, A., Narayan, R., Corsello, S. M., Peck, D. D., Natoli, T. E., Lu, X., Gould, J., Davis, J. F., Tubelli, A. A., Asiedu, J. K., Lahr, D. L., Hirschman, J. E., Liu, Z.,

Donahue, M., Julian, B., Khan, M., Wadden, D., Smith, I. C., Lam, D., … Golub, T. R. (2017). A Next Generation Connectivity Map: L1000 Platform and the First 1,000,000 Profiles. *Cell*, *171*(6), 1437-1452.e17. https://doi.org/10.1016/j.cell.2017.10.049

Sueldo, D., Ahmed, A., Misas-Villamil, J., Colby, T., Tameling, W., Joosten, M. H. A. J., & van der Hoorn, R. A. L. (2014). Dynamic hydrolase activities precede hypersensitive tissue collapse in tomato seedlings. *New Phytologist*, *203*(3), 913–925. https://doi.org/https://doi.org/10.1111/nph.12870

Sumaiya, K., Langford, D., Natarajaseenivasan, K., & Shanmughapriya, S. (2022). Macrophage migration inhibitory factor (MIF): A multifaceted cytokine regulated by genetic and physiological strategies. *Pharmacology & Therapeutics*, *233*, 108024. https://doi.org/10.1016/j.pharmthera.2021.108024

Sun, P., Shi, Y., Valerio, A. G. O., Borrego, E. J., Luo, Q., Qin, J., Liu, K., & Yan, Y. (2021). An updated census of the maize TIFY family. *PLOS ONE*, *16*(2), e0247271. https://doi.org/10.1371/journal.pone.0247271

Sun, Y., Wang, Y., Li, J.-H., Zhu, S.-H., Tang, H.-T., & Xia, Z.-F. (2013). Macrophage migration inhibitory factor counter-regulates dexamethasone-induced annexin 1 expression and influences the release of eicosanoids in murine macrophages. *Immunology*, *140*(2), 250–258. https://doi.org/https://doi.org/10.1111/imm.12135

Takahashi, F., Hanada, K., Kondo, T., & Shinozaki, K. (2019). Hormone-like peptides and small coding genes in plant stress signaling and development. *Current Opinion in Plant Biology*, *51*, 88–95. https://doi.org/https://doi.org/10.1016/j.pbi.2019.05.011

Tanaka, K., Choi, J., Cao, Y., & Stacey, G. (2014). Extracellular ATP acts as a damage-associated molecular pattern (DAMP) signal in plants. *Frontiers in Plant Science*, *5*(SEP), 1–9. https://doi.org/10.3389/fpls.2014.00446

Thulasi Devendrakumar, K., Copeland, C., & Li, X. (2019). The proteasome regulator PTRE1 contributes to the turnover of SNC1 immune receptor. *Molecular Plant Pathology*, *20*(11), 1566–1573. https://doi.org/https://doi.org/10.1111/mpp.12855

Thulasi Devendrakumar, K., Li, X., & Zhang, Y. (2018). MAP kinase signalling: interplays between plant PAMP- and effector-triggered immunity. *Cellular and Molecular Life Sciences*, *75*(16), 2981–2989. https://doi.org/10.1007/s00018-018-2839-3

Tornero, P, Conejero, V., & Vera, P. (1996). Primary structure and expression of a pathogen-induced protease (PR-P69) in tomato plants: Similarity of functional domains to subtilisin-like endoproteases. *Proceedings of the National Academy of Sciences*, *93*(13), 6332–6337. https://doi.org/10.1073/pnas.93.13.6332

Tornero, Pablo, Conejero, V., & Vera, P. (1997). Identification of a New Pathogen-induced Member of the Subtilisin-like Processing Protease Family from Plants *. *Journal of Biological Chemistry*, *272*(22), 14412–14419. https://doi.org/10.1074/jbc.272.22.14412

Tornero, Pablo, Mayda, E., Gómez, M. D., Cañas, L., Conejero, V., & Vera, P. (1996). Characterization of LRP, a leucine-rich repeat (LRR) protein from tomato plants that is processed during pathogenesis. *The Plant Journal*, *10*(2), 315–330. https://doi.org/https://doi.org/10.1046/j.1365-313X.1996.10020315.x

Trusova, S. V, Teplova, A. D., Golyshev, S. A., Galiullina, R. A., Morozova, E. A., Chichkova, N. V, & Vartapetian, A. B. (2019). Clathrin-Mediated Endocytosis Delivers Proteolytically Active Phytaspases Into Plant Cells. *Frontiers in Plant Science*, *10*.

Tsuda, K., & Katagiri, F. (2010a). Comparing signaling mechanisms engaged in pattern-triggered and effector-triggered immunity. *Current Opinion in Plant Biology*, *13*(4), 459–465. https://doi.org/https://doi.org/10.1016/j.pbi.2010.04.006

Tsuda, K., & Katagiri, F. (2010b). Comparing signaling mechanisms engaged in pattern-triggered and effector-triggered immunity. *Current Opinion in Plant Biology*, *13*(4), 459–465. https://doi.org/https://doi.org/10.1016/j.pbi.2010.04.006

van der Hoorn, R. A. L. (2008a). Plant Proteases: From Phenotypes to Molecular Mechanisms. *Annual Review of Plant Biology*, *59*(Volume 59, 2008), 191–223. https://doi.org/https://doi.org/10.1146/annurev.arplant.59.032607.092835

van der Hoorn, R. A. L. (2008b). Plant Proteases: From Phenotypes to Molecular Mechanisms. *Annual Review of Plant Biology*, *59*(Volume 59, 2008), 191–223. https://doi.org/https://doi.org/10.1146/annurev.arplant.59.032607.092835

Van Der Hoorn, R. A. L., & Klemenčič, M. (2021). Plant proteases: From molecular mechanisms to functions in development and immunity. *Journal of Experimental Botany*, *72*(9), 3337–3339. https://doi.org/10.1093/jxb/erab129

van der Linde, K. (2011). Funktionelle Charakterisierung von Wirtsgenen in der Ustilago maydis – Mais-Interaktion. *Dissertation*.

van der Linde, K., Egger, R. L., Timofejeva, L., & Walbot, V. (2018a). Application of the pathogen Trojan horse approach in maize (Zea mays). *Plant Signaling & Behavior*, *13*(12), e1547575. https://doi.org/10.1080/15592324.2018.1547575

van der Linde, K., Egger, R. L., Timofejeva, L., & Walbot, V. (2018b). Application of the pathogen Trojan horse approach in maize (Zea mays). *Plant Signaling & Behavior*, *13*(12), e1547575. https://doi.org/10.1080/15592324.2018.1547575

van der Linde, K., Hemetsberger, C., Kastner, C., Kaschani, F., van der Hoorn, R. A. L., Kumlehn, J., & Doehlemann, G. (2012). A maize cystatin suppresses host immunity by inhibiting apoplastic cysteine proteases. *Plant Cell*, *24*(3), 1285–1300. https://doi.org/10.1105/tpc.111.093732

van der Linde, K., Mueller, A. N., Hemetsberger, C., Kashani, F., van der Hoorn, R. A. L., & Doehlemann, G. (2012). The maize cystatin CC9 interacts with apoplastic cysteine proteases. *Plant Signaling and Behavior*, *7*(11), 1–5. https://doi.org/10.4161/psb.21902

Vij, S., & Tyagi, A. K. (2006). Genome-wide analysis of the stress associated protein (SAP) gene family containing A20/AN1 zinc-finger(s) in rice and their phylogenetic relationship with Arabidopsis. *Molecular Genetics and Genomics*, *276*(6), 565–575. https://doi.org/10.1007/s00438-006-0165-1

Wang, D., Wei, L., Liu, T., Ma, J., Huang, K., Guo, H., Huang, Y., Zhang, L., Zhao, J., Tsuda, K., & Wang, Y. (2023). Suppression of ETI by PTI priming to balance plant growth and defense through an MPK3/MPK6-WRKYs-PP2Cs module. *Molecular Plant*, *16*(5), 903–918. https://doi.org/10.1016/j.molp.2023.04.004

Wang, L., Tsuda, K., Truman, W., Sato, M., Nguyen, L. V, Katagiri, F., & Glazebrook, J. (2011). CBP60g and SARD1 play partially redundant critical roles in salicylic acid signaling. *The Plant Journal*, *67*(6), 1029–1041. https://doi.org/https://doi.org/10.1111/j.1365-313X.2011.04655.x

Wang, P., Yao, S., Kosami, K., Guo, T., Li, J., Zhang, Y., Fukao, Y., Kaneko-Kawano, T., Zhang, H., She, Y.-M., Wang, P., Xing, W., Hanada, K., Liu, R., & Kawano, Y. (2020). Identification of endogenous small peptides involved in rice immunity through

transcriptomics- and proteomics-based screening. *Plant Biotechnology Journal*, *18*(2), 415–428. https://doi.org/https://doi.org/10.1111/pbi.13208

Wang, Yan, Pruitt, R. N., Nürnberger, T., & Wang, Y. (2022). Evasion of plant immunity by microbial pathogens. *Nature Reviews Microbiology*, *20*(8), 449–464. https://doi.org/10.1038/s41579-022-00710-3

Wang, Yiming, Garrido-Oter, R., Wu, J., Winkelmüller, T. M., Agler, M., Colby, T., Nobori, T., Kemen, E., & Tsuda, K. (2019). Site-specific cleavage of bacterial MucD by secreted proteases mediates antibacterial resistance in Arabidopsis. *Nature Communications*, *10*(1), 2853. https://doi.org/10.1038/s41467-019-10793-x

Wasternack, C., & Song, S. (2017). Jasmonates: biosynthesis, metabolism, and signaling by proteins activating and repressing transcription. *Journal of Experimental Botany*, *68*(6), 1303–1321. https://doi.org/10.1093/jxb/erw443

Weiser, W. Y., Pozzi, L. M., & David, J. R. (1991). Human recombinant migration inhibitory factor activates human macrophages to kill Leishmania donovani. *The Journal of Immunology*, *147*(6), 2006–2011. https://doi.org/10.4049/jimmunol.147.6.2006

Wiermer, M., Feys, B. J., & Parker, J. E. (2005). Plant immunity: the EDS1 regulatory node. *Current Opinion in Plant Biology*, *8*(4), 383–389. https://doi.org/https://doi.org/10.1016/j.pbi.2005.05.010

Wildermuth, M. C., Dewdney, J., Wu, G., & Ausubel, F. M. (2001). Isochorismate synthase is required to synthesize salicylic acid for plant defence. *Nature*, *414*(6863), 562–565. https://doi.org/10.1038/35107108

Withers, J., & Dong, X. (2016). Posttranslational Modifications of NPR1: A Single Protein Playing Multiple Roles in Plant Immunity and Physiology. *PLOS Pathogens*, *12*(8), e1005707. https://doi.org/10.1371/journal.ppat.1005707

Wu, Y., Zhang, D., Chu, J. Y., Boyle, P., Wang, Y., Brindle, I. D., De Luca, V., & Després, C. (2012). The Arabidopsis NPR1 Protein Is a Receptor for the Plant Defense Hormone Salicylic Acid. *Cell Reports*, *1*(6), 639–647. https://doi.org/10.1016/j.celrep.2012.05.008

Yamaguchi, Y., Barona, G., Ryan, C. A., & Pearce, G. (2011). GmPep914, an Eight-Amino Acid Peptide Isolated from Soybean Leaves, Activates Defense-Related Genes . *Plant Physiology*, *156*(2), 932–942. https://doi.org/10.1104/pp.111.173096

Yamaguchi, Y., Huffaker, A., Bryan, A. C., Tax, F. E., & Ryan, C. A. (2010). PEPR2 Is a Second Receptor for the Pep1 and Pep2 Peptides and Contributes to Defense Responses in Arabidopsis . *The Plant Cell*, *22*(2), 508–522. https://doi.org/10.1105/tpc.109.068874

Yamaguchi, Y., Pearce, G., & Ryan, C. A. (2006). The cell surface leucine-rich repeat receptor for AtPep1, an endogenous peptide elicitor in Arabidopsis, is functional in transgenic tobacco cells. *Proceedings of the National Academy of Sciences*, *103*(26), 10104–10109. https://doi.org/10.1073/pnas.0603729103

Yang, C., Wang, E., & Liu, J. (2022). CERK1, more than a co-receptor in plant–microbe interactions. *New Phytologist*, *234*(5), 1606–1613. https://doi.org/https://doi.org/10.1111/nph.18074

Yang, H., Kim, X., Skłenar, J., Aubourg, S., Sancho-Andrés, G., Stahl, E., Guillou, M.-C., Gigli-Bisceglia, N., Tran Van Canh, L., Bender, K. W., Stintzi, A., Reymond, P., Sánchez-Rodríguez, C., Testerink, C., Renou, J.-P., Menke, F. L. H., Schaller, A., Rhodes, J., & Zipfel, C. (2023). Subtilase-mediated biogenesis of the expanded

family of SERINE RICH ENDOGENOUS PEPTIDES. *Nature Plants*, *9*(12), 2085–2094. https://doi.org/10.1038/s41477-023-01583-x

Yang, Y., Zhang, F., Zhou, T., Fang, A., Yu, Y., Bi, C., & Xiao, S. (2020). In Silico Identification of the Full Complement of Subtilase-Encoding Genes and Characterization of the Role of TaSBT1.7 in Resistance Against Stripe Rust in Wheat. *Phytopathology®*, *111*(2), 398–407. https://doi.org/10.1094/PHYTO-05-20-0176-R

Yee, D., & Goring, D. R. (2009). The diversity of plant U-box E3 ubiquitin ligases: from upstream activators to downstream target substrates. *Journal of Experimental Botany*, *60*(4), 1109–1121. https://doi.org/10.1093/jxb/ern369

Young, M. D., Wakefield, M. J., Smyth, G. K., & Oshlack, A. (2010). Gene ontology analysis for RNA-seq: accounting for selection bias. *Genome Biology*, *11*(2), R14. https://doi.org/10.1186/gb-2010-11-2-r14

Yu, L., Liu, D., Chen, S., Dai, Y., Guo, W., Zhang, X., Wang, L., Ma, S., Xiao, M., Qi, H., Xiao, S., & Chen, Q. (2020). Evolution and Expression of the Membrane Attack Complex and Perforin Gene Family in the Poaceae. In *International Journal of Molecular Sciences* (Vol. 21, Issue 16). https://doi.org/10.3390/ijms21165736

Yu, X.-Q., Niu, H.-Q., Liu, C., Wang, H.-L., Yin, W., & Xia, X. (2024). PTI-ETI synergistic signal mechanisms in plant immunity. *Plant Biotechnology Journal*, *22*(8), 2113–2128. https://doi.org/https://doi.org/10.1111/pbi.14332

Yuan, M., Ngou, B. P. M., Ding, P., & Xin, X. F. (2021a). PTI-ETI crosstalk: an integrative view of plant immunity. *Current Opinion in Plant Biology*, *62*, 102030. https://doi.org/10.1016/j.pbi.2021.102030

Yuan, M., Ngou, B. P. M., Ding, P., & Xin, X. F. (2021b). PTI-ETI crosstalk: an integrative view of plant immunity. *Current Opinion in Plant Biology*, *62*, 102030. https://doi.org/10.1016/j.pbi.2021.102030

Yuan, W., Chen, X., Du, K., Jiang, T., Li, M., Cao, Y., Li, X., Doehlemann, G., Fan, Z., & Zhou, T. (2024). NIa-Pro of sugarcane mosaic virus targets Corn Cysteine Protease 1 (CCP1) to undermine salicylic acid-mediated defense in maize. *PLOS Pathogens*, *20*(3), e1012086. https://doi.org/10.1371/journal.ppat.1012086

Zander, M., Lewsey, M. G., Clark, N. M., Yin, L., Bartlett, A., Saldierna Guzmán, J. P., Hann, E., Langford, A. E., Jow, B., Wise, A., Nery, J. R., Chen, H., Bar-Joseph, Z., Walley, J. W., Solano, R., & Ecker, J. R. (2020). Integrated multi-omics framework of the plant response to jasmonic acid. *Nature Plants*, *6*(3), 290–302. https://doi.org/10.1038/s41477-020-0605-7

Zavaliev, R., & Dong, X. (2024). NPR1, a key immune regulator for plant survival under biotic and abiotic stresses. *Molecular Cell*, *84*(1), 131–141. https://doi.org/10.1016/j.molcel.2023.11.018

Zeng, L., Hu, P., Zhang, Y., Li, M., Zhao, Y., Li, S., & Luo, A. (2024). Macrophage migration inhibitor factor (MIF): Potential role in cognitive impairment disorders. *Cytokine & Growth Factor Reviews*, *77*, 67–75. https://doi.org/https://doi.org/10.1016/j.cytogfr.2024.03.003

Zeng, W., Melotto, M., & He, S. Y. (2010). Plant stomata: a checkpoint of host immunity and pathogen virulence. *Current Opinion in Biotechnology*, *21*(5), 599–603. https://doi.org/https://doi.org/10.1016/j.copbio.2010.05.006

Zhang, C., Yang, R., Zhang, T., Zheng, D., Li, X., Zhang, Z. B., Li, L. G., & Wu, Z. Y.

(2023). ZmTIFY16, a novel maize TIFY transcription factor gene, promotes root growth and development and enhances drought and salt tolerance in Arabidopsis and Zea mays. *Plant Growth Regulation*, *100*(1), 149–160. https://doi.org/10.1007/s10725-022-00946-2

Zhang, X., Dai, Y.-S., Wang, Y.-X., Su, Z.-Z., Yu, L.-J., Zhang, Z.-F., Xiao, S., & Chen, Q.-F. (2022). Overexpression of the Arabidopsis MACPF Protein AtMACP2 Promotes Pathogen Resistance by Activating SA Signaling. In *International Journal of Molecular Sciences* (Vol. 23, Issue 15). https://doi.org/10.3390/ijms23158784

Zhang, Y., & Li, X. (2019). Salicylic acid: biosynthesis, perception, and contributions to plant immunity. *Current Opinion in Plant Biology*, *50*, 29–36. https://doi.org/10.1016/j.pbi.2019.02.004

Zhao, M., Chang, Q., Liu, Y., Sang, P., Kang, Z., & Wang, X. (2021). Functional Characterization of the Wheat Macrophage Migration Inhibitory Factor TaMIF1 in Wheat-Stripe Rust (Puccinia striiformis) Interaction. In *Biology* (Vol. 10, Issue 9). https://doi.org/10.3390/biology10090878

Ziemann, S., Van Der Linde, K., Lahrmann, U., Acar, B., Kaschani, F., Colby, T., Kaiser, M., Ding, Y., Schmelz, E., Huffaker, A., Holton, N., Zipfel, C., & Doehlemann, G. (2018). An apoplastic peptide activates salicylic acid signalling in maize. *Nature Plants*, *4*(3), 172–180. https://doi.org/10.1038/s41477-018-0116-y

6. Supplementary data

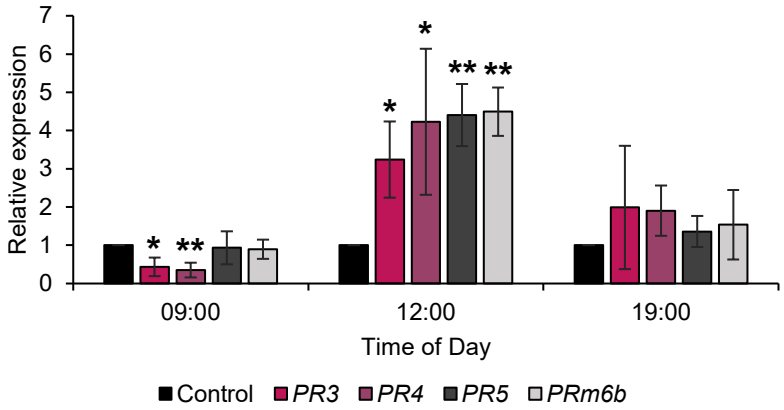

Figure S1: *PR*-gene expression 24 hours upon SA infiltration is daytime depending. Expression of four *PR*-genes (*PR3*, *PR4*, *PR5* and *PRm6b*) was measured 24 hours upon the treatment with 2 mM SA in the morning (9:00), at midday (12:00) and in the evening (19:00). The expression was set relative to *GAPDH* and the corresponding control. Significant differences were calculated based on students t-test (* =p<0.05, ** =p<0.01, *** =p<0.001).

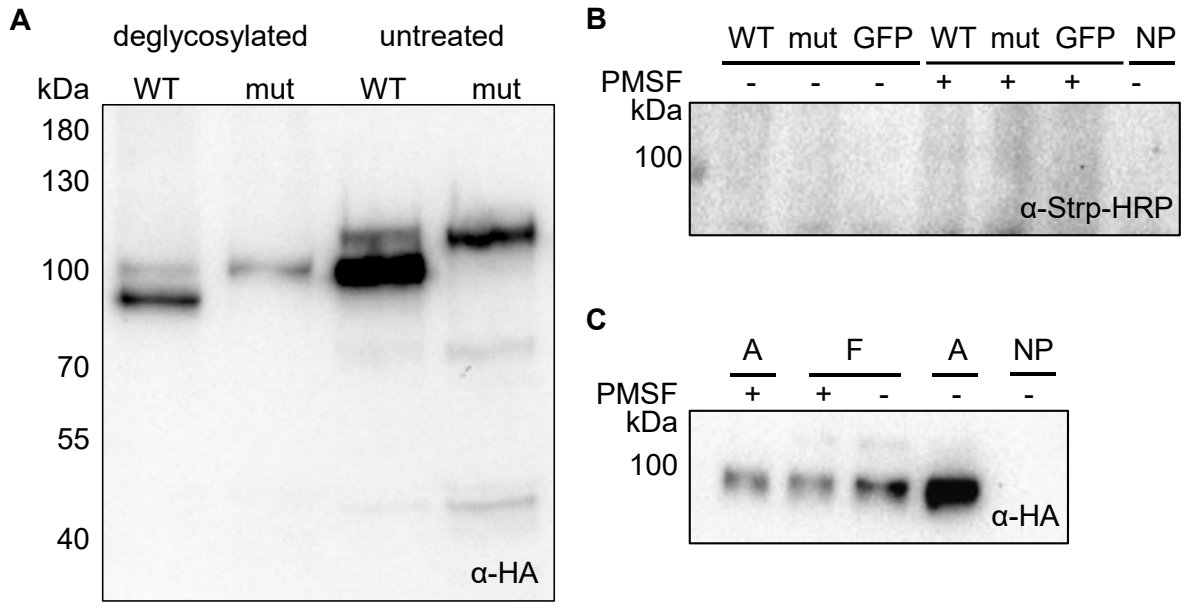

Figure S2: Heterologous expressed ZmSBT7 in *N. benthamiana* is glycosylated, but not active. ZmSBT7-HA (WT) and ZmSBT7_S540A-HA (mut) were transiently overexpressed in *N. benthamiana* using a 2x 35S promoter. Total leaf extract was diluted in 100 µl protein extraction buffer and incubated on ice for 30 min. Afterwards treated with the Protein Deglycosylation Mix II (NEB) for deglycosylation of proteins. Western blot analysis with α-HA antibody visualizes protein sizes of untreated and deglycosylated proteins (A). ABPP with protein extract and FP-Biotin was performed to identify Protease activity, visualized on western blot with α-Strp-HRP (B) and prove of protein abundance with α-HA (C). A = ABPP samples, F = samples without ABPP incubation. This figure was modified from Yannick Hoffmann (Bachelor Thesis)

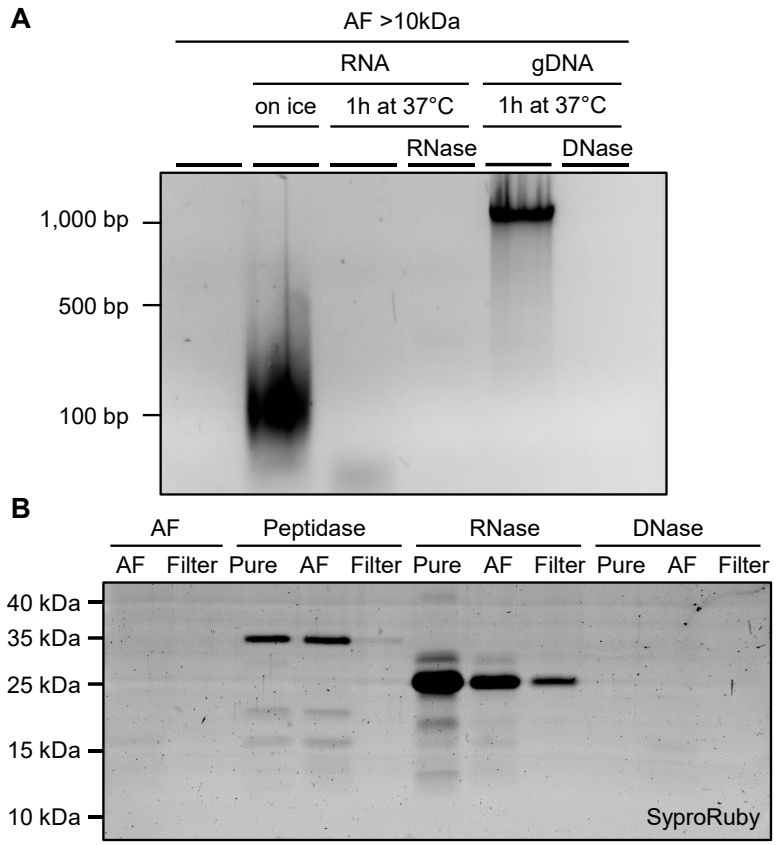

Figure S3: RNase and DNase degrade RNA and gDNA completely and gets partially removed by filters. 1 ml APF was incubated with 10 µg RNA and 2.5 µl gDNA (5U/ml) as well as 100 ng RNase and 100 ng DNase respectively to prove functionality of the enzymes in the APF. APF with RNA was incubated on ice as positive control RNA was added. Samples were run on an 2% agarose gel with 120 V for 20 min (A). To remove enzymes upon incubation with APF, the samples were run on an SDS PAGE and stained with SyproRuby.

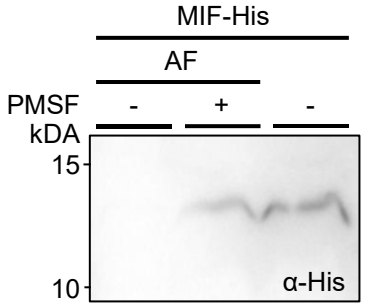

Figure S4: Cleavage of heterologous produced MIF can be inhibited by PMSF. MIF with His tag (MIF-His) was heterologous produced in *E. coli* and incubated with apoplastic fluid (AF) extracted SA treated maize leaves. AF was pre-treated with E64 (100µM), Pepstatin A (100µM) and EDTA (5mM) (-) and additional with PMSF (+). MIF-His was used as positive control. The figure was modified from Yannick Hoffmann (Bachelor Thesis)

Table S1: List of genes included in the three most prominent GO-terms for biological progress (BP) upon treatment with Zip1, SIGGI and PC13 respectively. GO enrichment analysis was provided by Novogene. Padj = adjusted p-value (to the hypothesis test P-value calibrated to control as the proportion of false positives (Young et al., 2010))

2 hpi

Treatment	**Zip1**			
Description	**cell recognition**			
(-Log10(padj))	(-Log10(pvalue))	pvalue	padj	Count
0	1.43	0.037	1	8
geneID				
Zm00001eb284690 Zm00001eb284380 Zm00001eb116650 Zm00001eb323690 Zm00001eb323640 Zm00001eb321390 Zm00001eb266160 Zm00001eb069410				
Description	**pollination**			
(-Log10(padj))	(-Log10(pvalue))	pvalue	padj	Count
0	1.43	0.037	1	8
geneID				
Zm00001eb284690 Zm00001eb284380 Zm00001eb116650 Zm00001eb323690 Zm00001eb323640 Zm00001eb321390 Zm00001eb266160 Zm00001eb069410				
Description	**pollen-pistil interaction**			
(-Log10(padj))	(-Log10(pvalue))	pvalue	padj	Count
0	1.43	0.037	1	8
geneID				
Zm00001eb284690 Zm00001eb284380 Zm00001eb116650 Zm00001eb323690 Zm00001eb323640 Zm00001eb321390 Zm00001eb266160 Zm00001eb069410				

Treatment	**SIGGI**			
Description	**protein modification by small protein conjugation or removal**			
(-Log10(padj))	(-Log10(pvalue))	pvalue	padj	Count
1.2	3.64	0	0.0633	36
geneID				
Zm00001eb190130 Zm00001eb290550 Zm00001eb368740 Zm00001eb300350 Zm00001eb371590 Zm00001eb385250 Zm00001eb379620 Zm00001eb149420 Zm00001eb038400 Zm00001eb252120 Zm00001eb422170 Zm00001eb204890 Zm00001eb020370 Zm00001eb134530 Zm00001eb010210 Zm00001eb145570 Zm00001eb244780 Zm00001eb239050 Zm00001eb008340 Zm00001eb083490 Zm00001eb174100 Zm00001eb425310 Zm00001eb136450 Zm00001eb204570 Zm00001eb144430 Zm00001eb407250 Zm00001eb102350 Zm00001eb026810 Zm00001eb253960 Zm00001eb081190 Zm00001eb241160 Zm00001eb178990 Zm00001eb225610 Zm00001eb367490 Zm00001eb147810 Zm00001eb119290				
Description	**protein ubiquitination**			
(-Log10(padj))	(-Log10(pvalue))	pvalue	padj	Count
1.2	3.48	0	0.0633	24

geneID
Zm00001eb190130 Zm00001eb290550 Zm00001eb368740 Zm00001eb371590 Zm00001eb385250 Zm00001eb379620 Zm00001eb149420 Zm00001eb252120 Zm00001eb422170 Zm00001eb204890 Zm00001eb020370 Zm00001eb010210 Zm00001eb145570 Zm00001eb239050 Zm00001eb083490 Zm00001eb174100 Zm00001eb425310 Zm00001eb136450 Zm00001eb144430 Zm00001eb407250 Zm00001eb253960 Zm00001eb241160 Zm00001eb178990 Zm00001eb119290

Description	**phosphorelay signal transduction system**			
(-Log10(padj))	(-Log10(pvalue))	pvalue	padj	Count
0.64	2.67	0.002	0.2309	16

geneID
Zm00001eb362820 Zm00001eb268260 Zm00001eb253970 Zm00001eb283590 Zm00001eb066570 Zm00001eb144290 Zm00001eb433500 Zm00001eb319590 Zm00001eb103490 Zm00001eb088180 Zm00001eb405030 Zm00001eb140730 Zm00001eb224010 Zm00001eb234170 Zm00001eb055280 Zm00001eb009140

Treatment	**PC13**			
Description	**fatty acid metabolic process**			
(-Log10(padj))	(-Log10(pvalue))	pvalue	padj	Count
1.07	3.67	0	0.0858	19

geneID
Zm00001eb385960 Zm00001eb366200 Zm00001eb008920 Zm00001eb240620 Zm00001eb398750 Zm00001eb377350 Zm00001eb399960 Zm00001eb167740 Zm00001eb018600 Zm00001eb270390 Zm00001eb085820 Zm00001eb285730 Zm00001eb203470 Zm00001eb376020 Zm00001eb277000 Zm00001eb004760 Zm00001eb006020 Zm00001eb148110 Zm00001eb258610

Description	**fatty acid biosynthetic process**			
(-Log10(padj))	(-Log10(pvalue))	pvalue	padj	Count
0.46	2.72	0.002	0.3447	13

geneID
Zm00001eb385960 Zm00001eb008920 Zm00001eb240620 Zm00001eb398750 Zm00001eb377350 Zm00001eb399960 Zm00001eb167740 Zm00001eb018600 Zm00001eb270390 Zm00001eb277000 Zm00001eb004760 Zm00001eb006020 Zm00001eb258610

Description	**monocarboxylic acid metabolic process**			
(-Log10(padj))	(-Log10(pvalue))	pvalue	padj	Count
0.46	2.59	0.003	0.3447	29

geneID
Zm00001eb293530 Zm00001eb385960 Zm00001eb366200 Zm00001eb280120 Zm00001eb008920 Zm00001eb240620 Zm00001eb398750 Zm00001eb377350 Zm00001eb399960 Zm00001eb339000 Zm00001eb167740 Zm00001eb018600 Zm00001eb020680 Zm00001eb339010 Zm00001eb144240 Zm00001eb270390 Zm00001eb085820 Zm00001eb337520 Zm00001eb285730 Zm00001eb203470 Zm00001eb376020 Zm00001eb277000 Zm00001eb004760 Zm00001eb196650 Zm00001eb006020 Zm00001eb148110 Zm00001eb258610 Zm00001eb386670 Zm00001eb066190

6 hpi

Treatment	Zip1			
Description	**carbon fixation**			
(-Log10(padj))	(-Log10(pvalue))	pvalue	padj	Count
0.68	2.44	0.004	0.2100	2
geneID				
Zm00001eb435060 Zm00001eb039150				
Description	**response to external stimulus**			
(-Log10(padj))	(-Log10(pvalue))	pvalue	padj	Count
0.68	2.38	0.004	0.2100	2
geneID				
Zm00001eb167710 Zm00001eb167720				
Description	**defense response**			
(-Log10(padj))	(-Log10(pvalue))	pvalue	padj	Count
0.40	1.85	0.014	0.4025	2
geneID				
Zm00001eb167710 Zm00001eb167720				

Treatment	SIGGI			
Description	**carbohydrate metabolic process**			
(-Log10(padj))	(-Log10(pvalue))	pvalue	padj	Count
0.16	2.42	0.004	0.6928	38
geneID				
Zm00001eb411380 Zm00001eb347530 Zm00001eb157610 Zm00001eb003440 Zm00001eb386660 Zm00001eb268650 Zm00001eb167360 Zm00001eb174340 Zm00001eb386670 Zm00001eb076600 Zm00001eb337520 Zm00001eb340080 Zm00001eb316070 Zm00001eb129970 Zm00001eb016920 Zm00001eb384280 Zm00001eb434590 Zm00001eb038060 Zm00001eb168350 Zm00001eb339380 Zm00001eb077490 Zm00001eb024960 Zm00001eb401220 Zm00001eb359080 Zm00001eb158930 Zm00001eb283530 Zm00001eb141540 Zm00001eb021270 Zm00001eb259620 Zm00001eb420100 Zm00001eb241670 Zm00001eb098910 Zm00001eb213180 Zm00001eb039820 Zm00001eb010420 Zm00001eb121310 Zm00001eb100790 Zm00001eb339720				
Description	**response to stress**			
(-Log10(padj))	(-Log10(pvalue))	pvalue	padj	Count
0.16	2.37	0.004	0.6928	21
geneID				
Zm00001eb260610 Zm00001eb009950 Zm00001eb167710 Zm00001eb288190 Zm00001eb195200 Zm00001eb167720 Zm00001eb429430 Zm00001eb204960 Zm00001eb028900 Zm00001eb264870 Zm00001eb264110 Zm00001eb047120 Zm00001eb104340 Zm00001eb352670 Zm00001eb330540 Zm00001eb033650 Zm00001eb355990 Zm00001eb014000 Zm00001eb271870 Zm00001eb111430 Zm00001eb074350				

Description	defense response			
(-Log10(padj))	(-Log10(pvalue))	pvalue	padj	Count
0.02	2.02	0.009	0.9638	5
geneID				
Zm00001eb167710 Zm00001eb288190 Zm00001eb167720 Zm00001eb014000 Zm00001eb271870				

Treatment	PC13			
Description	cellular potassium ion transport			
(-Log10(padj))	(-Log10(pvalue))	pvalue	padj	Count
0.25	2.26	0.006	0.5683	4
geneID				
Zm00001eb330230 Zm00001eb071150 Zm00001eb048930 Zm00001eb430810				
Description	potassium ion transmembrane transport			
(-Log10(padj))	(-Log10(pvalue))	pvalue	padj	Count
0.25	2.26	0.006	0.5683	4
geneID				
Zm00001eb330230 Zm00001eb071150 Zm00001eb048930 Zm00001eb430810				
Description	potassium ion transport			
(-Log10(padj))	(-Log10(pvalue))	pvalue	padj	Count
0.25	2.16	0.007	0.5683	4
geneID				
Zm00001eb330230 Zm00001eb071150 Zm00001eb048930 Zm00001eb430810				

12 hpi

Treatment	Zip1			
Description	cellulose metabolic process			
(-Log10(padj))	(-Log10(pvalue))	pvalue	padj	Count
1.94	3.41	0.000	0.0114	3
geneID				
Zm00001eb306030 Zm00001eb303110 Zm00001eb345740				
Description	cellulose biosynthetic process			
(-Log10(padj))	(-Log10(pvalue))	pvalue	padj	Count
1.94	3.41	0.000	0.0114	3
geneID				
Zm00001eb306030 Zm00001eb303110 Zm00001eb345740				
Description	polysaccharide biosynthetic process			
(-Log10(padj))	(-Log10(pvalue))	pvalue	padj	Count
1.94	2.93	0.001	0.0114	3
geneID				
Zm00001eb306030 Zm00001eb303110 Zm00001eb345740				

Treatment	SIGGI			
Description	**proteolysis**			
(-Log10(padj))	(-Log10(pvalue))	pvalue	padj	Count
0.42	1.23	0.059	0.3774	5
		geneID		
Zm00001eb248220 Zm00001eb340690 Zm00001eb305600 Zm00001eb334930 Zm00001eb031350				
Description	**negative regulation of cellular metabolic process**			
(-Log10(padj))	(-Log10(pvalue))	pvalue	padj	Count
0.42	1.21	0.062	0.3774	1
		geneID		
Zm00001eb326540				
Description	**negative regulation of nitrogen compound metabolic process**			
(-Log10(padj))	(-Log10(pvalue))	pvalue	padj	Count
0.42	1.21	0.062	0.3774	1
		geneID		
Zm00001eb326540				

Treatment	PC13			
Description	**DNA integration**			
(-Log10(padj))	(-Log10(pvalue))	pvalue	padj	Count
1.73	3.89	0.000	0.0187	4
		geneID		
novel.1927 novel.1496 novel.213 novel.1954				
Description	**mRNA processing**			
(-Log10(padj))	(-Log10(pvalue))	pvalue	padj	Count
0.79	2.39	0.004	0.1627	3
		geneID		
Zm00001eb271550 Zm00001eb292700 Zm00001eb375530				
Description	**DNA metabolic process**			
(-Log10(padj))	(-Log10(pvalue))	pvalue	padj	Count
0.79	2.28	0.005	0.1627	6
		geneID		
Zm00001eb352670 novel.1927 novel.1496 Zm00001eb280820 novel.213 novel.1954				

24 hpi

Treatment	Zip1			
Description	**drug catabolic process**			
(-Log10(padj))	(-Log10(pvalue))	pvalue	padj	Count
3.57	5.63	0.000	0.0003	7
geneID				
Zm00001eb078730 Zm00001eb425600 Zm00001eb272090 Zm00001eb246640 Zm00001eb002620 Zm00001eb379510 Zm00001eb346860				
Description	**carbohydrate derivative catabolic process**			
(-Log10(padj))	(-Log10(pvalue))	pvalue	padj	Count
3.57	5.22	0.000	0.0003	8
geneID				
Zm00001eb078730 Zm00001eb425600 Zm00001eb272090 Zm00001eb246640 Zm00001eb002620 Zm00001eb352530 Zm00001eb369390 Zm00001eb346860				
Description	**chitin metabolic process**			
(-Log10(padj))	(-Log10(pvalue))	pvalue	padj	Count
3.57	4.98	0.000	0.0003	6
geneID				
Zm00001eb078730 Zm00001eb425600 Zm00001eb272090 Zm00001eb246640 Zm00001eb002620 Zm00001eb346860				

Treatment	SIGGI			
Description	**chitin metabolic process**			
(-Log10(padj))	(-Log10(pvalue))	pvalue	padj	Count
1.94	3.46	0.000	0.0115	5
geneID				
Zm00001eb425600 Zm00001eb078730 Zm00001eb246640 Zm00001eb272090 Zm00001eb002620				
Description	**carbohydrate metabolic process**			
(-Log10(padj))	(-Log10(pvalue))	pvalue	padj	Count
1.55	2.96	0.001	0.0281	51
geneID				
Zm00001eb141540 Zm00001eb106410 Zm00001eb411380 Zm00001eb168350 Zm00001eb157820 Zm00001eb044860 Zm00001eb390820 Zm00001eb057230 Zm00001eb304560 Zm00001eb080890 Zm00001eb121310 Zm00001eb323370 Zm00001eb039820 Zm00001eb141500 Zm00001eb283110 Zm00001eb386670 Zm00001eb397970 Zm00001eb337520 Zm00001eb350090 Zm00001eb008530 Zm00001eb273940 Zm00001eb352530 Zm00001eb286760 Zm00001eb129970 Zm00001eb229440 Zm00001eb365200 Zm00001eb394740 Zm00001eb268650 Zm00001eb010420 Zm00001eb167360 Zm00001eb226470 Zm00001eb255140 Zm00001eb047940 Zm00001eb147120 Zm00001eb371630 Zm00001eb319710 Zm00001eb340080 Zm00001eb021270 Zm00001eb154520 Zm00001eb040260 Zm00001eb076600 Zm00001eb023950 Zm00001eb379070 Zm00001eb345740 Zm00001eb323400 Zm00001eb179730 Zm00001eb415630 Zm00001eb215900 Zm00001eb334460 Zm00001eb306030 Zm00001eb384280				

Description	defense response			
(-Log10(padj))	(-Log10(pvalue))	pvalue	padj	Count
0.72	2.05	0.009	0.1891	6

geneID

Zm00001eb014000 Zm00001eb014010 Zm00001eb167720 Zm00001eb167710 Zm00001eb167690 Zm00001eb167700

Treatment	PC13			
Description	**translation**			
(-Log10(padj))	(-Log10(pvalue))	pvalue	padj	Count
48.90	51.48	0.000	0.0000	144

geneID

Zm00001eb060730 Zm00001eb189260 Zm00001eb109330 Zm00001eb061760 Zm00001eb002640 Zm00001eb192860 Zm00001eb219500 Zm00001eb098510 Zm00001eb211900 Zm00001eb046430 Zm00001eb035770 Zm00001eb251610 Zm00001eb124750 Zm00001eb260960 Zm00001eb277530 Zm00001eb222240 Zm00001eb198180 Zm00001eb212470 Zm00001eb394940 Zm00001eb301420 novel.1776 Zm00001eb357570 Zm00001eb136620 Zm00001eb070200 Zm00001eb091900 Zm00001eb278610 Zm00001eb003180 Zm00001eb386940 Zm00001eb273640 Zm00001eb401700 Zm00001eb116930 Zm00001eb239530 Zm00001eb104470 Zm00001eb321960 Zm00001eb420570 Zm00001eb003420 Zm00001eb036020 Zm00001eb361700 Zm00001eb181430 Zm00001eb091870 Zm00001eb393200 Zm00001eb295950 Zm00001eb335620 Zm00001eb329680 Zm00001eb326540 Zm00001eb396730 Zm00001eb163700 Zm00001eb289870 Zm00001eb245740 Zm00001eb160260 Zm00001eb273650 Zm00001eb405580 Zm00001eb111360 Zm00001eb192140 Zm00001eb137550 Zm00001eb028980 Zm00001eb095960 Zm00001eb191550 Zm00001eb057690 Zm00001eb402880 Zm00001eb400820 Zm00001eb037310 Zm00001eb093610 Zm00001eb321580 Zm00001eb224520 Zm00001eb283950 Zm00001eb273660 Zm00001eb340580 Zm00001eb188040 Zm00001eb364190 Zm00001eb369510 Zm00001eb381630 Zm00001eb109610 Zm00001eb002520 Zm00001eb337800 Zm00001eb207850 Zm00001eb046340 Zm00001eb343830 Zm00001eb385150 Zm00001eb415410 Zm00001eb178210 Zm00001eb082960 Zm00001eb214650 Zm00001eb116830 Zm00001eb321600 Zm00001eb041340 Zm00001eb102250 Zm00001eb303080 Zm00001eb312560 Zm00001eb327250 Zm00001eb211090 Zm00001eb060550 Zm00001eb173470 Zm00001eb183420 Zm00001eb036530 Zm00001eb213080 Zm00001eb120260 Zm00001eb095190 Zm00001eb301640 Zm00001eb119260 Zm00001eb275200 Zm00001eb116850 Zm00001eb282450 Zm00001eb062450 Zm00001eb070950 Zm00001eb392950 Zm00001eb034830 novel.968 Zm00001eb215450 Zm00001eb157400 Zm00001eb402790 Zm00001eb273670 Zm00001eb333790 Zm00001eb078210 Zm00001eb373790 Zm00001eb013750 Zm00001eb327430 novel.1571 Zm00001eb072000 Zm00001eb374300 Zm00001eb430770 Zm00001eb301010 Zm00001eb212960 Zm00001eb339270 Zm00001eb105120 Zm00001eb232530 Zm00001eb341390 Zm00001eb379270 Zm00001eb329960 Zm00001eb009920 Zm00001eb172860 Zm00001eb352030 Zm00001eb229290 Zm00001eb097790 Zm00001eb020200 Zm00001eb219490 Zm00001eb148830 Zm00001eb359780 Zm00001eb154510 Zm00001eb183410 Zm00001eb426610 Zm00001eb330470 Zm00001eb074650 Zm00001eb240090

Description	peptide biosynthetic process			
(-Log10(padj))	(-Log10(pvalue))	pvalue	padj	Count
48.10	50.38	0.000	0.0000	144

geneID

Zm00001eb060730 Zm00001eb189260 Zm00001eb109330 Zm00001eb061760 Zm00001eb002640 Zm00001eb192860 Zm00001eb219500 Zm00001eb098510 Zm00001eb211900 Zm00001eb046430 Zm00001eb035770 Zm00001eb251610 Zm00001eb124750 Zm00001eb260960 Zm00001eb277530 Zm00001eb222240 Zm00001eb198180 Zm00001eb212470 Zm00001eb394940 Zm00001eb301420 novel.1776 Zm00001eb357570 Zm00001eb136620 Zm00001eb070200 Zm00001eb091900 Zm00001eb278610 Zm00001eb003180 Zm00001eb386940 Zm00001eb273640 Zm00001eb401700 Zm00001eb116930 Zm00001eb239530 Zm00001eb104470 Zm00001eb321960 Zm00001eb420570 Zm00001eb003420 Zm00001eb036020 Zm00001eb361700 Zm00001eb181430 Zm00001eb091870 Zm00001eb393200 Zm00001eb295950 Zm00001eb335620 Zm00001eb329680 Zm00001eb326540 Zm00001eb396730 Zm00001eb163700 Zm00001eb289870 Zm00001eb245740 Zm00001eb160260 Zm00001eb273650 Zm00001eb405580 Zm00001eb111360 Zm00001eb192140 Zm00001eb137550 Zm00001eb028980 Zm00001eb095960 Zm00001eb191550 Zm00001eb057690 Zm00001eb402880 Zm00001eb400820 Zm00001eb037310 Zm00001eb093610 Zm00001eb321580 Zm00001eb224520 Zm00001eb283950 Zm00001eb273660 Zm00001eb340580 Zm00001eb188040 Zm00001eb364190 Zm00001eb369510 Zm00001eb381630 Zm00001eb109610 Zm00001eb002520 Zm00001eb337800 Zm00001eb207850 Zm00001eb046340 Zm00001eb343830 Zm00001eb385150 Zm00001eb415410 Zm00001eb178210 Zm00001eb082960 Zm00001eb214650 Zm00001eb116830 Zm00001eb321600 Zm00001eb041340 Zm00001eb102250 Zm00001eb303080 Zm00001eb312560 Zm00001eb327250 Zm00001eb211090 Zm00001eb060550 Zm00001eb173470 Zm00001eb183420 Zm00001eb036530 Zm00001eb213080 Zm00001eb120260 Zm00001eb095190 Zm00001eb301640 Zm00001eb119260 Zm00001eb275200 Zm00001eb116850 Zm00001eb282450 Zm00001eb062450 Zm00001eb070950 Zm00001eb392950 Zm00001eb034830 novel.968 Zm00001eb215450 Zm00001eb157400 Zm00001eb402790 Zm00001eb273670 Zm00001eb333790 Zm00001eb078210 Zm00001eb373790 Zm00001eb013750 Zm00001eb327430 novel.1571 Zm00001eb072000 Zm00001eb374300

Zm00001eb430770 Zm00001eb301010 Zm00001eb212960 Zm00001eb339270 Zm00001eb105120 Zm00001eb232530
Zm00001eb341390 Zm00001eb379270 Zm00001eb329960 Zm00001eb009920 Zm00001eb172860 Zm00001eb352030
Zm00001eb229290 Zm00001eb097790 Zm00001eb020200 Zm00001eb219490 Zm00001eb148830 Zm00001eb359780
Zm00001eb154510 Zm00001eb183410 Zm00001eb426610 Zm00001eb330470 Zm00001eb074650 Zm00001eb240090

Description	**amide biosynthetic process**			
(-Log10(padj))	(-Log10(pvalue))	pvalue	padj	Count
47.24	49.34	0.000	0.0000	145

geneID

Zm00001eb060730 Zm00001eb189260 Zm00001eb109330 Zm00001eb061760 Zm00001eb002640 Zm00001eb192860
Zm00001eb219500 Zm00001eb098510 Zm00001eb211900 Zm00001eb046430 Zm00001eb035770 Zm00001eb251610
Zm00001eb124750 Zm00001eb260960 Zm00001eb277530 Zm00001eb222240 Zm00001eb198180 Zm00001eb212470
Zm00001eb394940 Zm00001eb301420 novel.1776 Zm00001eb357570 Zm00001eb136620 Zm00001eb070200
Zm00001eb091900 Zm00001eb278610 Zm00001eb003180 Zm00001eb386940 Zm00001eb273640 Zm00001eb401700
Zm00001eb116930 Zm00001eb239530 Zm00001eb104470 Zm00001eb321960 Zm00001eb420570 Zm00001eb003420
Zm00001eb036020 Zm00001eb361700 Zm00001eb181430 Zm00001eb091870 Zm00001eb393200 Zm00001eb295950
Zm00001eb335620 Zm00001eb329680 Zm00001eb326540 Zm00001eb396730 Zm00001eb163700 Zm00001eb289870
Zm00001eb245740 Zm00001eb160260 Zm00001eb273650 Zm00001eb405580 Zm00001eb111360 Zm00001eb192140
Zm00001eb137550 Zm00001eb028980 Zm00001eb095960 Zm00001eb191550 Zm00001eb057690 Zm00001eb402880
Zm00001eb400820 Zm00001eb037310 Zm00001eb093610 Zm00001eb321580 Zm00001eb224520 Zm00001eb283950
Zm00001eb273660 Zm00001eb340580 Zm00001eb188040 Zm00001eb364190 Zm00001eb369510 Zm00001eb381630
Zm00001eb109610 Zm00001eb002520 Zm00001eb337800 Zm00001eb207850 Zm00001eb046340 Zm00001eb343830
Zm00001eb385150 Zm00001eb415410 Zm00001eb178210 Zm00001eb082960 Zm00001eb214650 Zm00001eb116830
Zm00001eb321600 Zm00001eb041340 Zm00001eb102250 Zm00001eb303080 Zm00001eb312560 Zm00001eb327250
Zm00001eb211090 Zm00001eb060550 Zm00001eb173470 Zm00001eb183420 Zm00001eb036530 Zm00001eb213080
Zm00001eb120260 Zm00001eb095190 Zm00001eb301640 Zm00001eb119260 Zm00001eb275200 Zm00001eb116850
Zm00001eb282450 Zm00001eb062450 Zm00001eb070950 Zm00001eb392950 Zm00001eb034830 novel.968
Zm00001eb215450 Zm00001eb157400 Zm00001eb402790 Zm00001eb273670 Zm00001eb333790 Zm00001eb078210
Zm00001eb373790 Zm00001eb013750 Zm00001eb327430 novel.1571 Zm00001eb072000 Zm00001eb374300
Zm00001eb430770 Zm00001eb301010 Zm00001eb212960 Zm00001eb339270 Zm00001eb105120 Zm00001eb232530
Zm00001eb319990 Zm00001eb341390 Zm00001eb379270 Zm00001eb329960 Zm00001eb009920 Zm00001eb172860
Zm00001eb352030 Zm00001eb229290 Zm00001eb097790 Zm00001eb020200 Zm00001eb219490 Zm00001eb148830
Zm00001eb359780 Zm00001eb154510 Zm00001eb183410 Zm00001eb426610 Zm00001eb330470 Zm00001eb074650
Zm00001eb240090

Table S2: List of genes included in GO-terms for biological progress (BP) upon SIGGI treatment. Only genes were chosen, which are significantly upregulated (p-value < 0.05 and Log_2FC > 1) upon SIGGI treatment in comparison to MAP1 and only found upon SIGGI treatment. GO enrichment analysis was performed with ShinyGO 8.0 (Ge et al., 2020)

2 hpi

Treatment	**SIGGI**	
Description	**Regulation of defense response to fungus**	
Enrichment FDR	Fold Enrichment	Count
7.99E-05	12.561	8
geneID		
Zm00001eb015970 Zm00001eb149630 Zm00001eb159570 Zm00001eb195450 Zm00001eb330730 Zm00001eb344970 Zm00001eb368930 Zm00001eb395190		
Description	**Immune system processes**	
Enrichment FDR	Fold Enrichment	Count
0.002	2.956	20
geneID		
Zm00001eb015970 Zm00001eb030170 Zm00001eb047260 Zm00001eb047270 Zm00001eb062850 Zm00001eb062860 Zm00001eb099250 Zm00001eb149630 Zm00001eb159570 Zm00001eb195450 Zm00001eb199980 Zm00001eb295470 Zm00001eb330730 Zm00001eb331170 Zm00001eb344970 Zm00001eb364940 Zm00001eb368930 Zm00001eb370160 Zm00001eb371010 Zm00001eb395190		
Description	**Response to external stimulus**	
Enrichment FDR	Fold Enrichment	Count
0.001	2.593	30
geneID		
Zm00001eb015970 Zm00001eb030170 Zm00001eb044500 Zm00001eb047260 Zm00001eb047270 Zm00001eb062850 Zm00001eb062860 Zm00001eb066570 Zm00001eb099250 Zm00001eb143290 Zm00001eb149440 Zm00001eb149630 Zm00001eb151200 Zm00001eb159570 Zm00001eb195450 Zm00001eb195650 Zm00001eb199980 Zm00001eb220670 Zm00001eb220900 Zm00001eb295470 Zm00001eb330730 Zm00001eb331170 Zm00001eb333260 Zm00001eb344970 Zm00001eb364940 Zm00001eb368930 Zm00001eb370160 Zm00001eb371010 Zm00001eb393000 Zm00001eb395190		
Description	**Response to hormone**	
Enrichment FDR	Fold Enrichment	Count
0.001	2.246	41
geneID		
Zm00001eb009600 Zm00001eb015440 Zm00001eb045640 Zm00001eb066570 Zm00001eb066640 Zm00001eb074330 Zm00001eb082150 Zm00001eb084980 Zm00001eb104130 Zm00001eb122410 Zm00001eb122550 Zm00001eb142840 Zm00001eb146690 Zm00001eb149720 Zm00001eb150670 Zm00001eb153660 Zm00001eb154070 Zm00001eb158690 Zm00001eb177200 Zm00001eb177230 Zm00001eb177370 Zm00001eb179390 Zm00001eb182260 Zm00001eb206660 Zm00001eb227100 Zm00001eb253970 Zm00001eb256600 Zm00001eb258220 Zm00001eb271490 Zm00001eb289080 Zm00001eb301590 Zm00001eb317090 Zm00001eb324720 Zm00001eb336930 Zm00001eb362820 Zm00001eb370160 Zm00001eb390480 Zm00001eb402560 Zm00001eb415270 Zm00001eb417550 Zm00001eb433500		

Description	Response to endogenous stimulus	
Enrichment FDR	Fold Enrichment	Count
0.001	2.220	41

geneID

Zm00001eb009600 Zm00001eb015440 Zm00001eb045640 Zm00001eb066570
Zm00001eb066640 Zm00001eb074330 Zm00001eb082150 Zm00001eb084980
Zm00001eb104130 Zm00001eb122410 Zm00001eb122550 Zm00001eb142840
Zm00001eb146690 Zm00001eb149720 Zm00001eb150670 Zm00001eb153660
Zm00001eb154070 Zm00001eb158690 Zm00001eb177200 Zm00001eb177230
Zm00001eb177370 Zm00001eb179390 Zm00001eb182260 Zm00001eb206660
Zm00001eb227100 Zm00001eb253970 Zm00001eb256600 Zm00001eb258220
Zm00001eb271490 Zm00001eb289080 Zm00001eb301590 Zm00001eb317090
Zm00001eb324720 Zm00001eb336930 Zm00001eb362820 Zm00001eb370160
Zm00001eb390480 Zm00001eb402560 Zm00001eb415270 Zm00001eb417550
Zm00001eb433500

Description	Response to organic substance	
Enrichment FDR	Fold Enrichment	Count
0.002	1.974	45

geneID

Zm00001eb009600 Zm00001eb015440 Zm00001eb045640 Zm00001eb066570
Zm00001eb066640 Zm00001eb074330 Zm00001eb082150 Zm00001eb084980
Zm00001eb104130 Zm00001eb122410 Zm00001eb122550 Zm00001eb142840
Zm00001eb146690 Zm00001eb148420 Zm00001eb149720 Zm00001eb150670
Zm00001eb152120 Zm00001eb153660 Zm00001eb154070 Zm00001eb158690
Zm00001eb168550 Zm00001eb177200 Zm00001eb177230 Zm00001eb177370
Zm00001eb179390 Zm00001eb182260 Zm00001eb206660 Zm00001eb227100
Zm00001eb253970 Zm00001eb256600 Zm00001eb258220 Zm00001eb271490
Zm00001eb289080 Zm00001eb301590 Zm00001eb317090 Zm00001eb324720
Zm00001eb336930 Zm00001eb362820 Zm00001eb368000 Zm00001eb370160
Zm00001eb390480 Zm00001eb402560 Zm00001eb415270 Zm00001eb417550
Zm00001eb433500

Description	Protein phosphorylation	
Enrichment FDR	Fold Enrichment	Count
0.000	1.926	99

geneID

Zm00001eb002180 Zm00001eb004440 Zm00001eb011650 Zm00001eb013480 Zm00001eb017800
Zm00001eb025720 Zm00001eb034370 Zm00001eb042350 Zm00001eb043750 Zm00001eb044500
Zm00001eb047260 Zm00001eb047270 Zm00001eb055750 Zm00001eb059030 Zm00001eb062850
Zm00001eb062860 Zm00001eb063900 Zm00001eb063970 Zm00001eb066630 Zm00001eb069500
Zm00001eb072810 Zm00001eb077270 Zm00001eb077980 Zm00001eb079130 Zm00001eb085170
Zm00001eb098540 Zm00001eb100880 Zm00001eb104380 Zm00001eb105820 Zm00001eb108620
Zm00001eb121910 Zm00001eb123770 Zm00001eb124880 Zm00001eb127570 Zm00001eb134290
Zm00001eb135710 Zm00001eb143290 Zm00001eb144570 Zm00001eb149390 Zm00001eb149520
Zm00001eb155710 Zm00001eb157530 Zm00001eb167820 Zm00001eb174340 Zm00001eb186420
Zm00001eb191110 Zm00001eb195270 Zm00001eb199980 Zm00001eb211040 Zm00001eb217170
Zm00001eb220900 Zm00001eb227730 Zm00001eb228010 Zm00001eb234200 Zm00001eb246490
Zm00001eb253190 Zm00001eb253970 Zm00001eb271540 Zm00001eb272270 Zm00001eb273340
Zm00001eb274440 Zm00001eb277420 Zm00001eb278640 Zm00001eb288130 Zm00001eb292760
Zm00001eb298390 Zm00001eb316880 Zm00001eb323240 Zm00001eb323300 Zm00001eb324630
Zm00001eb326620 Zm00001eb327350 Zm00001eb328410 Zm00001eb334670 Zm00001eb339500
Zm00001eb354860 Zm00001eb357100 Zm00001eb357920 Zm00001eb366140 Zm00001eb368340
Zm00001eb368360 Zm00001eb368950 Zm00001eb371240 Zm00001eb375440 Zm00001eb380860
Zm00001eb385300 Zm00001eb388840 Zm00001eb389680 Zm00001eb397190 Zm00001eb400340
Zm00001eb401630 Zm00001eb402560 Zm00001eb403680 Zm00001eb404290 Zm00001eb405420
Zm00001eb421870 Zm00001eb422820 Zm00001eb425300 Zm00001eb425420

Description	Signal transduction

Enrichment FDR	Fold Enrichment	Count
0.001	1.829	63

geneID

Zm00001eb002180 Zm00001eb015440 Zm00001eb020120 Zm00001eb034370 Zm00001eb042350
Zm00001eb043750 Zm00001eb045640 Zm00001eb047260 Zm00001eb047270 Zm00001eb062850
Zm00001eb062860 Zm00001eb066570 Zm00001eb066640 Zm00001eb072810 Zm00001eb074330
Zm00001eb077270 Zm00001eb079190 Zm00001eb082150 Zm00001eb082280 Zm00001eb084980
Zm00001eb103490 Zm00001eb108620 Zm00001eb122410 Zm00001eb122550 Zm00001eb122740
Zm00001eb146690 Zm00001eb149390 Zm00001eb149720 Zm00001eb150670 Zm00001eb153660
Zm00001eb157530 Zm00001eb158690 Zm00001eb177230 Zm00001eb179390 Zm00001eb182260
Zm00001eb195270 Zm00001eb199980 Zm00001eb217170 Zm00001eb227100 Zm00001eb253970
Zm00001eb257410 Zm00001eb258220 Zm00001eb284020 Zm00001eb289080 Zm00001eb292760
Zm00001eb301590 Zm00001eb316880 Zm00001eb319590 Zm00001eb324720 Zm00001eb326900
Zm00001eb328410 Zm00001eb336820 Zm00001eb336930 Zm00001eb362820 Zm00001eb368360
Zm00001eb370160 Zm00001eb388100 Zm00001eb390480 Zm00001eb397190 Zm00001eb402560
Zm00001eb405420 Zm00001eb410350 Zm00001eb433500

Description	**Signaling**	
Enrichment FDR	Fold Enrichment	Count
0.001	1.811	63

geneID

Zm00001eb002180 Zm00001eb015440 Zm00001eb020120 Zm00001eb034370 Zm00001eb042350
Zm00001eb043750 Zm00001eb045640 Zm00001eb047260 Zm00001eb047270 Zm00001eb062850
Zm00001eb062860 Zm00001eb066570 Zm00001eb066640 Zm00001eb072810 Zm00001eb074330
Zm00001eb077270 Zm00001eb079190 Zm00001eb082150 Zm00001eb082280 Zm00001eb084980
Zm00001eb103490 Zm00001eb108620 Zm00001eb122410 Zm00001eb122550 Zm00001eb122740
Zm00001eb146690 Zm00001eb149390 Zm00001eb149720 Zm00001eb150670 Zm00001eb153660
Zm00001eb157530 Zm00001eb158690 Zm00001eb177230 Zm00001eb179390 Zm00001eb182260
Zm00001eb195270 Zm00001eb199980 Zm00001eb217170 Zm00001eb227100 Zm00001eb253970
Zm00001eb257410 Zm00001eb258220 Zm00001eb284020 Zm00001eb289080 Zm00001eb292760
Zm00001eb301590 Zm00001eb316880 Zm00001eb319590 Zm00001eb324720 Zm00001eb326900
Zm00001eb328410 Zm00001eb336820 Zm00001eb336930 Zm00001eb362820 Zm00001eb368360
Zm00001eb370160 Zm00001eb388100 Zm00001eb390480 Zm00001eb397190 Zm00001eb402560
Zm00001eb405420 Zm00001eb410350 Zm00001eb433500

Description	**Cell communication**	
Enrichment FDR	Fold Enrichment	Count
0.001	1.806	69

geneID

Zm00001eb002180 Zm00001eb015440 Zm00001eb020120 Zm00001eb034370 Zm00001eb042350
Zm00001eb043750 Zm00001eb044500 Zm00001eb045640 Zm00001eb047260 Zm00001eb047270
Zm00001eb062850 Zm00001eb062860 Zm00001eb063900 Zm00001eb066570 Zm00001eb066640
Zm00001eb072810 Zm00001eb074330 Zm00001eb077270 Zm00001eb079190 Zm00001eb082150
Zm00001eb082280 Zm00001eb084980 Zm00001eb103490 Zm00001eb105820 Zm00001eb108620
Zm00001eb122410 Zm00001eb122550 Zm00001eb122740 Zm00001eb143290 Zm00001eb146690
Zm00001eb149390 Zm00001eb149720 Zm00001eb150670 Zm00001eb153660 Zm00001eb157530
Zm00001eb158690 Zm00001eb177230 Zm00001eb179390 Zm00001eb182260 Zm00001eb195270
Zm00001eb199980 Zm00001eb217170 Zm00001eb220900 Zm00001eb227100 Zm00001eb253970
Zm00001eb257410 Zm00001eb258220 Zm00001eb284020 Zm00001eb289080 Zm00001eb292760
Zm00001eb301590 Zm00001eb316880 Zm00001eb319590 Zm00001eb324720 Zm00001eb326900
Zm00001eb328410 Zm00001eb336820 Zm00001eb336930 Zm00001eb362820 Zm00001eb368360
Zm00001eb370160 Zm00001eb385300 Zm00001eb388100 Zm00001eb390480 Zm00001eb397190
Zm00001eb402560 Zm00001eb405420 Zm00001eb410350 Zm00001eb433500

6 hpi

Treatment	SIGGI	
Description	**Salicylic acid biosynthetic proc.**	
Enrichment FDR	Fold Enrichment	Count
0.014	34.361	3
	geneID	
Zm00001eb042820 Zm00001eb125120 Zm00001eb410260		
Description	**Reg. of salicylic acid biosynthetic proc.**	
Enrichment FDR	Fold Enrichment	Count
0.014	34.361	3
	geneID	
Zm00001eb042820 Zm00001eb125120 Zm00001eb410260		
Description	**Phenol-containing compound biosynthetic proc.**	
Enrichment FDR	Fold Enrichment	Count
0.014	29.780	3
	geneID	
Zm00001eb042820 Zm00001eb125120 Zm00001eb410260		
Description	**Reg. of protein serine/threonine phosphatase activity**	
Enrichment FDR	Fold Enrichment	Count
0.023	22.335	3
	geneID	
Zm00001eb013990 Zm00001eb014000 Zm00001eb396710		
Description	**Response to hydrogen peroxide**	
Enrichment FDR	Fold Enrichment	Count
0.014	17.518	4
	geneID	
Zm00001eb013990 Zm00001eb014000 Zm00001eb145030 Zm00001eb397940		
Description	**Response to cold**	
Enrichment FDR	Fold Enrichment	Count
0.017	9.545	5
	geneID	
Zm00001eb013990 Zm00001eb014000 Zm00001eb145030 Zm00001eb145490 Zm00001eb187010		
Description	**Response to salt stress**	
Enrichment FDR	Fold Enrichment	Count
0.023	8.365	5
	geneID	
Zm00001eb013990 Zm00001eb014000 Zm00001eb145030 Zm00001eb314770 Zm00001eb397940		
Description	**Response to inorganic substance**	
Enrichment FDR	Fold Enrichment	Count
0.014	5.566	8

geneID		
Zm00001eb013990 Zm00001eb014000 Zm00001eb077130 Zm00001eb145030 Zm00001eb187010 Zm00001eb339970 Zm00001eb386040 Zm00001eb397940		
Description	**Response to temperature stimulus**	
Enrichment FDR	Fold Enrichment	Count
0.023	5.400	7
geneID		
Zm00001eb013990 Zm00001eb014000 Zm00001eb145030 Zm00001eb145490 Zm00001eb187010 Zm00001eb386040 Zm00001eb397940		

Table S3: List of genes included in GO-terms for biological progress (BP) upon PC13 treatment. Only genes were chosen, which are significantly upregulated (p-value < 0.05 and $Log_2FC > 1$) upon PC13 treatment in comparison to MAP1. GO enrichment analysis was performed with ShinyGO 8.0 (Ge et al., 2020)

2 hpi

Treatment	**PC13**	
Description	**Programmed cell death induced by symbiont**	
Enrichment FDR	Fold Enrichment	Count
0.001	10.168	6
geneID		
Zm00001eb153200 Zm00001eb180480 Zm00001eb241040 Zm00001eb267380 Zm00001eb272020 Zm00001eb313140		
Description	**Plant-type hypersensitive response**	
Enrichment FDR	Fold Enrichment	Count
0.001	10.168	6
geneID		
Zm00001eb153200 Zm00001eb180480 Zm00001eb241040 Zm00001eb267380 Zm00001eb272020 Zm00001eb313140		
Description	**Reg. of jasmonic acid mediated signaling pathway**	
Enrichment FDR	Fold Enrichment	Count
7.21E-06	9.559	11
geneID		
Zm00001eb005980 Zm00001eb005990 Zm00001eb006000 Zm00001eb048770 Zm00001eb099240 Zm00001eb100130 Zm00001eb121040 Zm00001eb223620 Zm00001eb300140 Zm00001eb312170 Zm00001eb314010		
Description	**Jasmonic acid mediated signaling pathway**	
Enrichment FDR	Fold Enrichment	Count
7.36E-05	7.034	11
geneID		
Zm00001eb005980 Zm00001eb005990 Zm00001eb006000 Zm00001eb048770 Zm00001eb099240 Zm00001eb100130 Zm00001eb121040 Zm00001eb223620 Zm00001eb300140 Zm00001eb312170 Zm00001eb314010		
Description	**Cellular response to jasmonic acid stimulus**	
Enrichment FDR	Fold Enrichment	Count
7.36E-05	6.657	11
geneID		

Zm00001eb005980 Zm00001eb005990 Zm00001eb006000 Zm00001eb048770
Zm00001eb099240 Zm00001eb100130 Zm00001eb121040 Zm00001eb223620
Zm00001eb300140 Zm00001eb312170 Zm00001eb314010

Description	**Response to jasmonic acid**	
Enrichment FDR	Fold Enrichment	Count
7.36E-05	6.070	12

geneID

Zm00001eb005980 Zm00001eb005990 Zm00001eb006000 Zm00001eb048770
Zm00001eb051200 Zm00001eb099240 Zm00001eb100130 Zm00001eb121040
Zm00001eb223620 Zm00001eb300140 Zm00001eb312170 Zm00001eb314010

Description	**Response to wounding**	
Enrichment FDR	Fold Enrichment	Count
0.001	4.960	12

geneID

Zm00001eb005980 Zm00001eb005990 Zm00001eb006000 Zm00001eb041390
Zm00001eb048770 Zm00001eb099240 Zm00001eb100130 Zm00001eb121040
Zm00001eb223620 Zm00001eb300140 Zm00001eb312170 Zm00001eb314010

Description	**Protein autophosphorylation**	
Enrichment FDR	Fold Enrichment	Count
1.69E-05	4.657	18

geneID

Zm00001eb001780 Zm00001eb031590 Zm00001eb070460 Zm00001eb078090
Zm00001eb107190 Zm00001eb207430 Zm00001eb213280 Zm00001eb220460
Zm00001eb239210 Zm00001eb248460 Zm00001eb282360 Zm00001eb299910
Zm00001eb310470 Zm00001eb312330 Zm00001eb324690 Zm00001eb426060
Zm00001eb428080 Zm00001eb431130

Description	**Reg. of defense response**	
Enrichment FDR	Fold Enrichment	Count
0.001	4.451	13

geneID

Zm00001eb005980 Zm00001eb005990 Zm00001eb006000 Zm00001eb012080
Zm00001eb048770 Zm00001eb099240 Zm00001eb100130 Zm00001eb111590
Zm00001eb121040 Zm00001eb223620 Zm00001eb300140 Zm00001eb312170
Zm00001eb314010

24 hpi

Treatment	**PC13**	
Description	**Maturation of LSU-rRNA**	
Enrichment FDR	Fold Enrichment	Count
6.12E-09	11.405	13

geneID

Zm00001eb053960 Zm00001eb131370 Zm00001eb150380 Zm00001eb176070
Zm00001eb189070 Zm00001eb198430 Zm00001eb253180 Zm00001eb253410
Zm00001eb255650 Zm00001eb295520 Zm00001eb326820 Zm00001eb414310
Zm00001eb420570

Description	Ribosomal large subunit biogenesis	
Enrichment FDR	Fold Enrichment	Count
6.14E-15	9.193	25

geneID

Zm00001eb002520 Zm00001eb053960 Zm00001eb091900 Zm00001eb093290
Zm00001eb098510 Zm00001eb124750 Zm00001eb131370 Zm00001eb150380
Zm00001eb173180 Zm00001eb176070 Zm00001eb189070 Zm00001eb192860
Zm00001eb198430 Zm00001eb204910 Zm00001eb245740 Zm00001eb251610
Zm00001eb253180 Zm00001eb253410 Zm00001eb255650 Zm00001eb257450
Zm00001eb295520 Zm00001eb326820 Zm00001eb347380 Zm00001eb414310
Zm00001eb420570

Description	Ribosome assembly	
Enrichment FDR	Fold Enrichment	Count
5.09E-10	9.044	17

geneID

Zm00001eb002520 Zm00001eb002640 Zm00001eb052970 Zm00001eb082850
Zm00001eb091900 Zm00001eb109330 Zm00001eb140330 Zm00001eb173180
Zm00001eb204910 Zm00001eb245740 Zm00001eb251610 Zm00001eb255650
Zm00001eb257450 Zm00001eb293800 Zm00001eb334050 Zm00001eb347380
Zm00001eb413810

Description	Ribosome biogenesis	
Enrichment FDR	Fold Enrichment	Count
5.55E-31	6.536	66

geneID

Zm00001eb002520 Zm00001eb002640 Zm00001eb016760 Zm00001eb016780 Zm00001eb031600
Zm00001eb036790 Zm00001eb052970 Zm00001eb053960 Zm00001eb067490 Zm00001eb072270
Zm00001eb082850 Zm00001eb091900 Zm00001eb093290 Zm00001eb098510 Zm00001eb109330
Zm00001eb114360 Zm00001eb124750 Zm00001eb131370 Zm00001eb135960 Zm00001eb139270
Zm00001eb140330 Zm00001eb150380 Zm00001eb163700 Zm00001eb172570 Zm00001eb173180
Zm00001eb176070 Zm00001eb183430 Zm00001eb189070 Zm00001eb191090 Zm00001eb192860
Zm00001eb198430 Zm00001eb200450 Zm00001eb204910 Zm00001eb209610 Zm00001eb218720
Zm00001eb228070 Zm00001eb229850 Zm00001eb245740 Zm00001eb251610 Zm00001eb253180
Zm00001eb253410 Zm00001eb255650 Zm00001eb257450 Zm00001eb272000 Zm00001eb278540
Zm00001eb292050 Zm00001eb293800 Zm00001eb295520 Zm00001eb303580 Zm00001eb311090
Zm00001eb326820 Zm00001eb328640 Zm00001eb333520 Zm00001eb334050 Zm00001eb347380
Zm00001eb355270 Zm00001eb376330 Zm00001eb378550 Zm00001eb379150 Zm00001eb386980
Zm00001eb394640 Zm00001eb405580 Zm00001eb413810 Zm00001eb414310 Zm00001eb420570
Zm00001eb428130

Description	Ribonucleoprotein complex biogenesis	
Enrichment FDR	Fold Enrichment	Count
5.55E-31	5.850	73

geneID

Zm00001eb002520 Zm00001eb002640 Zm00001eb016760 Zm00001eb016780 Zm00001eb031600
Zm00001eb036790 Zm00001eb037310 Zm00001eb052970 Zm00001eb053960 Zm00001eb067490
Zm00001eb072270 Zm00001eb080070 Zm00001eb082850 Zm00001eb091900 Zm00001eb093290
Zm00001eb098510 Zm00001eb107710 Zm00001eb109330 Zm00001eb114360 Zm00001eb124750
Zm00001eb131370 Zm00001eb135960 Zm00001eb139270 Zm00001eb140330 Zm00001eb150380
Zm00001eb163700 Zm00001eb172570 Zm00001eb173180 Zm00001eb176070 Zm00001eb183430
Zm00001eb189070 Zm00001eb191090 Zm00001eb192860 Zm00001eb198430 Zm00001eb200450
Zm00001eb204910 Zm00001eb206810 Zm00001eb209610 Zm00001eb218720 Zm00001eb228070
Zm00001eb229850 Zm00001eb245740 Zm00001eb251610 Zm00001eb253180 Zm00001eb253410
Zm00001eb255650 Zm00001eb257450 Zm00001eb272000 Zm00001eb278540 Zm00001eb292050
Zm00001eb293800 Zm00001eb295520 Zm00001eb296070 Zm00001eb303580 Zm00001eb311090
Zm00001eb325580 Zm00001eb326820 Zm00001eb328640 Zm00001eb333520 Zm00001eb334050
Zm00001eb339230 Zm00001eb347380 Zm00001eb355270 Zm00001eb376330 Zm00001eb378550
Zm00001eb379150 Zm00001eb386980 Zm00001eb394640 Zm00001eb405580 Zm00001eb413810
Zm00001eb414310 Zm00001eb420570 Zm00001eb428130

Description	Ribosomal small subunit biogenesis	
Enrichment FDR	Fold Enrichment	Count
8.90E-06	5.834	14

geneID			
Zm00001eb002640	Zm00001eb072270	Zm00001eb082850	Zm00001eb109330
Zm00001eb140330	Zm00001eb163700	Zm00001eb209610	Zm00001eb229850
Zm00001eb272000	Zm00001eb293800	Zm00001eb334050	Zm00001eb378550
Zm00001eb405580	Zm00001eb413810		

Description	Ribonucleoprotein complex assembly	
Enrichment FDR	Fold Enrichment	Count
3.01E-09	5.583	23

geneID			
Zm00001eb002520	Zm00001eb002640	Zm00001eb037310	Zm00001eb080070
Zm00001eb082850	Zm00001eb091900	Zm00001eb107710	Zm00001eb109330
Zm00001eb140330	Zm00001eb173180	Zm00001eb204910	Zm00001eb206810
Zm00001eb245740	Zm00001eb251610	Zm00001eb255650	Zm00001eb292050
Zm00001eb293800	Zm00001eb296070	Zm00001eb325580	Zm00001eb334050
Zm00001eb339230	Zm00001eb347380	Zm00001eb413810	

Description	RRNA metabolic proc.	
Enrichment FDR	Fold Enrichment	Count
4.12E-15	5.508	38

geneID			
Zm00001eb031600	Zm00001eb053960	Zm00001eb067490	Zm00001eb072270
Zm00001eb114360	Zm00001eb131370	Zm00001eb135960	Zm00001eb139270
Zm00001eb150380	Zm00001eb163700	Zm00001eb176070	Zm00001eb183430
Zm00001eb189070	Zm00001eb191090	Zm00001eb198430	Zm00001eb200450
Zm00001eb209610	Zm00001eb218720	Zm00001eb228070	Zm00001eb229850
Zm00001eb253180	Zm00001eb253410	Zm00001eb255650	Zm00001eb272000
Zm00001eb293800	Zm00001eb295520	Zm00001eb303580	Zm00001eb311090
Zm00001eb326820	Zm00001eb328370	Zm00001eb328640	Zm00001eb333520
Zm00001eb376330	Zm00001eb378550	Zm00001eb386980	Zm00001eb405580
Zm00001eb414310	Zm00001eb420570		

Description	RRNA processing	
Enrichment FDR	Fold Enrichment	Count
8.53E-15	5.507	37

geneID			
Zm00001eb031600	Zm00001eb053960	Zm00001eb067490	Zm00001eb072270
Zm00001eb114360	Zm00001eb131370	Zm00001eb135960	Zm00001eb139270
Zm00001eb150380	Zm00001eb163700	Zm00001eb176070	Zm00001eb183430
Zm00001eb189070	Zm00001eb191090	Zm00001eb198430	Zm00001eb200450
Zm00001eb209610	Zm00001eb218720	Zm00001eb228070	Zm00001eb229850
Zm00001eb253180	Zm00001eb253410	Zm00001eb255650	Zm00001eb272000
Zm00001eb293800	Zm00001eb295520	Zm00001eb303580	Zm00001eb311090
Zm00001eb326820	Zm00001eb328640	Zm00001eb333520	Zm00001eb376330
Zm00001eb378550	Zm00001eb386980	Zm00001eb405580	Zm00001eb414310
Zm00001eb420570			

Publication Licenses – Figures

49 Spadina Ave. Suite 200
Toronto ON M5V 2J1 Canada
www.biorender.com

Confirmation of Publication and Licensing Rights

January 10th, 2025

Subscription Type:	*Lab - Academic*
Agreement number:	*YL27RXCF53*
Publisher Name:	*PhD thesis*
Citation to Use:	*Created in BioRender. Doehlemann, G. (2025) https://BioRender.com/q13r760*

To whom this may concern,

This document is to confirm that Gunther Doehlemann has been granted a license to use the BioRender Content, including icons, templates, and other original artwork, appearing in the attached Completed Graphic pursuant to BioRender's Academic License Terms. This license permits BioRender Content to be sublicensed for use in publications (journals, textbooks, websites, etc.).

All rights and ownership of BioRender Content are reserved by BioRender. All Completed Graphics must be accompanied by the following citation: "Created in BioRender. Doehlemann, G. (2025) https://BioRender.com/q13r760".

BioRender Content included in the Completed Graphic is not licensed for any commercial uses beyond use in a publication. For any commercial use of this figure, users may, if allowed, recreate it in BioRender under an Industry BioRender Plan.

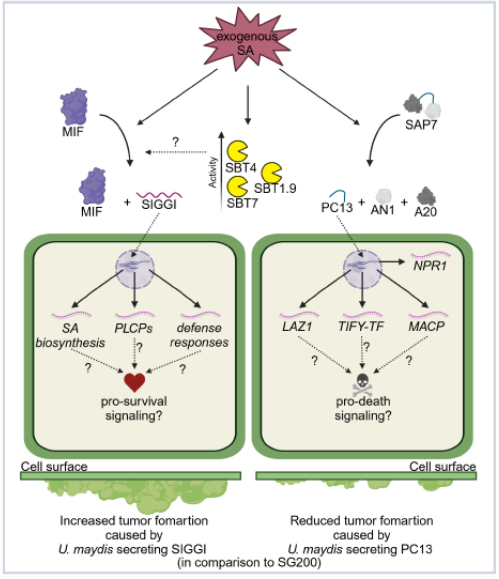

For any questions regarding this document, or other questions about publishing with BioRender, please refer to our BioRender Publication Guide, or contact BioRender Support at support@biorender.com.

7. Delimitation of own contribution

- **Dr. Farnusch Kaschani**, Center of Medical Biotechnology (ZMB), University of Duisburg-Essen, performed OBD following mass spectrometry analysis
- **Dr. Jan-Wilm Lackmann**, CECAD/ZMMK Proteomics Facility, University of Cologne, performed Mass spectrometry analysis of peptidomics
- **Novogene Company Limited** for the RNA sequencing and standard analysis

During the course of my dissertation, I was responsible for the supervision of the following student, whose final theses contributed to this thesis:

Bachelor Thesis:

- **Yannick Hoffmann** (2024): Characterisation of serine proteases potentially involved in immune signaling of *Zea mays*

Yannick Hoffmann produced recombinant MIF-His and SAP7-His, performed the overexpression and purification of the ZmSBT7 in *N. benthamiana* with following activity tests and deglycosylation.